Electric Dipole Moments within and beyond the Standard Model

A DISSERTATION
SUBMITTED TO THE FACULTY OF THE GRADUATE SCHOOL
OF THE UNIVERSITY OF MINNESOTA
BY

Ting Gao

IN PARTIAL FULFILLMENT OF THE REQUIREMENTS
FOR THE DEGREE OF
DOCTOR OF PHILOSOPHY

Maxim Pospelov

June, 2025

Acknowledgements

Writing the thesis is an experience that is both delightful and painful, as this important milestone also signals having to say goodbye to so many memorable people in Minnesota. As the last part remaining to be finished in this thesis, I hope this acknowledgment can express my gratitude to the people who have helped me over the years, without whom this thesis would have been impossible.

First and foremost, I want to thank my advisor, Maxim, who introduced me to the research in particle physics and provided the greatest support throughout my PhD experience. I am particularly grateful for Maxim's confidence in my academic potential, his guidance and support for helping me to grow into an independent researcher, and the incredible academic freedom I have while working with him. The experience of paving the way out of complicated problems with Maxim is invaluable to me. I appreciate how hard Maxim has been trying to get financial support for me over the years, which has led to many fellowship and research assistantship opportunities in an area where getting teaching assistantships throughout one's PhD is typical. I am also indebted to all the summer schools and conference opportunities Maxim introduced to me. With Maxim's influence on me coming from all aspects of physics and a significant part of my personal life, it is impossible to overstate how much Maxim has changed my life.

As the standard in particle theory, it is always beneficial to keep open to new ideas. To this end, I want to thank Zhen for introducing me to the topic of scattering amplitudes, which, although it didn't appear in this thesis, constitutes an important part of my research. I also want to thank Zhen for bridging many conversations with the visitors of the particle theory group and for all the advice for my academic development.

Learning how to do research requires a lot of guidance, and I want to thank Yohei for being an excellent collaborator for almost all the research projects I have participated

in and for shaping the standard of what a mature researcher should be like during the years of collaboration. I am impressed by Yohei's serious and calming attitude towards science and his efficiency and passion in carrying out research.

I also want to thank all my other collaborators, Adam, Ishmam, Wenqi, and Kun-Feng, for all the insightful discussions we had and for the nice work that resulted from that. In particular, I benefited a lot from the discussions with Ishmam. The research would have been impossible without everyone's expertise, and I want to thank you all for the great collaboration.

I am fortunate to be in a large particle physics group with many students, postdocs, and faculty to exchange ideas and learn from other people's expertise. I am particularly grateful to Peiran for our conversations about all the different topics. I want to thank the student journal club lectures, as well as informal discussions, from Theo, Chao-Hsiang, Tom, Ravneet, Arpon, Saif, Maria, Stephen, Sami, Yuxin, Batu, and Hao-Ran, where I got a better understanding of many physics topics. The interactions with Saarik, Evgenii, Shi, and Raymond were also beneficial. I also want to thank the entire particle theory group for building a warm and welcoming atmosphere where everyone's development is encouraged.

Next, I want to thank Andy, Dan, and Yong (along with Maxim and Zhen) for devoting their valuable time to be on my preliminary and final oral exam committee, and for the helpful suggestions for my growth.

Going to the non-academic side, I want to thank all my friends for the time we spent together. I am especially grateful to Sirui, Wei, He, and Yanting for being great roommates during my PhD, and I want to give special thanks to Shaowei and Yuqin for taking me to see the aurora and the meteor shower multiple times. My life here would have been a lot more pale without Panmei, Guopeng, Pengyan, Siqi, Yan, Longyu, Wanling, Hao, Yi, Yifei, Yu, Xi, Yuxuan, Rongfeng, Zaifu, Zixiang, Daren, Haiyao, and Yang. I appreciate having you as my friend; the memories with you will be a treasure in my life.

Finally, I want to thank my parents, Shuxia and Yuan, for their support to the best of their ability and for understanding my attending graduate school in a country far away from my hometown.

This thesis is based on the published works [1–5] in collaboration with Yohei Ema,

Maxim Pospelov, and Adam Ritz. The other works completed during my PhD [6–8] with Yohei Ema, Wenqi Ke, Zhen Liu, Kun-Feng Lyu, Ishmam Mahbub, and Maxim Pospelov, along with papers in preparation, are not included. Part of my work that led to this thesis is supported by U.S. Department of Energy Grant No. desc0011842 and three fellowships at the University of Minnesota: Hoff Lu Fellowship, Mikhail Voloshin Fellowship, and Doctoral Dissertation Fellowship.

Dedication

To the summers in Minnesota

Abstract

Searches for electric dipole moments (EDMs) in fundamental particles, nucleons, atoms, and molecules provide a powerful test of fundamental symmetries. The smallness of the CP-violation in the Standard Model (SM) gives a clean background for the EDM experiments, making any non-zero signals of EDMs directly sensitive to the beyond Standard Model (BSM) physics. The interpretation of EDM experiments requires a wide range of inputs from particle physics, hadron physics, nuclear physics, to atomic physics. In this thesis, a series of work on the theory of EDMs from the point of view of particle physics is presented. Starting from the Kobayashi-Maskawa (KM) phase in the SM, the size of the electron-spin-dependent CP-odd electron-nucleon interaction (usually denoted as the C_S operator), which contributes to the EDMs of paramagnetic systems, is calculated. The result is three orders of magnitude larger than previously believed. Using the QCD sum rule technique, arbitrary choices of the interpolating current are shown to lead to inconsistent results in the calculations involving the QCD theta term, and the proper procedure is identified to solve this issue. In the presence of EDMs of heavy SM fermions, the effective CP-odd operators generated below the heavy fermion mass threshold and the further induced neutron and atomic EDMs are derived, which in turn allows indirect constraints on the muon, charm quark, and bottom quark EDMs to be set based on existing experiments.

Contents

List of Tables

List of Figures

Chapter 1

Introduction

Symmetries have been playing a central role in physics since the beginning of the twentieth century. Among all the symmetries, our spacetime is believed to be invariant (at least when gravity is negligible) under continuous Lorentz transformations, which is the transformation of the proper, orthochronous Lorentz group $\mathrm{SO}^+(1,3)$. On the other hand, the invariance of physics laws under *discrete* Lorentz transformations, namely charge conjugation (C), parity (P), and time reversal (T), cannot be assumed a priori. C and P are separately violated by the weak interaction [9,10], and the combined symmetry of C and P (CP) is also violated, but at a much smaller level [11]. However, it is believed that the continuous Lorentz symmetry implies the combined symmetry of CPT [12–14].

The Standard Model is by far the most successful theory of the particle world, but there is accumulating evidence reminding us it is not the ultimate theory. One such piece of evidence comes from Baryogenesis. As pointed out by Sakharov [15], three conditions are required to generate baryon-antibaryon asymmetry observed today: Baryon number violation, C and CP violation, and deviation from thermal equilibrium. The Standard Model allows two CP violation parameters: the complex phase of the Cabibbo–Kobayashi–Maskawa (CKM) matrix δ_{KM} and the QCD theta term θ_{QCD}. The former is observed in the flavor-changing channel from Kaon and B meson decays and is well determined; the latter is physically allowed but has not yet been observed in experiments. However, the observed CP violation within the SM is insufficient to produce the amount of asymmetry needed, which makes it essential to test CP violations

within and beyond the SM from other aspects.

Intrinsic EDMs of particles, atoms, and molecules require the breaking of T symmetry[1], and, assuming CPT invariance, implies CP symmetry, this can be seen from the fact that EDMs can only align on (or opposite to) the direction of total angular momentum. Angular momentum flips the sign under T, so EDMs also need to flip the sign to keep the action invariant.[2] Therefore, searches for EDMs provide a way of probing CP violations in the flavor-neutral channel. Due to the clean background from low energy physics and the superior precision, any experimental signal of EDMs can be interpreted as direct evidence of the CP violation in the heavy new physics and will be an important hint for probing the new physics on-shell with colliders.

Experimental efforts searching for EDMs were first proposed in the 1950s by Purcell and Ramsey [16]. Since then, the accuracy of EDM experiments has been improving by nearly two orders of magnitude per decade [17]. The best sensitivity on EDMs is achieved in three main classes of EDMs measured in experiments: EDM of paramagnetic systems, diamagnetic systems, and the neutron [18]. Making full use of EDM experiments, therefore, requires complete analysis of both the SM and BSM physics from the fundamental high-energy scale to the relevant experimental scale. In the context of the effective field theory (EFT), by integrating out the heavy degrees of freedom, the effects coming from high energy can be categorized as higher-dimensional operators that contribute to the low energy physics, with the coefficients in front of them, known as Wilson coefficients, characterizing the specific features of the high energy physics. Below the electroweak scale, the CP-odd operators up to dimension 6 include the dimension-4 QCD theta term, the dimension-5 fermion EDMs and color EDMs (CEDMs), and the dimension-6 Weinberg operator and the four-fermion operators :

$$\begin{aligned}\mathcal{L}_{CPV} =& \frac{\bar{\theta}\alpha_s}{8\pi} G^a_{\mu\nu}\tilde{G}^{a\mu\nu} + \sum_i \frac{d_i}{2}\bar{\psi}_i(\tilde{F}\sigma)\psi_i + \sum_i \frac{g_s\tilde{d}_i}{2}\bar{\psi}_i(\tilde{G}\sigma)\psi_i \\ &+ \frac{1}{3}wf^{abc}\tilde{G}^{a\mu}_{\nu}G^{b\nu}_{\rho}G^{c\rho}_{\mu} + \sum_{i,j,k,l} C_{ijkl}(\bar{\psi}_i\psi_j)(\bar{\psi}_k i\gamma^5\psi_l) + \cdots .\end{aligned} \tag{1.1}$$

[1] Some molecules have classical EDMs which do not give $\boldsymbol{J}\cdot\boldsymbol{E}$ correlation, this type of EDM does not require the breaking of CP symmetry and is not of our interest.

[2] Magnetic dipole moments, however, exists without the requirement of CP violation, this is because the magnetic field flips the sign under T, which allows the correct action to be obtained without flipping the sign of magnetic dipole moments.

As the energy scale further goes down, the operators involving quarks become the interactions with nucleons and mesons due to the confinement, and heavy fermions are further integrated out to contribute to the effective operators involving only light degrees of freedom. These operators together contribute to the EDMs measured in experiments. As systems with an electron in the open shell, paramagnetic systems get EDMs mainly from a linear combination of the EDM of the unpaired electron and the C_S operator, which characterizes the electron spin-dependent CP-odd interaction between electron and nucleon. For this reason, the result of paramagnetic EDM experiments can be interpreted as a constraint on the equivalent electron EDM d_e^{equiv} by normalizing the coefficient in front of the electron EDM to 1. Diamagnetic atoms, on the other hand, get EDMs mainly from the CP-violation on the nucleon side, including the nucleon EDMs, the CP-odd nucleon forces, and the nuclear spin-dependent CP-odd interactions between electron and nucleon. Neutron EDM can also be directly searched for, and its EDM could come from the CP-odd nucleon forces, CP-odd gluon interactions, quark EDMs, and quark color EDMs (CEDMs). The current experimental upper limit for these three types of EDMs is listed in Table 1.1.

Table 1.1: Experimental upper limits for paramagnetic, diamagnetic, and neutron EDMs.

Type of EDM	Experimental bound
Paramagnetic atoms	$\lvert d_e^{\text{equiv}}(\text{ThO})\rvert < 1.1 \times 10^{-29} e\text{cm}$ (90% C.L.) [19]
	$\lvert d_e^{\text{equiv}}(\text{HfF}^+)\rvert < 4.1 \times 10^{-30} e\text{cm}$ (90% C.L.) [20]
Diamagnetic atoms	$\lvert d(^{199}\text{Hg})\rvert < 7.4 \times 10^{-30} e\text{cm}$ (95% C.L.) [21]
Neutron	$\lvert d_n\rvert < 1.8 \times 10^{-26} e\text{cm}$ (90% C.L.) [22]

The equivalent electron EDM constrained in Table 1.1 can be compared with the electron's magnetic dipole moment (MDM),

$$|\mu_e| = \frac{e}{2m_e} = 1.9 \times 10^{-11} e\text{cm}. \tag{1.2}$$

This shows the smallness of the CP-violating effects and how far the EDM experiments have pushed the experimental accuracy to search for CP-violations.

With the SM sources of CP violation it is possible to generate EDMs within the

SM, either through the $\delta_{\rm KM}$ phase by combining several flavor changing processes, or through the $\theta_{\rm QCD}$ by considering the topological effects in the strong sector. A number of efforts have been made to predict the SM EDMs; the current results are shown in Table 1.2. In particular, the calculation for the paramagnetic EDM from the CKM phase is part of this thesis, and the neutron EDM from the QCD theta term is also reconfirmed in this thesis.

Table 1.2: SM estimates for paramagnetic, diamagnetic, and neutron EDMs, in units of $e$cm

Type of EDM	theta term	CKM phase
Paramagnetic $\lvert d_e^{\rm eq}({\rm ThO})\rvert$	$5\times10^{-22}\bar{\theta}$ [23, 24]	1.0×10^{-35} [2]
Diamagnetic $d(^{199}{\rm Hg})$	$(1.5\pm1.8)\times10^{-19}\bar{\theta}$ [25]	$(0.4-2.4)\times10^{-35}$ [26]
Neutron $\lvert d_n\rvert$	$(0.8-1.2)\times10^{-16}\bar{\theta}$ [5, 27–30]	$(1-6)\times10^{-32}$ [31]

Comparing the SM prediction from $\delta_{\rm KM}$ and the experimental constraints, there is still a six orders of magnitude gap between them; the smallness of the SM contribution to EDMs then provides a clean environment for the searches for BSM sources of CP-violation. A simple dimensional analysis, assuming possible BSM CP violation contributing to EDMs at one-loop, gives the scaling

$$d_e/e \simeq \frac{m_e}{\Lambda_{CP}^2}\times(\text{loop factors}) \;\rightarrow\; \Lambda_{CP} > 10^2\text{TeV} \tag{1.3}$$

So the current limit on EDMs translates to a constraint on the CP-violating new physics at the 10^2TeV scale, a scale which is challenging to probe on-shell in the foreseeable future.

The goal of this thesis is to accomplish the following:

- Despite the enormous experimental progress on the measurement of electron EDM in atomic, molecular, and optical physics (AMO), a proper theoretical prediction on the EDMs of paramagnetic systems within the SM is still missing. While previous SM calculations mainly focus on the contribution from d_e, the contribution from C_S, which might be dominant, is not well estimated. This gap is filled in Chapter 2

- The neutron, as a bound state dominated by QCD effects, requires the use of non-perturbative methods to calculate its EDM, and a self-consistent starting point for such calculations has to be defined. Starting from the θ-induced neutron EDM, Chapter 3 evaluates the suitability of the three-quark interpolating field based on their properties under $\mathrm{U}(1)_A$ transformation, which has important implications in lattice QCD calculations.

- Given the advances in the loop calculation techniques, adapting them in EDM calculations becomes desirable. Based on the methods of projection, integration by parts, and master integrals used in modern multi-loop calculations, Chapter 4 calculates the electron EDM induced by the heavy leptons and the light quark EDMs induced by the charm and bottom quark EDMs. Additionally, based on the external field method, the CP-odd interactions among four gauge bosons are derived.

- Given the new experiment to measure the muon EDM at PSI [32], in Chapter 5, the indirect limit on the muon EDM is determined from existing AMO EDM data. Different from the EFT below the electroweak scale, the mass of the muon is at the borderline of being heavy when one considers the nuclear scale; therefore, an EDM of the muon could potentially contribute to EDMs of atoms through dimension-8 operators. The constraints on the muon EDM obtained in this way are shown to be stronger than the direct constraints from [33].

- Given the proposal to measure the charm EDM at LHC [34–38], in Chapter 6, the indirect limits on the charm and bottom quark EDMs are determined from existing experiments based on the effects of dimension-8 CP-odd photon-gluon operators generated by the charm and bottom quark EDMs.

Finally, Chapter 7 provides a summary of the thesis and an outlook for the future. A number of appendices are included for reference, with Appendix A focusing on the conventions used in the thesis, Appendix B-D concentrating on technical details, and Appendix E providing a list of acronyms used in this thesis.

Chapter 2

Standard Model prediction for paramagnetic EDMs

Recent breakthrough sensitivity to CP violation connected to electron spin (that we will refer to as "paramagnetic EDMs") [20, 39] established a new limit on the linear combination of the electron EDM d_e and semileptonic nucleon-electron $\bar{N}N\bar{e}i\gamma_5 e$ operators, commonly parametrized by a C_S coefficient. Given rapid progress of the last decade, as well as some additional hopes for increased accuracy (see *e.g.* [40–42]), in this chapter we revisit the Standard Model (SM) sources of CP violation and the expected size of the paramagnetic EDMs in the SM. We point out that the paramagnetic EDMs are dominated by the combination of the electroweak penguin diagrams and $\Delta I = 1/2$ weak transitions in the baryon sector, and are calculable within chiral perturbation theory. The predicted size of the semileptonic operator C_S is 7×10^{-16} which corresponds to the *equivalent* electron EDM $d_e^{\rm eq} = 1.0 \times 10^{-35} e\,{\rm cm}$. While still far from the current observational limits, this result is three orders of magnitude larger than previously believed.

2.1 Overview of previous calculations

As discussed in the introduction, the SM sources of CP-violation include the non-perturbative effects parametrized by the QCD vacuum angle θ and the (KM) phase $\delta_{\rm KM}$. We discuss here the past efforts in calculating the paramagnetic EDMs from these

sources.

CP violation due to θ comes through the $\pi^0(\eta)\bar{N}N$ coupling, recently it has been shown [23] that paramagnetic EDMs are dominated by the two-photon exchange mechanism, and the leading chiral behavior of the hadronic part of the diagram is given by the t-channel exchange by π^0, η. The result, in combination with the experimental bound [39], sets the independent limit on $|\theta| < 3 \times 10^{-8}$, which is still subdominant to the limit provided by $d_n(\theta)$.

The predictions of EDM-like observables induced by $\delta_{\rm KM}$ thus far can be summarized by two adjectives: small and uncertain. The suppression comes from the necessity to involve at least two W-bosons and multiple loops [43–45] involving all three generations of quarks. As a result, short distance contributions to quark EDMs do not exceed $10^{-33}\, e\,$cm level [46]. At the same time, it is clear that long-distance nonperturbative contributions, typically described as a combination of two transitions changing strangeness by one unit, $\Delta S = \pm 1$, dominate d_n and nucleon-nucleon forces [47–51]. More recent estimate [31] places d_n in the ballpark of few $\times\, 10^{-32}\, e\,$cm with a wide order-of-magnitude expected range. It is fair to say that magnitudes of d_n and nucleon-nucleon forces (that feeds into the nuclear-spin-dependent atomic EDMs) cannot be accurately predicted at this point.

$\delta_{\rm KM}$ induces paramagnetic EDMs through a combination of d_e and C_S. Recent estimates of d_e [52] (dominated again by long-distance effects) converge at the tiniest value of $\sim 6 \times 10^{-40}\, e\,$cm, presumably with considerable uncertainties corresponding to hadronic modelling of quark loops. This result is subdominant to the C_S estimate due to the two-photon exchange mechanism in combination with $\Delta S = \pm 1$ transitions [53], that corresponds to equivalent d_e of $\sim 10^{-38}\, e\,$cm. To introduce useful notations, this is EW^{2}EM^2 order effect, where EW/EM stands for electroweak/electromagnetic.

2.2 C_S operator from $\delta_{\rm KM}$ in EW^3 order

In this section, we demonstrate that the dominant contribution to paramagnetic EDMs associated with the KM CP-violation is given by the semileptonic C_S induced in EW^3 order. It has an unambiguous answer in the flavor-$SU(3)$ chiral limit, and is calculable to $\sim 30\%$ accuracy that can be further improved. Remarkably, the result reaches the

level of $\sim 10^{-35}\, e\,\text{cm}$ in terms of the d_e equivalent, which is three orders of magnitude larger than previously believed [53].

Our starting point is the expression for the *equivalent* d_e that follows from atomic and molecular theory, and defines the linear combination of two Wilson coefficients constrained by the most precise paramagnetic EDM measurements performed with ThO molecule [1]:

$$d_e^{\text{equiv}} = d_e + C_S \times 1.5 \times 10^{-20}\, e\,\text{cm}, \tag{2.1}$$

where e is the positron charge. Current experimental limit [39] stands as $|d_e^{\text{equiv}}| < 1.1 \times 10^{-29}\, e\,\text{cm}$. As per convention, C_S is defined with the Fermi constant factored out, and γ_5 corresponds to the $\frac{1}{2}\gamma_\mu(1-\gamma_5)$ definition of the left-handed current:

$$\mathcal{L}_{eN} = C_S \frac{G_F}{\sqrt{2}} (\bar{e} i\gamma_5 e)(\bar{p}p + \bar{n}n). \tag{2.2}$$

Our goal is to calculate $C_S(\delta_{\text{KM}})$.

2.2.1 Leading chiral order C_S calculation

Because of the conservation of the electron chirality in the SM, it is clear that $C_S \propto m_e$. This in turn rules out single photon exchange (EM penguin) as origin of $m_e \bar{e} i\gamma_5 e$, and one would need either a two-photon mechanism [23, 53] or the EW penguin Z-boson exchange/W-box diagram. The most crucial property of EW penguins is that although they are formally of the second order in weak interactions, their size is enhanced by the heavy top, so that the result scales as $G_F^2 m_t^2$. EW penguins[2] induce $B_{s,d} \to \mu^+\mu^-$ decays, and dominate the dispersive part of $K_L \to \mu^+\mu^-$ amplitude. Dropping the vector part of the lepton current (as not leading to $m_e \bar{e} i\gamma_5 e$), and integrating out heavy W, Z, t particles, one can concisely write down the semileptonic operator as

$$\mathcal{L}_{\text{EWP}} = -\mathcal{P}_{\text{EW}} \times \bar{e}\gamma_\mu\gamma_5 e \times \bar{s}\gamma^\mu(1-\gamma_5)d + (h.c.), \tag{2.3}$$

[1] The sign convention of C_S can be checked, *e.g.*, with [54]. We define $\gamma_5 = i\gamma^0\gamma^1\gamma^2\gamma^3$ that has the opposite sign as theirs.

[2] As is well known, EW penguins must also include W-box diagrams, and we include both.

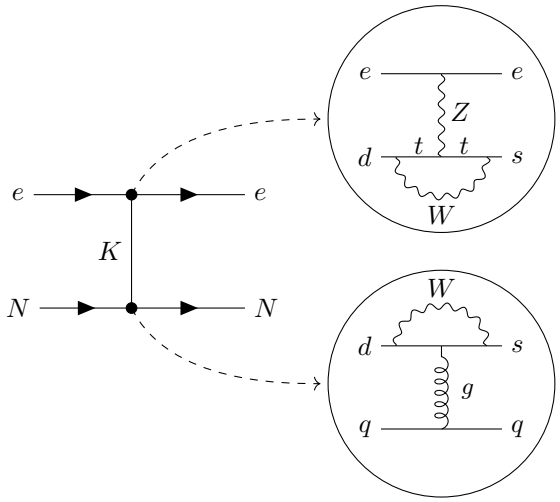

Figure 2.1: EW^3 order diagram that dominates in the chiral limit. The top vertex is the CP-odd, P-even $K_S\bar{e}i\gamma_5 e$ generated in EW^2 order, and the bottom vertex is CP-even, P-odd $K_S\bar{N}N$ coupling generated at EW^1 order.

where

$$\mathcal{P}_{\rm EW} = \frac{G_F}{\sqrt{2}} \times V_{ts}^* V_{td} \times \frac{\alpha_{\rm EM}(m_Z)}{4\pi \sin^2\theta_W} I(x_t), \tag{2.4}$$

and the loop function is given by [55]

$$I(x_t) = \frac{3}{4}\left(\frac{x_t}{x_t-1}\right)^2 \log x_t + \frac{1}{4}x_t - \frac{3}{4}\frac{x_t}{x_t-1}, \; x_t = \frac{m_t^2}{m_W^2}. \tag{2.5}$$

These results are well established, and unlike the case of four-quark operators, the subsequent renormalization group evolution of (2.3) introduces only small corrections (see *e.g.* [56, 57]). This is because the QCD evolution is trivial (apart from small threshold corrections at m_W) due to the partially conserved nature of the quark current, and QED evolution is small $\propto \alpha_{\rm EM}/\pi$.

The most convenient representation of the CKM matrix is when $\delta_{\rm KM}$ enters mostly in V_{td}. It enters the imaginary part of $\mathcal{P}_{\rm EW}$ and couples the axial vector current of leptons to the $\bar{s}\gamma_\mu(1-\gamma_5)d - \bar{d}\gamma_\mu(1-\gamma_5)s$ quark current. This current can create/annihilate CP-even combination of the neutral kaons that (in neglection of small ϵ_K) can be

identified with K_S field. Same operator in the muon channel induces $K_S \to \mu^+\mu^-$ meson decay [58, 59]. Within chiral perturbation theory, the axial vector current of leptons is treated as an external left-handed current, which gives rise to

$$\mathcal{L}_{Uee} = -\frac{if_0^2}{2}\mathcal{P}_{\rm EW} \times \bar{e}\gamma_\mu\gamma_5 e \times {\rm Tr}\left[h^\dagger \left(\partial^\mu U\right) U^\dagger\right] + (h.c.), \tag{2.6}$$

where U is the exponential of the meson octet M, $U = \exp[2iMf_0^{-1}]$, in our convention it transforms as $U' = LUR^\dagger$, and $h_{ij} = \delta_{i2}\delta_{j3}$. At linear order, this leads to $\partial_\mu K \times \bar{e}\gamma^\mu\gamma_5 e$, and upon application of the equation of motion for electrons we arrive to

$$\mathcal{L}_{Kee} = -2\sqrt{2}f_0 m_e \bar{e} i\gamma_5 e \left(K_S \times {\rm Im}\mathcal{P}_{\rm EW} + K_L \times {\rm Re}\mathcal{P}_{\rm EW}\right). \tag{2.7}$$

In this expression, f_0 is the meson coupling constant, that in the $SU(3)$ symmetric limit is equal to $\simeq 134\,{\rm MeV}$, and we follow Ref. [60] conventions. Subsequent m_s-dependent corrections renormalize this coupling to $f_0 \to f_K \simeq 160\,{\rm MeV}$. While other s-quark containing resonances may also contribute, the neutral kaon exchange, Fig. 2.1, will give the only m_s^{-1}-enhanced contribution in the chiral limit.

We now need to find out how the neutral kaons couple to the nucleon scalar densities, $\bar{p}p$ and $\bar{n}n$ that occur due to $\Delta S = \pm 1$ transitions in the EW[1] order. Instead of attempting such calculation from first principles (see *e.g.* [61]) we will use flavor $SU(3)$ relations and connect this coupling to the s-wave amplitudes of hadronic decays of strange hyperons, following [60]. It is well known that empirical $\Delta I = 1/2$ rule holds for hyperon decays, and the leading order $SU(3)$ relations fit s-wave amplitudes with $O(10\%)$ accuracy. It is strongly suspected that these amplitudes are indeed induced by strong penguins (SP), although this assumption is not crucial for us. With that, one can write down the two types of couplings consistent with $(8_L, 1_R)$ transformation properties:

$$\mathcal{L}_{\rm SP} = -a{\rm Tr}(\bar{B}\{\xi^\dagger h\xi, B\}) - b{\rm Tr}(\bar{B}[\xi^\dagger h\xi, B]) + (h.c.). \tag{2.8}$$

In this expression, B is the baryon octet matrix, and $\xi = \exp[iMf_0^{-1}]$. Assuming a and

b to be real, and taking $f_0 = f_\pi$, they are fit by [60] to be[3]

$$a = 0.56 G_F f_\pi \times [m_{\pi^+}]^2; \quad b = -1.42 G_F f_\pi \times [m_{\pi^+}]^2. \tag{2.9}$$

Brackets over m_{π^+} indicate that these are numerical values taken, 139.5 MeV, rather than $m_u + m_d$-proportional theoretical quantity m_π. These value can be easily found via the least square fit to the nonleptonic s-wave amplitude, that also indicate 10% theoretical accuracy of this fit. In the assumption of a and b being real, only the K_S meson couples to nucleons, $2^{1/2} f_0^{-1}((b-a)\bar{p}p + 2b\bar{n}n)K_S$, which will provide the dominant contribution. This type of coupling breaks P but respects CP symmetry. Restoring the CKM factors, one can also include much subdominant coupling to K_L so that we have:

$$\begin{aligned}\mathcal{L}_{KNN} \simeq -\frac{\sqrt{2}\, G_F \times [m_{\pi^+}]^2 f_\pi}{|V_{ud}V_{us}| f_0} \times 2.84(0.7\bar{p}p + \bar{n}n) \\ \times \left(\mathrm{Re}(V_{ud}^* V_{us}) K_S + \mathrm{Im}(V_{ud}^* V_{us}) K_L\right).\end{aligned} \tag{2.10}$$

At the last step, we integrate out the K mesons as shown in Fig. 2.1. Adopting it for a nucleus containing $A = Z + N$ nucleons, one arrives to a straightforward prediction for the $\delta_{\rm KM}$-induced size of the electron-nucleon interaction:

$$C_S \simeq \mathcal{J} \times \frac{N + 0.7Z}{A} \times \frac{13[m_{\pi^+}]^2 f_\pi m_e G_F}{m_K^2} \times \frac{\alpha_{\rm EM} I(x_t)}{\pi \sin\theta_W^2}, \tag{2.11}$$

where $\mathcal{J}$ is the rephasing invariant combination of the CKM angles,

$$\mathcal{J} = \mathrm{Im}(V_{ts}^* V_{td} V_{ud}^* V_{us}) \simeq 3.1 \times 10^{-5}, \tag{2.12}$$

that carries about $\sim 6\%$ uncertainty. Notice that the f_0 factor in the numerator of (2.7) cancels against f_0 in the denominator of (2.10), and this cancellation would persist even one changes f_0 for f_K.

[3] The overall sign of a and b is not fixed by the hyperon nonleptonic decay (the relative sign between a and b is fixed to be negative). We use the sign motivated by the vacuum factorization of strong penguins [61, 62]. If the overall sign is opposite, it only affects the overall sign of C_S (and $d_e^{\rm equiv}$) and not its absolute value.

The overall scaling of this formula in the chiral limit and at large x_t is

$$G_F C_S \propto \mathcal{J} G_F^3 m_t^2 m_e m_s^{-1} \Lambda_{\rm hadr}^2. \tag{2.13}$$

where $\Lambda_{\rm hadr}$ is a typical hadronic energy/momentum scale. Notice that this is far more singular behavior with m_q of a light quark than that arising in the chiral-loop-induced expressions for d_n. Also notice that the K_S exchange dominates for any conventional parametrization of the CKM matrix, and the role of K_L exchange is to add small pieces of the amplitude that take $\mathrm{Re}(V_{ud}V_{us}^*)\mathrm{Im}(V_{ts}V_{td}^*)$, arising from K_S exchange, to full $\mathcal{J}$. Substituting all SM parameters, we obtain the following leading order result:

$$C_S(\mathrm{LO}) \simeq 5 \times 10^{-16}. \tag{2.14}$$

2.2.2 Next to leading order calculation

In order to estimate accuracy of the leading order (LO) $\sim O(m_s^{-1})$ result, one could try to evaluate the next-to-leading order (NLO) corrections in the expansion over small m_s. These corrections can be divided into two groups: A. corrections to the $K\bar{N}N$ vertex at $m_s \log m_s$ order, B. diagrams that do not reduce to the t-channel K-meson exchange. Type A corrections involve essentially same diagrams as those appearing in the corresponding corrections to the s-wave hyperon decays [60, 63]. The analysis of Ref. [63] showed that when the loop corrections are included with the tree-level a and b parameters and the total theoretical result is fit to experimental data, one notices that the tree level values for a and b come out smaller than in (2.9), while *total* result is rather close to the tree-level fit for a, b. This comes mostly from the renormalization of the meson and baryon wave functions. The lesson from this is that the corrections of type A for KNN weak coupling are expected to mirror results of Ref. [63] for s-wave amplitudes, and therefore would not deviate substantially from Eq. (2.10).

We then estimate type B corrections. It turns out that they parametrically dominate over other types of corrections, as the baryon pole diagrams, Fig. 2.2, contribute. The m_s scaling of these corrections is set by the ratio of the loop integral, proportional to m_K (at $m_K^2 \gg m_\pi^2$ limit), divided by mass splitting Δm_B in the baryon octet, *e.g.* $m_\Lambda - m_n$. This quantity scales as $m_s^{-1/2}$ and therefore these baryon pole diagrams

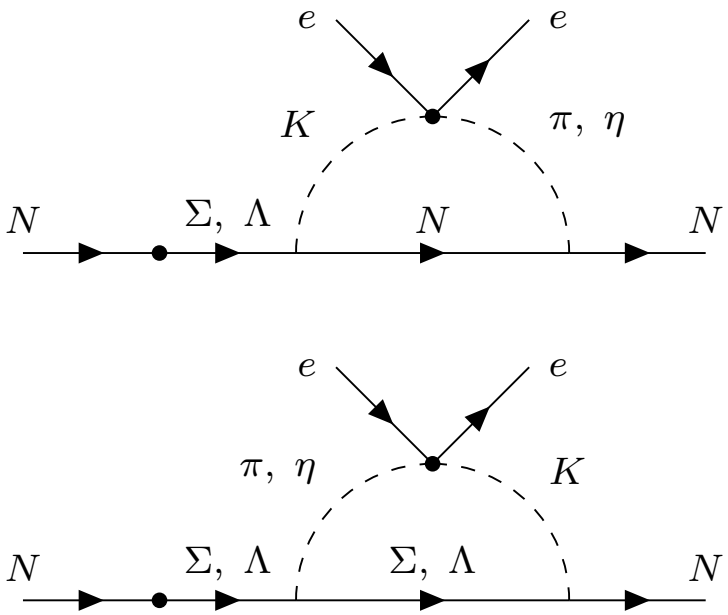

Figure 2.2: The baryon pole diagrams that contribute to C_S at the NLO level in the chiral limit. The left vertex is the nucleon-hyperon mixing induced by Eq. (2.8), while the top vertex is induced by Eq. (2.6). The vertices without black dots are the strong interaction with the coupling constants D and F. The diagrams with the nulceon-hyperon mixing on the right side give the same amount of contribution.

dominate the NLO contributions in the chiral limit. They are fully calculable (*i.e.* do not depend on unknown counterterms), and the result for these corrections are:

$$\frac{C_{S,NLO}(p)}{C_{S,LO}(p)} = \frac{m_K^3(0.77D^2 + 2.7DF - 2.3F^2)}{24\pi f_0^2(m_{\Sigma^+} - m_p)} \tag{2.15}$$

$$\begin{aligned}\frac{C_{S,NLO}(n)}{C_{S,LO}(n)} = \frac{m_K^3}{24\pi f_0^2}\Bigg(&\frac{(a/b+3)}{2\sqrt{6}(m_\Lambda - m_n)} \\ &\times(-0.44D^2 + 3.2DF + 1.3F^2) \\ +\frac{a/b-1}{2\sqrt{2}(m_{\Sigma^0} - m_n)}&\left(-0.53D^2 - 1.9DF + 1.6F^2\right)\Bigg).\end{aligned} \tag{2.16}$$

It has been obtained using heavy baryon chiral perturbation theory, and D, F are the coupling constants characterizing the strength of the $SU(3)$-invariant baryon-meson strong interaction, with $F = 0.46$, $D = 0.8$ typically used [60]. Since the dominant contribution comes from loops with $K-\pi$ transition, it is appropriate to take $f_0^2 \simeq f_\pi f_K$. Using these numbers, we discover that NLO corrections interfere constructively with LO, and give 30% correction for the proton, and 40% for the neutron, correspondingly.

Combining LO and NLO, we arrive at our final result,

$$C_S(\text{LO}+\text{NLO}) \simeq 6.9\times 10^{-16}$$
$$\Longrightarrow\ d_e^{\text{equiv}} \simeq 1.0\times 10^{-35}\, e\,\text{cm}. \tag{2.17}$$

The size of the NLO corrections also allows us to estimate the accuracy of this computation as $O(30\%)$.

As stated at the beginning of this chapter, this result is much larger than previously believed, and exceeds any contributions of d_e into d_e^{equiv} by at least four orders of magnitude. The enhancement of C_S at EW^3 order compared to EW^2EM^2 can be roughly ascribed to $\alpha_W/\alpha_{\text{EM}}^2 \sim O(10^3)$. We note that, although translating C_S to d_e^{equiv} depends on atoms/molecules that one considers (ThO above), this dependence is mild and d_e^{equiv} is within the same ballpark if we instead consider, *e.g.*, Tl or YbF [53].

Stepping away from chiral expansion, one can formulate the necessary hadronic matrix element that will be required to generate C_S in combination with the dominant $\text{Im}\mathcal{P}_{\text{EW}}$ channel of Eq. (2.3). The corresponding d-to-s transitions need to be taken in the first order, EW^1, that break P and C separately but conserve CP.

$$\langle N|i(\bar{s}\gamma_\mu(1-\gamma_5)d - \bar{d}\gamma_\mu(1-\gamma_5)s)|N\rangle_{\text{EW}^1} \tag{2.18}$$
$$= \frac{f_S}{m_N} i q_\mu \bar{N}N + \frac{f_T}{m_N} q_\nu \bar{N}\sigma_{\mu\nu}\gamma_5 N.$$

In this formula, q_μ stands for the momentum transfer. It turns out that there are only two form factors on the r.h.s. of this expression that have the same CP properties as the left-hand side. Moreover, f_T in combination with $\text{Im}\mathcal{P}_{\text{EW}}$ leads to CP-odd P-even interactions that do not induce EDMs. Therefore only f_S form factor (that sometimes is called induced scalar) at $q^2 \to 0$ is relevant. We have provided first two terms in the chiral expansion of f_S for neutrons and protons, so that effectively $f_S \propto a(b)\times m_N m_K^{-2} + ...$ While we use chiral perturbation theory, in principle, calculation of f_S can be attempted using lattice QCD methods.

Finally, we note that other semi-leptonic operators such as $\bar{e}e\bar{N}i\gamma_5 N$ that lead to nuclear-spin-dependent effects are not generated the same way at EW^3 order and therefore will be suppressed compared to (2.11).

2.3 Discussion

We have shown that $\delta_{\rm KM}$ induces the CP-odd electron nucleon interaction at the level much larger than previous estimates [53]. The main mechanism is not a two-photon exchange, $\mathrm{EW}^2\mathrm{EM}^2$, between electron and the nucleus, but the combination of weak non-leptonic EW^1 transition with the semileptonic EW^2 electroweak penguin. Although the result is still small, it is not unthinkable that the progress in sensitivity to paramagnetic EDMs may reach the level of $d_e^{\rm equiv}$ in the future. Indeed, some novel proposals [40] envision that statistical sensitivity to paramagnetic EDMs can be brought down to $d_e \sim O(10^{-35}\text{–}10^{-37})\, e\,\mathrm{cm}$.

It is not surprising that the C_S operator can be predicted, at least in the $SU(3)$ chiral expansion, rather precisely. This puts in clear distinction with $d_n(\delta_{\rm KM})$ estimate that carries an order of magnitude uncertainty with unclear prospects for improvement. In contrast, the only significant source of uncertainty in C_S is in the induced scalar form factor (2.18) that can be improved in the future with the use of lattice QCD methods.

Even if one takes chiral $SU(3)$ expansion sceptically, it is clear that unique m_s^{-1} (LO) and $m_s^{-1/2}$ (NLO) contributions to C_S identified in our work would not be cancelled - unless completely accidentally - by other contributions, mirroring a similar argument of [27] made for $d_n(\theta)$. Therefore, $10^{-35}\, e\,\mathrm{cm}$ should be adopted as the robust $\delta_{\rm KM}$-induced SM benchmark value for all experiments attempting the search of d_e using electron spins in heavy atoms and molecules. It also allows for establishing the *maximum* sensitivity to CP-violating New Physics via d_e. Taking a one-loop perturbative scaling, $d_e \propto (\alpha/\pi) m_e \Lambda_{\rm NP}^{-2}$, and equating it to $d_e^{\rm equiv}(\delta_{\rm KM})$ one arrives at the maximum scale that is possible to probe with paramagnetic EDMs: $\Lambda_{\rm NP}^{\rm max} \sim 5 \times 10^7\,\mathrm{GeV}$. Notice, however, that in models with no chiral m_e suppression of d_e and/or tree level C_S generation by new physics, the ultimate scale can be larger [64, 65].

Chapter 3

Calculation of θ-induced nucleon EDM with interpolating currents

Being the last undetected parameter in the SM, the smallness of the QCD θ term way below the natural level implied by QCD has been known as the strong CP-problem [21, 22]. A reliable determination of how a non-zero θ gives rise to experimental observables plays a crucial role in understanding the nature of this problem.

While the nonperturbative treatment of QCD in the hadronic regime is of course nontrivial, an important guide in elucidating the nature of θ-dependent observables is the strong violation of chiral symmetry in the nonet of pseudoscalar Nambu-Goldstone mesons, $m_{\eta'} \gg m_{\pi,\eta_8}$. The nonvanishing of $m_{\eta'}$ in the chiral limit, $m_{u,d,s} \to 0$, was identified in [66] as the necessary and sufficient condition for θ-dependence of physical observables. The dependence of the vacuum energy on θ (or equivalently the axion mass, if one promotes θ_G to a dynamical variable), the θ-induced CP-odd pion-nucleon coupling, and the electric dipole moments (EDMs) of nucleons, all rely on a finite m'_η in the chiral limit.

Among the nonperturbative approaches to θ-dependent observables, lattice QCD promises to provide a systematic approach to the computation of the neutron EDM, $d_n(\theta)$, but results thus far are inconclusive and the program is ongoing; for a partial list of relevant papers, see *e.g.* Refs. [30, 67–76]. Approaches using chiral perturbation theory show relatively stable answers for the leading IR-singular terms [27, 70, 77–79].

The QCD sum rule method, originating in Ref. [80], is conceptually much closer to lattice QCD, and has also been employed to calculate $d_n(\theta)$ [18, 29, 81, 82], with results consistent with chiral estimates, but slightly smaller numerically. Nucleon magnetic moments have also been found within this method to be in reasonable agreement with observations [83].

Given this situation, in this chapter we present a careful analysis of the chiral properties of the nucleon interpolating currents used in both lattice QCD and QCD sum rules, and to reassess the sum rules calculations of $d_n(\theta)$, as a concrete means of testing the symmetry-based constraints inferred from more general considerations. In this context, the sum rule approach, based on calculations of the operator product expansion (OPE) for hadronic current correlators in an external θ background, offers the advantage that many symmetries of the problem, such as chiral symmetry, and the chiral re-phasing invariance, can be made manifest at the quark-gluon level. These symmetries will allow us to determine physical choices for nucleon interpolating currents that ensure the required scaling of observables in the chiral limit.

3.1 The θ term and the chiral limit of θ-dependent observables

The physical θ angle, $\bar{\theta} = \theta_G + \theta_m$, includes the phase θ_G of the topological term $\mathcal{L} = \frac{\theta_G g_s^2}{32\pi^2} G^a_{\mu\nu} \widetilde{G}^{a\mu\nu}$ in QCD and the phase $\theta_m = \mathrm{ArgDet}\mathcal{M}_q$ of the quark mass matrix $\mathcal{M}_q$, and thus any physical dependence on θ necessarily vanishes in the chiral limit. This is conveniently observed within QCD itself by using the anomalous $U(1)_A$ symmetry to rotate away θ_G, so that the physical phase is captured entirely by a complex singlet mass term. Restricting to the case of two light flavours, this term has the form

$$\mathcal{L}_{m_*} = -m_* \bar{\theta} (\bar{u} i\gamma_5 u + \bar{d} i\gamma_5 d) + \frac{1}{2} m_* \bar{\theta}^2 (\bar{u}u + \bar{d}d) + \cdots , \tag{3.1}$$

where $m_* = m_u m_d/(m_u + m_d)$. It follows that any physical dependence on θ must vanish as $m_* \to 0$. This is immediately apparent in CP-even observables such as the topological susceptibility $d^2 E_{\mathrm{vac}}/d\bar{\theta}^2 = -m_* \langle 0|\bar{u}u + \bar{d}d|0\rangle$, and the θ-dependence of the nucleon mass $d^2 m_N/d\bar{\theta}^2 = -m_* \langle N|\bar{u}u + \bar{d}d|N\rangle$.

CP-odd observables of considerable phenomenological interest first arise at linear order in θ, such as nucleon EDMs and CP-odd pion nucleon couplings, and must also vanish in the $m_* \to 0$ limit. Our focus in this chapter will be on the properties of nucleon interpolating currents that are required to ensure this behaviour. For example, we can write the most general interpolating current for neutrons that just involves the leading quark fields and no derivatives as follows,

$$j_n^\beta(x) = j_1(x) + \beta j_2(x), \tag{3.2}$$

where β is a numerical coefficient, and the two currents with the quantum numbers of the neutron are given by $j_1(x)=2\epsilon_{ijk}(d_i^T \mathcal{C}\gamma_5 u_j)d_k$ and $j_2(x)=2\epsilon_{ijk}(d_i^T \mathcal{C} u_j)\gamma_5 d_k$ (see Sec. 3.2 for further details). The notation in (3.2) reflects the fact that only j_1 is nonzero in the nonrelativistic limit, and thus the value of β is apparently unimportant for generic observables in the neutron rest frame. However, the nonrelativistic limit for nucleons, encapsulated by the naive quark model, may not always be a good starting point for real life QCD, which corresponds to the limit of nearly massless quarks. This distinction proves to be important for CP-odd observables that are intrinsically sensitive to chirality-violating parameters such as m_*, and the choice of interpolating current deserves further scrutiny. Indeed, we will show below that only the choices $\beta = \pm 1$, namely

$$j_n^\pm(x) = j_1(x) \pm j_2(x), \tag{3.3}$$

are fully consistent when computing the leading dependence of observables on quantities, such as θ, that transform under the anomalous $U(1)_A$ symmetry. Other choices allow for an unphysical dependence of observables in the chiral limit. For example, we show that away from these two special points, nucleon current correlators depend explicitly on θ in the $m_* \to 0$ limit, in contradiction with (3.1).

Subtleties in the treatment of nucleon correlators in the chiral limit are well known, but are only important when studying chirally sensitive observables such as those dependent on θ. It was highlighted in [29] that in the presence of CP-violation, the coupling of the physical nucleon state (represented by a spinor v) to the nucleon interpolator acquires an additional unphysical phase α, where $\langle 0|j_n|N\rangle = \lambda e^{i\alpha_n\gamma_5/2}v$. This phase can mix magnetic and electric dipole structures, and complicates the extraction of physical

observables from two-point correlation functions. As we discuss below, one can consider special tensor structures from which the phase α_n decouples, such as $\{F \cdot \sigma\gamma_5, \not{p}\}$ as considered in [29], or explicitly calculate the phase as advocated for the specific approaches to computing $d_n(\theta)$ in lattice QCD [69]. The lack of chiral invariance for the generic nucleon interpolators also manifests in nontrivial mixing with CP-conjugate currents (denoted i_1 and i_2 in [29]), dependent on the unphysical combination $\theta_G - \theta_m$ orthogonal to $\bar{\theta}$. In this work, we will further argue that the chiral non-invariance of j_n^β leads in fact to a generic and unphysical dependence on θ in the chiral limit unless $\beta = \pm 1$.

We then proceed to systematically analyze the leading order results for the magnetic and electric dipole moments of nucleons using QCD sum rules for both consistent choices of the current interpolator $j_n^\pm$, extending earlier work [29, 82]. We report new results for the $\beta = -1$ choice finding that $d_n(\theta)$ is consistent, both in sign and magnitude, with earlier estimates of $d_n(\theta)$ using $\beta = +1$ [18, 29, 81, 82]. This analysis also allows us to directly relate $d_{n,p}$ to the nucleon magnetic dipole moment (MDM) $\mu_{n,p}$. From general principles, it is clear that one should expect the scaling $d_n \propto (\bar{\theta} m_*/m_n) \times \mu_n$, and determining a concrete coefficient in this relation is another goal of this chapter. Since $\mu_{n,p}$ are reproduced rather reliably in the QCD SR approach [83], and recently on the lattice [84], this may be considered as a useful/natural normalisation for the EDMs.

The remaining sections of this chapter are organized as follows. In Sec. 3.2, we define the nucleon interpolating currents, and illustrate their transformation under $U(1)_A$ in a general basis. We find that only the combinations $\beta = \pm 1$ transform covariantly. In Sec. 3.3, we consider the chiral $m_* \to 0$ limit, and demonstrate the unphysical dependence of correlation functions on θ in the chiral limit unless $\beta = \pm 1$. In Sec. 3.4, we generalize earlier calculations of the nucleon EDMs using QCD sum rules for both covariant choices of the interpolating current $j_{n,p}^\pm$, and use alternate channels sensitive to the magnetic moment to express EDMs in the ratio $d_{n,p}/\mu_{n,p}$. We conclude by discussing the implications of our results for calculations of θ-dependent observables, *e.g.* using the j_1 current, in Sec. 3.5.

3.2 Nucleon currents and chirality

In general, at lowest dimension, there are two independent nucleon interpolating currents (after applying the Fierz identity) that have the same quantum numbers as the nucleons:

$$j_1^a = 2\epsilon_{ijk}\left(d_i^T \mathcal{C}\gamma_5 u_j\right) q_k^a, \tag{3.4}$$

$$j_2^a = 2\epsilon_{ijk}\left(d_i^T \mathcal{C} u_j\right) \gamma_5 q_k^a, \tag{3.5}$$

where i, j, k are the color indices and $\mathcal{C}$ is the charge conjugate matrix that satisfies $(\gamma^\mu)^T\mathcal{C} = -\mathcal{C}\gamma^\mu$. The index "$a$" represents the isospin and $q^a = (u, d)^T$. We note that $d_i^T\mathcal{C}\gamma_5 u_j = u_j^T\mathcal{C}\gamma_5 d_i$ and $d_i^T\mathcal{C}u_j = u_j^T\mathcal{C}d_i$, and hence we can rewrite the currents as

$$j_1^a = \epsilon_{ijk}\left(q_i^{bT}\epsilon_{bc}\mathcal{C}\gamma_5 q_j^c\right) q_k^a, \tag{3.6}$$

$$j_2^a = \epsilon_{ijk}\left(q_i^{bT}\epsilon_{bc}\mathcal{C} q_j^c\right) \gamma_5 q_k^a, \tag{3.7}$$

where ϵ_{ab} is the anti-symmetric tensor with $\epsilon^{12} = +1$ and hence $\epsilon_{12} = -1$. This form makes it explicit that the diquark products inside the brackets are invariant under both chiral and vector $SU(2)$ transformations. This immediately leads to the conclusion that all linear combinations of the currents transform covariantly under the $SU(2)$ chiral and vector rotation.

Parametrizing a general linear combination of the two interpolation functions as

$$j_a^\beta = j_1^a + \beta j_2^a, \tag{3.8}$$

we see that for the special choices of $\beta = \pm 1$,

$$j_a^+ = 2\epsilon_{ijk}\left[-\left(q_{iL}^T\mathcal{C}q_{jL}\right) q_{kL}^a + \left(q_{iR}^T\mathcal{C}q_{jR}\right) q_{kR}^a\right], \tag{3.9}$$

$$j_a^- = 2\epsilon_{ijk}\left[\left(q_{iR}^T\mathcal{C}q_{jR}\right) q_{kL}^a - \left(q_{iL}^T\mathcal{C}q_{jL}\right) q_{kR}^a\right], \tag{3.10}$$

where we suppress the isospin indices of the quark products, and the subscripts "L/R" indicate the projections onto left-/right-handed components. This tells us that $j_a^\pm$ are covariant under the anomalous $U(1)_A$ transformation $q_i \to e^{i\theta_A\gamma_5}q_i$, while the current

j_a^β is not covariant under the $U(1)_A$ rotation for $\beta \neq \pm 1$.[1] In general, the current transforms as

$$j_a^\beta \to \frac{1+\beta}{2} e^{3i\theta_A\gamma_5} j_a^+ + \frac{1-\beta}{2} e^{-i\theta_A\gamma_5} j_a^- . \tag{3.11}$$

Note, in particular, that the current j_a^0 which contains the unique non-relativistic structure, and so is widely used in lattice QCD computations, does not transform covariantly under the $U(1)_A$ rotation.

We anticipate that this non-covariance for $\beta \neq \pm 1$ may complicate the extraction of physical quantities from nucleon correlators that depend sensitively on the realization of the anomalous chiral symmetry in QCD. To see this, recall that current correlators may be computed by introducing an external fermionic source term η_a, with

$$\mathcal{L}_\eta = \mathcal{L} + \bar{\eta}_a j_a^\beta + (\text{h.c.}), \tag{3.12}$$

where $\mathcal{L}$ is the original QCD Lagrangian (including CP-odd θ phases). The nucleon current correlator then follows from a second-order variation of action with respect to η_a. If j_a^β transforms covariantly under a $U(1)_A$ rotation, *i.e.* if $\beta = \pm 1$, we can preserve the anomalous $U(1)_A$ symmetry by re-absorbing the chiral phases in the source η_a. In other words, we can treat η_a as a spurion to render the Lagrangian, including the source term, invariant. On the other hand, if j_a^β does not transform covariantly under the $U(1)_A$ rotation, we cannot keep the whole Lagrangian, including the source term, invariant under the $U(1)_A$ rotation.[2] As a result, it is not guaranteed that the final correlators maintain the anomalous $U(1)_A$ symmetry of the original theory, for example being independent of the unphysical phase combination $\theta_G - \theta_m$. Nor does it guarantee the restoration of $\bar{\theta}$-independence in the chiral $m_* \to 0$ limit.[3] This consideration

[1] Here we call a current "covariant" if its transformation can be expressed as multiplying only a single chiral phase. In this sense, the currents $\beta \neq \pm 1$, including the one with $\beta = 0$, are not covariant since they are composed of two parts obtaining different chiral phases, $3\theta_A$ and $-\theta_A$. This notion of the (non-)covariance is essential for our discussion in the following.

[2] This naturally requires us to treat the external sources that couple to the $j_a^\pm$ components inside j_a^β separately. In other words, we are required to introduce two distinct sources, so that $\mathcal{L}_\eta = \mathcal{L} + \bar{\eta}_a^\pm j_a^\pm +$ (h.c.), to maintain the invariance. It then follows that the correlators are defined by the chiral covariant currents $j_a^\pm$.

[3] The approach introduced in [29,81] to account for leading-order mixing with CP-conjugate currents $i_1 = \gamma_5 j_2$ and $i_2 = \gamma_5 j_1$ removes dependence on $\theta_G - \theta_m$, but may still induce an unphysical $\bar{\theta}$ dependence

naturally invites us to use the covariant currents $j_a^{\pm}$.

In the rest of this chapter, we compute the nucleon correlators explicitly and confirm our general argument above; the unphysical phase $\theta_G - \theta_m$ in general shows up in the correlators of j_a^{β} with $\beta \neq \pm 1$, while only the physical combination $m_*\bar{\theta}$ appears in higher-point correlators of $j_a^{\pm}$ (after properly subtracting the chiral phase of the two-point function; see Sec. 3.4).

3.3 Nucleon correlators in the chiral limit

In Sec. 3.2, we have seen that the lowest dimension nucleon interpolation currents are in general not covariant under the $U(1)_A$ transformation, with the exception of two linear combinations, $j_a^{\pm}$ with $\beta = \pm 1$. In this section, we begin our investigation of the consequence of this non-covariance by taking the chiral limit, $m_q \to 0$, with m_*/m_q fixed. In this limit, from the general properties of QCD, all dependence on θ should disappear from physical quantities, as it can be rotated away by the $U(1)_A$ transformation of the quarks. Despite this general expectation, as we see below, unphysical dependence on θ remains in the correlators of the currents for general choices of β. The unphysical dependence disappears only for $\beta = \pm 1$, indicating that only these choices of currents produce physical results.

In the chiral limit, we take the QCD Lagrangian as

$$\mathcal{L} = \bar{q} i \not{D} q - \frac{1}{4} G^a_{\mu\nu} G^{a\mu\nu} + \frac{\theta_G \alpha_s}{8\pi} G^a_{\mu\nu} \tilde{G}^{a\mu\nu}, \tag{3.13}$$

where $\tilde{G}^{a\mu\nu} = \epsilon^{\mu\nu\rho\sigma} G^a_{\rho\sigma}/2$ with $\epsilon^{0123} = +1$. We define the electromagnetic part of the covariant derivative as $D_\mu = \partial_\mu + i e_q A_\mu$ with $e_u = 2e/3$ and $e_d = -e/3$. We have $e > 0$ with this convention. We define the nucleon correlator as

$$\Pi_n^{\beta}(p) = i \int d^4x \, e^{ip\cdot x} \langle 0 | \mathcal{T}\{ j_n^{\beta}(x), \bar{j}_n^{\beta}(0) \} | 0 \rangle. \tag{3.14}$$

In the following, we compute correlator structures corresponding to the nucleon mass and EDM in the presence of θ, employing the operator product expansion (OPE) with large $p^2 < 0$, as the first crucial step in constructing the QCD sum rule.

in the chiral limit unless $\beta = \pm 1$.

3.3.1 Nucleon mass

We begin our discussion with correlators that are often used for the calculation of the nucleon mass. We first note that, as argued above, we can rotate away the gluonic θ term via a $U(1)_A$ transformation, $q \to e^{i\theta_G m_* \gamma_5/2m_q} q$.[4] This indicates that we can write down the (color-diagonal) quark propagator in the presence of θ_G as

$$S_q(\theta_G) = e^{i\theta_G \gamma_5/4} S_q(\theta_G = 0) e^{i\theta_G \gamma_5/4}. \tag{3.15}$$

The massless quark propagator is given at leading order by

$$S_q(\theta_G = 0) = \frac{i\not{x}}{2\pi^2 x^4} - \frac{\langle \bar{q}q \rangle}{12}. \tag{3.16}$$

Here $\langle \bar{q}q \rangle$ is short-hand notation for the vacuum condensate of quarks, $\langle 0|\bar{q}q|0\rangle$. We then insert this expression into the nucleon correlator, simplify the Dirac matrix structures, and perform the Fourier transformation to momentum space. Correlators with an odd number of gamma-matrices, $\not{p}$ in this particular case, are explicitly θ-independent at leading order. However, chirality flipping Dirac structures, proportional to Dirac matrices $\mathbb{1}$ or γ_5, acquire θ-dependence. The leading order OPE terms are linear in the quark condensate and are given by:

$$\begin{aligned} \Pi_n^\beta\Big|_{\mathbb{1},\gamma_5} =& \frac{\langle \bar{q}q \rangle}{16\pi^2} p^2 \log\left(-\frac{p^2}{\mu^2}\right) \\ & \times (1-\beta)\left[6(1+\beta)e^{i\theta_G\gamma_5/2} + (1-\beta)e^{-i\theta_G\gamma_5/2}\right]. \end{aligned} \tag{3.17}$$

This is a generalization of a well known result [85, 86] for an arbitrary θ angle. A dual description of the same physics is achieved via a sum over nucleon states, including the excited states, $\propto \sum_i \lambda_i^2 e^{i\alpha_i\gamma_5}(\not{p} - m_i)^{-1} e^{i\alpha_i\gamma_5}$. We see that, if the currents are covariant, $\beta = \pm 1$, we have only one chiral phase.[5] We can then interpret the phase as the chiral phase of the nucleon states α_i that needs to be subtracted to obtain a physical result. In equivalent language, we can reabsorb this phase into the definition of the source η_a

[4] For brevity, in the rest of this subsection, we choose $m_u = m_d$ and thus $m_*/m_q = 1/2$ so that the chiral rotations of u, d quarks are pure $U(1)_A$ transformations.

[5] The correlator vanishes at this order for $\beta = +1$. One can repeat the computation at $\mathcal{O}(\langle \bar{q}q \rangle^3)$ and obtain the same conclusion that the correlator with $\beta = +1$ contains only one chiral phase.

so that the nucleon mass correlator does not depend on θ.

On the other hand, if the currents are not covariant, $\beta \neq \pm 1$, the correlator contains two chiral phases, $e^{\pm i\theta_G\gamma_5/2}$, and we cannot absorb both phases in the overall chiral phase of the nucleon state. We may choose the phase so that it absorbs the term linear in θ_G, but the term quadratic in θ_G remains. This would lead to the erroneous conclusion that the nucleon mass should acquire θ^2-dependent contributions in the $m_* \to 0$ limit, which is entirely an artifact of using non-covariant currents. For instance, for $\beta = 0$, the correlator can be expressed as

$$\Pi_n^0\big|_{\mathbb{1},\gamma_5} \propto e^{5i\gamma_5\theta_G/28}\left(1 - \frac{3}{49}\theta_G^2 + \cdots\right)e^{5i\gamma_5\theta_G/28}, \tag{3.18}$$

where the dots indicate higher order terms in θ_G. We may absorb the phase $e^{5i\gamma_5\theta_G/28}$ into the nucleon state, but the terms in the bracket, including the term of order θ_G^2, will still contribute to the chirality flipping structure. Therefore, if we use this expression to estimate the nucleon mass, we obtain an unphysical dependence on θ even in the chiral limit. This is inconsistent with the general constraint following from Eq. (3.1), indicating that the calculation based on the non-covariant currents, in general, is flawed. At a technical level, this occurs because the nucleon currents away from $\beta = \pm 1$ contain "built-in" flips of the quark chiralities $q_L \leftrightarrow q_R$ that persist in the chiral limit.

3.3.2 Nucleon EDM

In the above subsection, we have seen that the nucleon mass term acquires unphysical dependence on θ in the chiral limit for general $\beta \neq \pm 1$. This raises concerns about the use of *e.g.* the "non-relativistic" $\beta = 0$ current for calculation of any θ-dependent nucleon observable. We should anticipate similar issues for CP-odd operators such as nucleon EDMs that are intrinsically sensitive to the θ-phases, and we indeed confirm this expectation below. In the following, we again focus on the chirality flipping part, as used in lattice QCD calculations of the neutron EDM [67–76].

In the chiral limit, with a background electromagnetic field, the quark propagator

is given by

$$S_q = \frac{i\not{x}}{2\pi^2 x^4} - \frac{\langle\bar{q}q\rangle}{12}\left(1 + i\gamma_5\theta_G\frac{m_*}{m_q}\right) - \frac{\tilde{\chi}_q}{24}F\cdot\sigma\left(1 + i\gamma_5\theta_G\frac{m_*}{m_q}\right), \tag{3.19}$$

where we have restored the dependence on m_*/m_q for clarity, $F\cdot\sigma = F_{\mu\nu}\sigma^{\mu\nu}$, and the vacuum condensate in the presence of the external electromagnetic field is parametrized as $\langle\bar{q}\sigma_{\mu\nu}q\rangle_F = \chi_q F_{\mu\nu}\langle\bar{q}q\rangle = \tilde{\chi}_q F_{\mu\nu}$. The quantity χ_q is the so-called magnetic susceptibility of the QCD vacuum introduced in [83], while $\tilde{\chi}_q$ is introduced here for brevity. By focusing on the chirality flipping structures relevant to the sum rule (see the discussion around Eq. (3.45) below) and retaining only the leading singular part, the correlator in the external field is given by

$$\Pi_n^\beta\Big|_{\{\not{p},\{\not{p},F\cdot\sigma/2\}\}} = -\frac{(1-\beta)^2\tilde{\chi}_u}{96\pi^2}\log\left(-\frac{p^2}{\mu^2}\right), \tag{3.20}$$

$$\Pi_n^\beta\Big|_{\{\not{p},\{\not{p},iF\cdot\sigma\gamma_5/2\}\}} = -\theta_G\frac{(1-\beta)^2\tilde{\chi}_u}{96\pi^2}\frac{m_*}{m_u}\log\left(-\frac{p^2}{\mu^2}\right), \tag{3.21}$$

Notice that the dependence on the unphysical phase θ does not disappear in this expression.

In the context of lattice computations of the neutron EDM, Refs. [69, 72] have proposed canceling the spurious phase by subtracting the corresponding phase computed via the two-point function (representing the chiral phase of the nucleon state), α_n^β, from the phase of the three-point function. The chirality flipping part of the two-point function was computed in (3.17), and upon linearization in θ takes the following form,

$$\Pi_n^\beta\Big|_{\mathbb{1},\gamma_5} = \frac{\langle\bar{q}q\rangle}{16\pi^2}p^2\log\left(-\frac{p^2}{\mu^2}\right)(1-\beta) \times\left[7 + 5\beta + i\gamma_5\theta_G\left(6(1+\beta)\frac{m_*}{m_d} - (1-\beta)\frac{m_*}{m_u}\right)\right], \tag{3.22}$$

where we retain only the leading-order terms with the logarithm. From this expression,

we can read off the chiral phase, acting on the nucleon mass operator, as

$$\alpha_n^\beta = \left[\frac{6(1+\beta)}{7+5\beta}\frac{m_*}{m_d} - \frac{1-\beta}{7+5\beta}\frac{m_*}{m_u}\right]\theta_G. \tag{3.23}$$

Following [69, 72], we may subtract this chiral phase from the three-point function to obtain

$$\begin{aligned}\Pi_n^\beta\Big|_{\{\not{p},\{\not{p},iF\cdot\sigma\gamma_5/2\}\}} + \alpha_n^\beta \times \Pi_n^\beta\Big|_{\{\not{p},\{\not{p},F\cdot\sigma/2\}\}} \\ = -\frac{\tilde{\chi}_u\theta_G}{16\pi^2}\log\left(-\frac{p^2}{\mu^2}\right)\times\frac{(1-\beta)^2(1+\beta)}{7+5\beta},\end{aligned} \tag{3.24}$$

where we note the minus sign arising from commuting γ_5 with $\not{p}$, resulting in $+\alpha_n^\beta$ instead of $-\alpha_n^\beta$ in the first line.

As one can observe, the removal of the unphysical phase does not occur in the EDM correlator for a generic choice β. Since physical quantities must be independent of θ in the chiral limit, it appears that the procedure outlined in [69, 72] requires the use of $\beta = \pm 1$ currents to ensure the cancelation of spurious θ-dependence in nucleon EDMs.

3.4 EDM and MDM sum rules for $\beta = \pm 1$

Thus far we have seen that calculations based on the non-covariant currents generically induce spurious θ dependence even in the chiral limit. As discussed in Sec. 3.2, the interpolation functions with $\beta = \pm 1$ are covariant under the $U(1)_A$ transformation. This property allows us to define two distinct procedures to obtain correlators invariant under the $U(1)_A$ transformation and thus free from unphysical θ dependence:

- Use the chirality conserving structure (with an odd number of γ_μ) in the correlator.
- Use the chirality flipping structure (with an even number of γ_μ) in the correlator, and subtract the chiral phase computed from the two-point correlator.

The former procedure was originally proposed in [29], as dependence on the chiral phase θ_A automatically cancels due to the gamma-matrix identity:

$$e^{i\alpha\gamma_5}(\text{odd number of }\gamma_\mu)e^{i\alpha\gamma_5} = \text{odd number of }\gamma_\mu. \tag{3.25}$$

As a result, the EDM correlator structure proportional to $\{F\cdot\sigma\gamma_5, \not{p}\}$ is guaranteed to depend only on the physical combination $m_*\bar{\theta}$, and unphysical phases do not make an appearance for $\beta = \pm 1$. This method makes it possible to calculate EDM correlators without the need to consider the two-point functions and rotation angles α_n. For a generic choice of β, Ref. [29] suggested to add the specific admixture of CP-rotated currents (i_1, i_2) that restore the invariance under the $U(1)_A$ rotation in this channel and guarantee $m_*\bar{\theta}$-proportionality of the OPE.

The second procedure (using the channel with an even number of γ_μ) has been applied in lattice QCD computations of the neutron EDM [69, 72], with the $\beta = 0$ current choice. We would like to follow this path and calculate EDMs in the channel with an even number of γ matrices, but with the important observation that we must use the covariant currents $\beta = \pm 1$ to ensure physical dependence on $\bar{\theta}$. Since the currents are covariant, the two- and three-point functions obtain the same chiral phase after performing the chiral rotation of the quarks, and hence their difference is guaranteed to be independent of the $U(1)_A$ rotation angle. This, again, leads to the dependence only on the physical combination $m_*\bar{\theta}$.

In the following, we confirm that the neutron EDM indeed depends only on the physical combination $m_*\bar{\theta}$ for both procedures, based on the QCD sum rule technique. Moreover, we observe that results obtained this way are consistent between the two different channels, using tensor structures with odd and even numbers of γ matrices.

We focus on the terms up to linear order in m_q and the θ-angles, and begin from the QCD Lagrangian

$$\begin{aligned}\mathcal{L} &= \bar{q}\left[i\not{D} - m_q\right] q \\ &\quad - \frac{1}{4}G^a_{\mu\nu}G^{a\mu\nu} - \theta_m m_* \bar{q} i\gamma_5 q + \frac{\theta_G \alpha_s}{8\pi} G^a_{\mu\nu}\tilde{G}^{a\mu\nu}.\end{aligned} \tag{3.26}$$

Following the QCD sum rule approach, we compute the correlator of the nucleon interpolation current, given by

$$\Pi_n^{\pm}(p) = i\int d^4x\, e^{ip\cdot x}\langle 0|\mathcal{T}\{j_n^{\pm}(x), \bar{j}_n^{\pm}(0)\}|0\rangle, \tag{3.27}$$

based on the OPE (the relevant diagrams are shown in Fig. 3.1), and compare it with

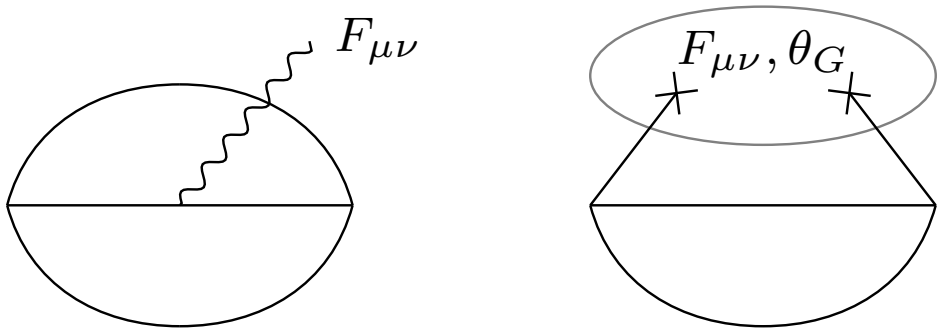

Figure 3.1: Diagrams that induce the nucleon MDM and EDM in the nucleon correlator (3.27) with an external electromagnetic field. For $\beta = +1$, the first diagram generates the MDM while the second diagram induces the EDM at the leading order. For $\beta = -1$, the MDM and EDM receive contributions from both diagrams. The dependence on θ_G arises from the vacuum condensate as indicated, while the dependence on θ_m comes from the mass dependence of the quark propagator and the equation of motion.

the phenomenological expression to extract the nucleon MDM and EDM. To avoid sensitivity to IR divergences, it is convenient to use the first procedure (using chirality conserving structures) for $\beta = +1$, and the second procedure (using chirality flipping structures) for $\beta = -1$, respectively. We discuss each of them in the following subsections.

3.4.1 Sum rules for $\beta = +1$

We begin with the QCD sum rules of the neutron MDM and EDM for $\beta = +1$ and focus on the chirality conserving part, as in [29, 81, 82]. Since the current with $\beta = +1$ is covariant, the chiral phase automatically cancels when we focus on the chirality conserving structure, leading to the dependence only on the physical combination $m_*\bar{\theta}$, as shown in the following.

In this case, Eq. (3.9) tells us that only the chirality conserving part of the quark propagator contributes to the correlator, and hence we can take

$$S_q = \frac{i\not{x}}{2\pi^2 x^4} - \frac{ie_q}{8\pi^2}\frac{x^\mu}{x^2}\tilde{F}_{\mu\nu}\gamma^\nu\gamma_5 - \frac{i\tilde{\chi}_q}{24}m_*\bar{\theta}x^\mu F_{\mu\nu}\gamma^\nu\gamma_5, \tag{3.28}$$

where we keep only the leading order terms contributing to the MDM and EDM. Note that only the physical combination $m_*\bar{\theta}$ appears in this expression since the chirality

conserving part does not depend on the spurious chiral phase. As explained in App. B.1, the relevant part of the correlator can be written as follows,

$$\Pi_n^+ = \frac{4e_d - e_u}{64\pi^4} p^2 \log\left(-\frac{p^2}{\mu^2}\right) \{\not{p}, F\cdot\sigma\} - \frac{4\tilde{\chi}_d - \tilde{\chi}_u}{16\pi^2} m_* \bar{\theta} \log\left(-\frac{p^2}{\mu^2}\right) \{\not{p}, iF\cdot\sigma\gamma_5\}\,, \tag{3.29}$$

where we retain only the leading parts relevant for a Borel transformation. The transformed correlator is given by

$$\mathcal{B}\left[\Pi_n^+\right]_{\{\not{p},F\cdot\sigma\}} = -\frac{4e_d - e_u}{64\pi^4} M^2, \tag{3.30}$$

$$\mathcal{B}\left[\Pi_n^+\right]_{\{\not{p},iF\cdot\sigma\gamma_5\}} = \frac{4e_d - e_u}{16\pi^2} m_* \bar{\theta}\chi\langle\bar{q}q\rangle, \tag{3.31}$$

where the subscripts denote the corresponding Dirac structures and we assume $\chi_q = e_q\chi$. Remarkably, both the MDM and EDM depend on the linear combination, $4e_d - e_u$, that appears in the constituent quark model.[6] On the phenomenological side of QCD sum rules, we represent the correlator, with a sum over hadron resonances and a continuum. For our leading order estimates below, we can neglect the continuum and single pole contributions, concentrating only on the leading nucleon double pole terms associated with the neutron ground state:

$$\Pi_n^+ = -\frac{|\lambda_n|^2 m_n}{2(p^2 - m_n^2)^2}\left[\mu_n\{\not{p}, F\cdot\sigma\} + d_n\{\not{p}, iF\cdot\sigma\gamma_5\}\right]. \tag{3.32}$$

This expression includes both the MDM and EDM terms, and λ_n denotes the coupling to the neutron state, $\langle 0|j_n^\pm|n\rangle = \lambda_n v$, up to an overall phase [29] which as noted above cancels in the chirality conserving channel. After the Borel transformation we obtain,

$$\mathcal{B}\left[\Pi_n^+\right]_{\{\not{p},F\cdot\sigma\}} = -\frac{|\lambda_n|^2 m_n}{2M^4}\mu_n e^{-m_n^2/M^2}, \tag{3.33}$$

$$\mathcal{B}\left[\Pi_n^+\right]_{\{\not{p},iF\cdot\sigma\gamma_5\}} = -\frac{|\lambda_n|^2 m_n}{2M^4} d_n e^{-m_n^2/M^2}. \tag{3.34}$$

[6] This property of the EDM correlator was noted in [29], while here we note that the same property holds for the MDM.

Taking the ratio to eliminate λ_n, we obtain

$$d_n = -\mu_n m_* \bar{\theta} \frac{4\pi^2 \chi \langle \bar{q} q \rangle}{M^2}. \tag{3.35}$$

As advertised, this result indeed depends only on the physical combination $m_* \bar{\theta}$, as required.

In writing the estimate in the form (3.35), relating d_n to μ_n, one should also make sure that the estimate for the MDM is reasonably close to its measured value. Normalizing the MDM expression (3.33) using the sum rule for $\not{p}$ to eliminate λ_n, one obtains the following expressions:

$$\mu_n = \frac{2}{m_n} \times \left(\frac{4}{3} e_d - \frac{1}{3} e_u \right); \quad \frac{\mu_n}{\mu_p} = -\frac{2}{3}. \tag{3.36}$$

The observed ratio of MDM is, famously, in agreement with the $-2/3$ value that follows from the constituent quark model and is also obtained using QCD sum rules at $\beta = +1$.

The magnitudes of $\mu_{n,p}$ at leading order are within 50% of the observed values. For example, for the neutron the prediction is $-8/3 = -2.67$ in units of the nuclear Bohr magneton, while the observed value is -1.91. The estimate (3.36) can be improved further upon the inclusion of the subleading OPE terms in both the MDM and $\not{p}$ channels. The subleading terms include gluon and quark condensate corrections. While the quark condensate corrections explicitly vanish for $\beta = +1$, the inclusion of the gluon corrections for the $\not{p}$ (see [86] and references therein) and MDM structures, calculated here, lead to the result:

$$\frac{\mu_n}{e/(2m_n)} = -\frac{8}{3} \times \frac{1 + \frac{b}{24M^4}}{1 + \frac{b}{4M^4}} \simeq -2.05 \text{ at } M = m_n. \tag{3.37}$$

Here $b \equiv (2\pi)^2 \langle (\alpha_s/\pi) G^a_{\mu\nu} G^a_{\mu\nu} \rangle \sim 1.2\,\text{GeV}^4$ parametrizes the strength of the gluon vacuum condensate. This result is indeed remarkably close to the observed value of the MDM, and the corrections do not spoil the $-2/3$ prediction for μ_n/μ_p. Therefore, we can be confident that the $\beta = +1$ sum rules perform at least as well as the $\beta = -1$ sum rules [83] in the MDM channel.

To obtain a numerical estimate for the EDM, we re-write the above result in terms

of the pion mass,

$$F_\pi^2 m_\pi^2 = -(m_u + m_d)\langle \bar{q}q \rangle, \tag{3.38}$$

with $F_\pi \simeq 93\,\text{MeV}$ as this reduces the dependence on the normalization scale,

$$d_n = \mu_n \bar{\theta} m_\pi^2 \times \frac{m_u m_d}{(m_u + m_d)^2} \frac{4\pi^2 \chi F_\pi^2}{M^2}. \tag{3.39}$$

Taking the Borel normalization scale to be $M = m_n$, with $m_u/m_d = 0.48$, leads to the result

$$d_n|_{\beta=+1} \simeq 2 \times 10^{-16}\, e\,\text{cm} \times \bar{\theta} \times \left(\frac{|\chi|}{6\,\text{GeV}^{-2}} \right). \tag{3.40}$$

Although this is a leading order estimate, it is consistent with the result obtained in [29] which accounts for higher-order terms. Notably, its value is sensitive to the magnetic susceptibility χ of the QCD vacuum. Initial estimates [83,87] put the value of χ close to $-6\,\text{GeV}^{-2}$ ($-5.7 \pm 0.6\,\text{GeV}^{-2}$ [87]), while later work based on considerations of the chiral anomaly in asymmetric kinematics and the pion pole dominance [88], estimates this quantity to be $\chi \sim -N_c/(4\pi^2 F_\pi^2) \simeq -9\,\text{GeV}^{-2}$. One should also note that available lattice studies [89] have found this quantity to be a factor of 2-to-3 smaller than Refs. [83,87], albeit with a higher normalization scale. Therefore, we conclude that the value of χ still provides the leading source of numerical uncertainty.

Finally, for completeness, we also note that the proton EDM in this approach is obtained by replacing $n \to p$ and $u \leftrightarrow d$, and is numerically $d_p(\bar{\theta}) = (-3/2) \times d_n(\bar{\theta})$.

3.4.2 Sum rules for $\beta = -1$

We next consider the sum rules for the neutron MDM and EDM using $\beta = -1$ and focusing on the chirality flipping structure. Following Ioffe [85], this is the most widely used current in the QCD SR literature, including the MDM analysis of Ref. [83]. However, the EDM has not previously been computed using this channel, or with this choice of current. In this approach, the unphysical chiral phase does not automatically cancel in the three-point function (that depends on $F_{\mu\nu}$), but can be subtracted by computing it directly from the two-point function (that does not depend on $F_{\mu\nu}$). Since j_a^- is covariant under the $U(1)_A$ transformation, this subtraction procedure [69,72] defines a quantity that is invariant under the $U(1)_A$ transformation, leading to dependence only

on the physical combination $m_*\bar{\theta}$.

The relevant part of the quark propagator is given by

$$\begin{aligned} S_q = & \frac{i\not{x}}{2\pi^2 x^4} \\ & - \frac{m_q}{4\pi^2 x^2}\left(1 - i\gamma_5\theta_m\frac{m_*}{m_q}\right) - \frac{\langle\bar{q}q\rangle}{12}\left(1 + i\gamma_5\theta_G\frac{m_*}{m_q}\right) \\ & - \frac{ie_q}{8\pi^2}\frac{x^\mu}{x^2}\tilde{F}_{\mu\nu}\gamma^\nu\gamma_5 - \frac{\tilde{\chi}_q}{24}F\cdot\sigma\left(1 + i\gamma_5\theta_G\frac{m_*}{m_q}\right) \\ & + \frac{e_q m_q}{32\pi^2}\log\left(-\mu_{\mathrm{IR}}^2 x^2\right)F\cdot\sigma\left(1 - i\gamma_5\theta_m\frac{m_*}{m_q}\right). \end{aligned} \tag{3.41}$$

Notice that for the final term, the propagator perturbed by both m_q and $F_{\mu\nu}$, is sufficiently infrared-singular to necessitate the introduction of the corresponding cutoff μ_{IR}. As described above, we first compute the chiral phase of the two-point function (see App. B.2), given by

$$\begin{aligned} \Pi_n^-\big|_{\mathbb{1},\gamma_5} = & \frac{\langle\bar{q}q\rangle}{4\pi^2}\left(1 - i\gamma_5\theta_G\frac{m_*}{m_u}\right)p^2\log\left(-\frac{p^2}{\mu^2}\right) \\ & - \frac{m_u}{32\pi^4}\left(1 + i\gamma_5\theta_m\frac{m_*}{m_u}\right)p^4\log\left(-\frac{p^2}{\mu^2}\right), \end{aligned} \tag{3.42}$$

where the subscript denotes the Dirac structures we focus on. By performing the Borel transformation, we obtain

$$\begin{aligned} \mathcal{B}\left[\Pi_n^-\right]_{\mathbb{1},\gamma_5} = & -\frac{\langle\bar{q}q\rangle M^2}{4\pi^2}\left(1 - i\gamma_5\theta_G\frac{m_*}{m_u}\right) \\ & + \frac{m_u M^4}{16\pi^4}\left(1 + i\gamma_5\theta_m\frac{m_*}{m_u}\right). \end{aligned} \tag{3.43}$$

From this expression, we extract the chiral phase α_n^- as

$$\alpha_n^- = -\frac{m_*}{m_u}\theta_G - \frac{m_* M^2}{4\pi^2\langle\bar{q}q\rangle}\bar{\theta}. \tag{3.44}$$

Note that the first term depends on both the physical and unphysical combinations of the phases, $2\theta_G = \bar{\theta} + (\theta_G - \theta_m)$.

To compute the external field dependent three-point function, we note that the

correlator on the phenomenological side of the sum rule takes the form

$$\not{p}F\cdot\sigma\not{p}+m_n^2F\cdot\sigma=\frac{1}{2}\left\{\not{p},\{\not{p},F\cdot\sigma\}\right\}-(p^2-m_n^2)F\cdot\sigma, \tag{3.45}$$

for the MDM, and $F\cdot\sigma$ is replaced by $iF\cdot\sigma\gamma_5$ for the EDM. Therefore, to focus on the double-pole contributions, we consider the Dirac structures $\{\not{p},\{\not{p},F\cdot\sigma/2\}\}$ for the MDM and $\{\not{p},\{\not{p},iF\cdot\sigma\gamma_5/2\}\}$ for the EDM, respectively [83]. We denote the former structure as "μ" and the latter as "$\tilde{d}$" for brevity, with the tilde indicating that the latter quantity is computed *before* subtracting the chiral phase. As explained in App. B.2, these structures are given by

$$\begin{aligned}\Pi_n^-|_\mu=&-\frac{\tilde{\chi}_u}{24\pi^2}\log\left(-\frac{p^2}{\mu^2}\right)\\&+\frac{m_u}{32\pi^4}\left[e_uI(p^2)+e_d\log\left(-\frac{p^2}{\mu^2}\right)\right],\end{aligned} \tag{3.46}$$

for the MDM, and

$$\begin{aligned}\Pi_n^-|_{\tilde{d}}=&-\frac{\tilde{\chi}_u}{24\pi^2}\frac{m_*\theta_G}{m_u}\log\left(-\frac{p^2}{\mu^2}\right)\\&-\frac{m_*\theta_m}{32\pi^4}\left[e_uI(p^2)+e_d\log\left(-\frac{p^2}{\mu^2}\right)\right],\end{aligned} \tag{3.47}$$

for the EDM (before the chiral phase subtraction), where $I(p^2)$ is a function that encodes both UV and IR divergences, given explicitly as $I(p^2;\epsilon_{\rm IR},\epsilon_{\rm UV})$ in [3]. Here we only require its Borel transform, given by

$$\mathcal{B}[I(p^2)]=\log\left(\frac{M^2}{\mu_{\rm IR}^2}\right). \tag{3.48}$$

We then obtain

$$\mathcal{B}\left[\Pi_n^-\right]_\mu=\frac{\tilde{\chi}_u}{24\pi^2}+\frac{e_um_u}{32\pi^4}\left[\log\left(\frac{M^2}{\mu_{\rm IR}^2}\right)-\frac{e_d}{e_u}\right], \tag{3.49}$$

$$\mathcal{B}\left[\Pi_n^-\right]_{\tilde{d}}=\frac{\tilde{\chi}_u}{24\pi^2}\frac{m_*}{m_u}\theta_G-\frac{e_um_*\theta_m}{32\pi^4}\left[\log\left(\frac{M^2}{\mu_{\rm IR}^2}\right)-\frac{e_d}{e_u}\right]. \tag{3.50}$$

Although the second term in Eq. (3.49) is subdominant for the nucleon MDM, it is important to obtain the physical combination, $m_*\bar{\theta}$, for the nucleon EDM after subtracting the chiral phase. Also, we distinguish $e_u \log\left(M^2/\mu_{\rm IR}^2\right)$ and e_d since they depend on different charges.

By subtracting the chiral phase α_n^- from the three-point functions, we obtain

$$\begin{aligned}\mathcal{B}\left[\Pi_n^-\right]_d &\equiv \mathcal{B}\left[\Pi_n^-\right]_{\tilde{d}} + \alpha_n^- \times \mathcal{B}\left[\Pi_n^-\right]_\mu \\ &= -\left[\frac{\chi_u M^2}{96\pi^4} + \frac{e_u}{32\pi^4}\left(\log\left(\frac{M^2}{\mu_{\rm IR}^2}\right) - \frac{e_d}{e_u}\right)\right] m_*\bar{\theta},\end{aligned} \tag{3.51}$$

where we again note the minus sign arising from commuting γ_5 with $\not{p}$, resulting in $+\alpha_n^-$ instead of $-\alpha_n^-$ in the first line. Notice that this now depends only on the physical combination, $m_*\bar{\theta}$, as expected. On the phenomenological side of the sum rule, we have

$$\Pi_n^- = -\frac{|\lambda_n|^2}{4(p^2-m_n^2)^2}\left\{\not{p}, \left\{\not{p}, F\cdot\sigma\left(\mu_n + i\gamma_5 d_n\right)\right\}\right\}, \tag{3.52}$$

for the MDM and EDM parts, where it is understood that this correlator holds *after* rotating away the unphysical chiral phase. Therefore we obtain our final result, after re-expressing $|\lambda_n|^2$ via the sum rule for the MDM,

$$d_n = -\mu_n m_*\bar{\theta}\left[\frac{M^2}{4\pi^2\langle\bar{q}q\rangle} + \frac{3}{4\pi^2\chi\langle\bar{q}q\rangle}\left(\log\left(\frac{M^2}{\mu_{\rm IR}^2}\right) - \frac{e_d}{e_u}\right)\right], \tag{3.53}$$

where we denoted $\chi_u = e_u\chi$.

We note the following qualitative features of this result:

- As stated above, we see that the use of the covariant $\beta = -1$ current automatically leads to the correct dependence of EDM on $m_*\bar{\theta}$.

- The $M^2/(4\pi^2\langle\bar{q}q\rangle)$ term in (3.53) results from the extraction of the α_n^- phase, and interferes destructively with the remaining terms. Using the leading order sum rule for the nucleon mass, $m_n M^2 = -8\pi^2\langle\bar{q}q\rangle$, known as the Ioffe formula approximation, this term can be rewritten as $-2/m_n$.

- Dependence on the infrared regulator $\mu_{\rm IR}$ means that the $\beta = -1$ result (3.53) is less precise than for $\beta = +1$ due to the breakdown of the OPE. In particular, it

is doubtful that using the scale separation one can calculate next-to-leading order corrections to (3.53) without encountering power-like sensitivity to infrared scales.

- The factor of m_* in the numerator and $\langle\bar{q}q\rangle$ in the denominator form a combination that is far more sensitive to the normalization scale than the $\beta = +1$ result in Eq. (3.39).

With the caveats above, one can still make a parametric estimate of the EDM, by tentatively taking $M \sim 1\,\text{GeV}$, $\mu_{\text{IR}} \sim 0.3\,\text{GeV}$, and $\langle\bar{q}q\rangle \simeq -(0.225\,\text{GeV})^3$. Depending on the assumed value for χ, that now enters in the denominator, numerical values for the EDM are in the range

$$d_n|_{\beta=-1} \sim (0.5-1.5) \times 10^{-16}\, e\,\text{cm} \times \bar{\theta}. \tag{3.54}$$

This result for the EDM indicates that we obtain the same sign for both $\beta = +1$ and $\beta = -1$ channels. This sign is also consistent with the chiral calculation, assuming the dominance of the chirally-enhanced $\log m_\pi$ contributions. The upper range of (3.54) is for smaller values of $\chi \sim -3\,\text{GeV}^{-2}$, at which point the $\beta = +1$ and $\beta = -1$ values for the EDM are approximately the same, and about two times smaller than chiral estimates for the $\log m_\pi$ contributions.

Finally, the proton EDM for $\beta = -1$ is again obtained by replacing $n \to p$ and $u \leftrightarrow d$, and is numerically $d_p(\bar{\theta}) \sim -(2.5-4) \times d_n(\bar{\theta})$, where the range is mainly driven by the uncertainty in χ.

3.5 Discussion

The physical hadronic effects induced by the QCD vacuum angle $\bar{\theta}$ are subtle and depend sensitively on quantities that break chiral symmetry. Indeed, any matrix elements that depend on $\bar{\theta}$ also depend on m_q, rendering the quantitative impact at the per mille level when the quark mass is properly normalized on the hadronic mass, $m_*/m_n \sim O(10^{-3})$. This property follows directly from the QCD Lagrangian and the action of the anomalous $U(1)_A$ symmetry, but its implementation within modern methods that address hadronic/nucleon physics is far from straightforward.

Among a multitude of leading dimension nucleon interpolating currents j_a^β parametrized by the angle β, only the choices $\beta = \pm 1$ correspond to currents that transform covariantly under chiral rotations, *i.e.* preserving the same structure of the current, and acquiring an overall $e^{i\gamma_5 \times \text{phase}}$ phase. Importantly, one can then show that correlators of the corresponding currents $\Pi_n^\pm$ have the correct chiral properties and depend only on the physical combination $m_* \bar{\theta}$ for $m_* \ll m_n$, with $\theta_G + \theta_m = \bar{\theta}$.

Conversely, we exhibited problematic features of correlators computed using other choices of currents, and in particular the $\beta = 0$ choice often used in lattice QCD computations. The leading order OPE terms, that were calculated both for the two- and three-point functions, retain their θ dependence even in the chiral limit, $m_q \to 0$. This is because these currents, away from the $\beta = \pm 1$ point, contain spurious $q_L \leftrightarrow q_R$ chirality flips built into the interpolators that retain the phase dependence upon chiral rotations. Technically this manifests in the non-covariant transformation properties of such currents, and as a consequence $\Pi_n^{\beta \neq \pm}$ correlators retain unphysical phases dependence both in the mass and EDM/MDM channels even in the $m_q \to 0$ limit. While these calculations are performed in the leading order of the OPE, it is nevertheless clear that this problem is a consequence of symmetries and not specific to this regime. As lattice QCD calculations approach the sensitivity required to see the physical effects of $\bar{\theta}$, use of the $\beta = \pm 1$ interpolating currents will ensure that the appropriate chiral extrapolation is under control. It is also worth emphasizing that the chiral covariance problem discussed here is unique to the $U(1)_A$ transformation. In contrast, $SU(2)$ chiral rotations, of the form $\exp(i\gamma_5 \tau^a \phi^a)$, will always result in a covariant transformation of all currents, due to the invariance of the diquark structure. Therefore, calculations of nucleon properties in the *e.g.* constant pion field background should produce physical results regardless of the choice of current.

We also revisited EDM calculations for both the covariant $\beta = \pm 1$ choices of current, and calculated the EDM in parallel to the MDM. For $\beta = +1$ we reproduce the leading order result of Ref. [29], conveniently re-expressed as $d_{n,p}(\bar{\theta})$ being proportional to the MDM, $\mu_{n,p}$. We note that this channel does reproduce the measured values of the MDM reasonably well, including the $\mu_n/\mu_p = -2/3$ relation, and therefore μ_n can be used for normalization.

A new calculation was presented using the $\beta = -1$ currents for the neutron and

proton EDM. We utilized the channel with an even number of γ matrices, and observed explicitly how the combination of the two- and three-point functions (*i.e.* explicit removal of the overall chiral phase) leads to physical results. We obtained a different, but nevertheless numerically consistent result for the neutron EDM. Extraction of quantitative predictions, and their systematic improvement within the QCD sum rules approach is problematic in this channel, as the leading order result already depends on the IR cutoff $\mu_{\rm IR}$. While this is a problem for the sum rules approach to nucleon correlators, it can be resolved within lattice QCD. Thus we hope that the procedure described here, using covariant $\beta = \pm 1$ currents can be followed in lattice QCD computations of the nucleon EDMs.

We conclude by noting that for phenomenological purposes, it may be useful to revisit previous calculations of the neutron EDM due to higher-dimensional CP-odd sources such as the EDMs and chromo EDMs of quarks, using the approach pursued here of adding numerical stability by normalizing them on the MDM. Such sources are the primary targets in analyzing nucleon and atomic and molecular EDM sensitivity to new sources of CP violation in nature [18]. In this context, we recall that while the inferred value of $\bar{\theta}$ is small possibly hinting at dynamical relaxation via the axion mechanism, the numerical value of $d_n(\bar{\theta})$ still plays an important role in this context as the axion vacuum expectation value, $\bar{\theta} = \theta_{\rm ind}$, can be shifted away from zero in the presence of higher-dimensional sources.

Chapter 4

CP-odd operators from heavy fermion EDMs

Going beyond the SM, new physics sources of CP violation are generally allowed given the extra degrees of freedom and expected due to the mismatch between the baryogenesis predicted in the SM and the one observed in the universe. Through interactions between the SM and the new physics, those new sources of CP violation could induce higher-dimensional CP-odd interactions among the SM particles. For heavy particles, direct probes of those CP-odd operators often turn out to be difficult; on the other hand, if those operators indeed exist, they could contribute to the EDMs measured at the nuclear and atomic scale through loop effects. Understanding the details of this mechanism, therefore, opens the possibility of indirectly probing CP-odd SM effective operators. In this chapter, we start from the heavy fermions in the SM with EDMs and integrate out loops containing those fermions to derive the CP-odd operators that connect the heavy fermion energy scale with the energy scale of EDM experiments. The relevant Lagrangian is given by

$$\mathcal{L} = \bar{f}\left[i\not{D} - m_f - \frac{id_f}{2}\sigma_{\mu\nu}\gamma_5 F^{\mu\nu}\right] f - \frac{1}{4}F^{\mu\nu}F_{\mu\nu} - \frac{1}{4}G^{a\mu\nu}G^a_{\mu\nu}, \tag{4.1}$$

with the covariant derivative defined by

$$iD_\mu = i\partial_\mu + eA_\mu, \tag{4.2}$$

for leptons, and

$$iD_\mu = i\partial_\mu + g_s G_\mu - eQ_Q A_\mu, \quad G_\mu = T^a G^a_\mu, \tag{4.3}$$

for quarks, where the U(1) charge $Q_c = Q_t = +2/3$ and $Q_b = -1/3$.

4.1 Heavy-lepton-induced electron EDM

A non-zero heavy fermion EDM, through loops, can induce EDMs of lighter fermions. It is first shown by Grozin, Khriplovich, and Rudenko in [90] that heavy leptons (muon and tau lepton) can induce an electron EDM at $\alpha^3_{\rm EM}$ order. (Here the subscript EM stands for electromagnetic.) In this section, we reevaluate the same set of diagrams and show that there is an omission made in the previous work [90]. We present an updated calculation that includes this missing contribution.

A total number of 24 diagrams contribute to the heavy lepton induced electron EDM at three-loop, including the diagrams in Fig. 4.1 and their permutations.

To get the EDM operator, we expand the amplitude up to linear order in the external photon momentum q. While a full expression for arbitrary mass hierarchy can be found following [91], in practice, we would like to explore the smallness of the electron mass compared to a fermion mass inside the closed loop. Thus, observing that $m_l/m_L \ll 1$, where $l = e$ refers to the electron, and $L = \mu, \tau$ refers to heavy leptons, we evaluate the amplitude up to leading order in m_l/m_L. Noticing that on account of the Dirac equation $\left(\not{p} - m_l\right) l(p) = 0$, the expansion in m_l needs to be accompanied with an expansion in p. So, most generally, after the expansion, one would get an expression of the following form:

$$\mathcal{M} = -im_l q^\alpha A^\beta \bar{l} S^{(1)}_{\alpha\beta} l - ip^\rho q^\alpha A^\beta \bar{l} S^{(2)}_{\alpha\beta\rho} l. \tag{4.4}$$

By performing this expansion, the resulting integrals do not contain any external momentum p or q, this type of integral is commonly known as the vacuum integral. Eq. (4.4) contains two structures. While it is possible to convert one structure to the other with the help of the Dirac equation, we will keep both structures for later clarity, in order to

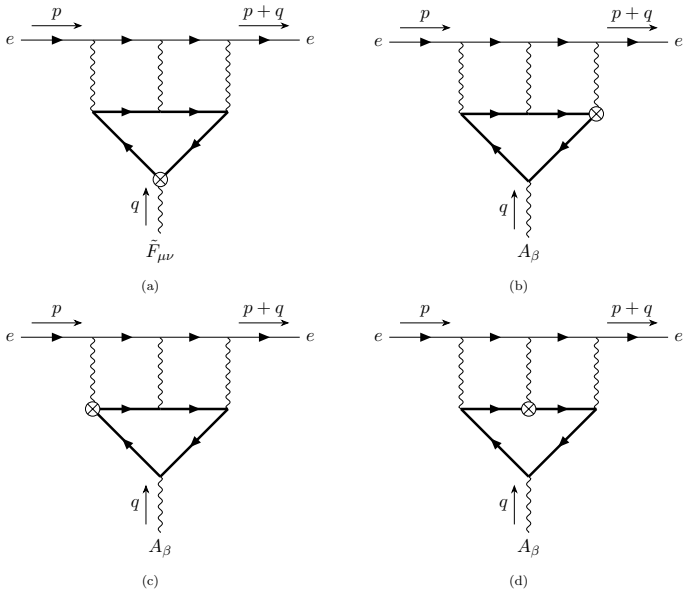

Figure 4.1: Examples of three-loop QED diagrams for heavy lepton EDM contribution to electron EDM. The upper fermion line represents the electron and the lower fermion loop is formed by the heavy lepton. The crossed dot is the EDM vertex and replaces one of the 4 regular EM vertices on the heavy lepton loop. The three photon lines connecting the heavy lepton loop and electron line have 6 possible permutations.

compare our result with the previous one. The EDM operator can be written as

$$\mathcal{M}_{\rm EDM} = -\frac{id_l}{2}\epsilon_{\mu\nu\alpha\beta}q^\alpha A^\beta \bar{l}\sigma^{\mu\nu}l = -\frac{id_l}{4m_l}p^\rho\epsilon_{\mu\nu\alpha\beta}q^\alpha A^\beta \bar{l}\{\sigma^{\mu\nu},\gamma_\rho\}l, \tag{4.5}$$

where q is the incoming photon momentum as in Fig. 4.1. Comparing Eqs. (4.4) and (4.5), we see $S^{(1)}_{\alpha\beta} \propto \epsilon_{\mu\nu\alpha\beta}\sigma^{\mu\nu}$ and $S^{(2)}_{\alpha\beta\rho} \propto \epsilon_{\mu\nu\alpha\beta}\{\sigma^{\mu\nu},\gamma_\rho\}$. Using completeness of Dirac matrices and properties of the Levi-Civita tensor, we find

$$\begin{aligned} S^{(1)}_{\alpha\beta} &= -\frac{1}{8d(d-1)(d-2)(d-3)}\mathrm{Tr}\left[S^{(1)}_{\gamma\delta}\epsilon^{\gamma\delta\kappa\lambda}\sigma_{\kappa\lambda}\right]\times\epsilon_{\mu\nu\alpha\beta}\sigma^{\mu\nu}, \\ S^{(2)}_{\alpha\beta\rho} &= -\frac{1}{32d(d-1)(d-2)^2(d-3)}\mathrm{Tr}\left[S^{(2)}_{\gamma\delta\eta}\epsilon^{\gamma\delta\kappa\lambda}\{\sigma_{\kappa\lambda},\gamma^\eta\}\right]\times\epsilon_{\mu\nu\alpha\beta}\{\sigma^{\mu\nu},\gamma_\rho\}. \end{aligned} \tag{4.6}$$

This expression is generalized to arbitrary dimension d for later use inside the dimensionally-regularized loop expressions. By writing $S^{(1)}_{\alpha\beta}$ and $S^{(2)}_{\alpha\beta\rho}$ in the form of Eq. (4.6), we can focus on the scalar integral inside the trace, rather than a complicated integral with open

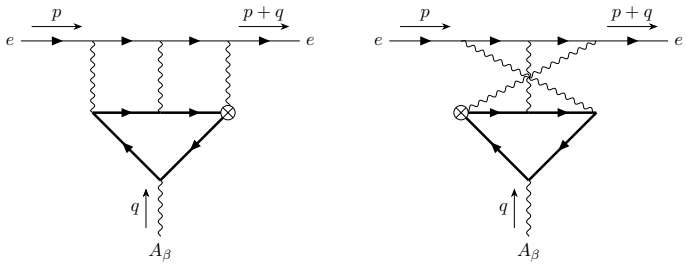

Figure 4.2: An example of related diagrams.

tensor and Dirac indices. The scalar vacuum integral has a simple topology described by B_M in [92] and can be reduced to two master integrals by repeated use of integration by parts [93–97]. One of the master integral is simply the product of three one-loop integrals, and the other is a three-loop integral corresponding to $\mathbf{E}(0,0,x,x)$ in [97]. We use the `FIRE6` [98] package to perform the integration-by-parts reduction and use the analytical expressions of master integrals in [97]. Divergences and gauge dependencies in the two structures cancel out separately and leave us with a finite result. Using the same notation as [90], we get

$$\Delta d_l = a \frac{m_l}{m_L} \left(\frac{\alpha}{\pi}\right)^3 d_L, \tag{4.7}$$

with

$$\begin{aligned}
&a_1^{(1)} = \frac{3}{2}\zeta(3) - \frac{19}{12}, \quad a_2^{(1)} = \frac{9}{4}\zeta(3) - 1, \quad a^{(1)} = a_1^{(1)} + a_2^{(1)} = \frac{15}{4}\zeta(3) - \frac{31}{12} \approx 1.924, \\
&a_1^{(2)} = \frac{1}{2}\zeta(3) - \frac{1}{6}, \quad a_2^{(2)} = \frac{1}{2}\zeta(3) - \frac{5}{24}, \quad a^{(2)} = a_1^{(2)} + a_2^{(2)} = \zeta(3) - \frac{3}{8} \approx 0.827, \\
&a = a^{(1)} + a^{(2)} = \frac{19}{4}\zeta(3) - \frac{71}{24} \approx 2.751,
\end{aligned} \tag{4.8}$$

where $\zeta(s)$ is the Riemann zeta function with $\zeta(3) \approx 1.202$. The contribution from expansion in m_l/m_L is labeled by the upper index "(1)", and the contribution from expansion in p/m_L is labeled by the upper index "(2)". The lower index indicates which set of diagrams the result comes from, with "1" representing the diagram (a) (and its permutations), and "2" representing the sum of diagrams (b), (c), (d) (and

their permutations).

We note in passing a couple of observations that reduce the amount of calculation. First, the CP-odd light-by-light operator induced by the heavy lepton loop vanishes at $q = 0$ limit due to the Ward identity. This tells us that we need to keep q at linear order in the heavy lepton part, so q dependence on the photon propagator and light lepton part can be neglected, as long as we fix the momentum assignment of the photons. Second, not all 24 diagrams are independent. For example, the two diagrams in Fig. 4.2 are the same (or in the general SU(N) case, differ only by a color factor). Similar relations hold for other diagrams and reduce the number of diagrams we need to calculate by half.

Comparing with [90], we see that their result corresponds to our $a^{(1)}$, while the contribution from $a^{(2)}$ is not included. This means they expanded the amplitude in m_e/m_τ but missed the expansion in p/m_τ. Our calculation shows that both expansions contribute to the electron EDM at the same order. Numerically our result is $\sim 40\%$ larger than [90]. Throughout the calculation, we have assumed the "contact" nature of the EDM source, that is no q^2 dependence of d_L within the relevant range of momenta, $|q^2| \lesssim m_L^2$.

As a double-check of our procedure, we also reevaluated the leading order contribution to the electron $g-2$ from light-by-light scattering induced by a muon loop (without the EDM operator insertion). Compared to the CP-odd EDM case discussed here, the CP-even magnetic dipole moment (MDM) case, which is also known as $g-2$, has been extensively studied by many groups and is better known [91, 99]. The same procedure reproduces the known result correctly, and both expansions in m_e/m_μ and in p/m_μ need to be included to get the correct result.

4.2 Heavy-quark-induced light quark EDM

The same idea discussed in Section 4.1 also allows the heavy quark EDMs to be transferred to light quarks; however, due to the strong force between quarks, the contributions shown in Fig. 4.1 are subdominant compared to an analog of Fig. 4.1(a) with internal photons replaced by gluons, as is shown in Fig. 4.3 The calculation is similar to the one

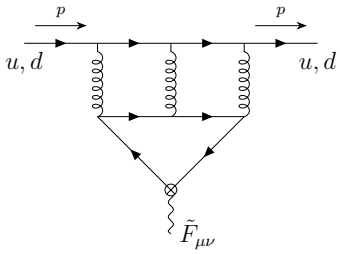

Figure 4.3: An example of the three-loop diagrams that generate the light quark EDMs. The cross dot indicates the heavy quark EDM d_Q insertion, the wavy line is the external photon, the closed solid line is the heavy quark and the upper solid line is the light quark, respectively. There are five additional diagrams that are permutations of the gluon lines attached to the light quark line.

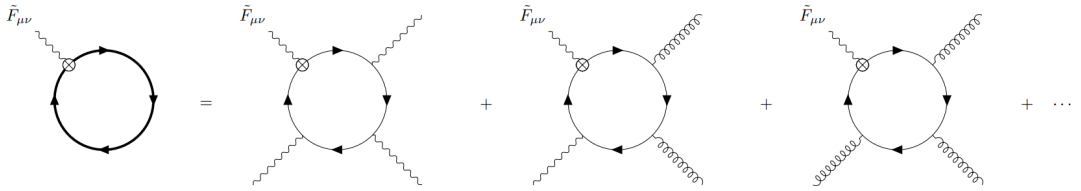

Figure 4.4: The effective action to linear order in d_f after integrating out the heavy fermion. The thick line on the left hand side indicates the full heavy fermion propagator with the covariant derivative D_μ, and the cross dot indicates the EDM operator insertion. The full propagator is expanded with respect to the field strengths, which results in the CP-odd light-by-light and photon-gluon operators as shown on the right hand side.

discussed in Section 4.1, except for the need to include color factors. We then obtain

$$d_q = \frac{5\,(8\zeta(3)-7)}{72} \times \left(\frac{\alpha_s}{\pi}\right)^3 \frac{m_q}{m_Q} d_Q, \tag{4.9}$$

where $\alpha_s = g_s^2/4\pi$.

4.3 CP-odd four-gauge operators

The heavy fermion EDMs induces CP-odd light-by-light and photon-gluon operators through the diagrams in Fig. 4.4. The effective action after integrating out the heavy

quark, to linear order in d_f, is given by

$$S_{\text{eff}} = -\frac{id_f}{2}\text{Tr}\left[\frac{1}{i\not{D} - m_f}\sigma_{\mu\nu}\tilde{F}^{\mu\nu}\right], \tag{4.10}$$

the trace is taken over the spinor indices and the spacetime; for quarks, the trace is taken over the color as well. In the following, we evaluate this expression for heavy quarks and take the result for leptons as the special case where there is no interaction with the gluon. We expand Eq.(4.10) with respect to the field strength $H_{\mu\nu}$, given by

$$H_{\mu\nu} = g_s G_{\mu\nu} - eQ_Q F_{\mu\nu}, \tag{4.11}$$

which satisfies $[iD_\mu, iD_\nu] = iH_{\mu\nu}$. Eq.(4.10) then can be simplified as

$$S_{\text{eff}} = -\frac{id_Q}{2}\text{Tr}\left[\frac{i\not{D} + m_Q}{i\not{D} + m_Q}\frac{1}{i\not{D} - m_Q}\sigma_{\mu\nu}\tilde{F}^{\mu\nu}\right] = -\frac{id_Q m_Q}{2}\text{Tr}\left[\frac{1}{(iD)^2 - m_Q^2 + \frac{1}{2}\sigma\cdot H}(\sigma\cdot\tilde{F})\right], \tag{4.12}$$

where $(iD)^2 = iD_\mu iD^\mu$ and we used that the traces of odd γ's vanish in the second equality. We further expand the denominator with respect to H, and obtain up to fourth-order in the gauge fields

$$S_{\text{eff}} = -\frac{id_Q m_Q}{2}\left(T_2 + T_3 + T_4\right), \tag{4.13}$$

where

$$T_2 = -\frac{1}{2}\text{Tr}\left[\frac{1}{(iD)^2 - m_Q^2}(\sigma\cdot H)\frac{1}{(iD)^2 - m_Q^2}(\sigma\cdot\tilde{F})\right], \tag{4.14}$$

$$T_3 = +\frac{1}{4}\text{Tr}\left[\frac{1}{(iD)^2 - m_q^2}(\sigma\cdot H)\frac{1}{(iD)^2 - m_Q^2}(\sigma\cdot H)\frac{1}{(iD)^2 - m_Q^2}(\sigma\cdot\tilde{F})\right], \tag{4.15}$$

$$T_4 = -\frac{1}{8}\text{Tr}\left[\frac{1}{(iD)^2 - m_Q^2}(\sigma\cdot H)\frac{1}{(iD)^2 - m_Q^2}(\sigma\cdot H)\frac{1}{(iD)^2 - m_Q^2}(\sigma\cdot H)\frac{1}{(iD)^2 - m_Q^2}(\sigma\cdot\tilde{F})\right]. \tag{4.16}$$

The term linear in $\sigma_{\mu\nu}$ vanishes after taking the trace of the spinor index. In order to compute T_2, we use the following identity [100]:

$$\begin{aligned}&\mathrm{Tr}\left[\frac{1}{\left((iD)^2-m_q^2\right)^3}f(H,F)\right]\\&=\mathrm{Tr}\left[\frac{1}{\left((i\partial)^2-m_q^2\right)^3}f(H,F)\right]-\mathrm{Tr}\left[\frac{1}{\left((iD)^2-m_q^2\right)^5}H_{\mu\nu}H^{\mu\nu}f(H,F)\right],\end{aligned}\tag{4.17}$$

where $f(H,F)$ is an arbitrary function of $H_{\mu\nu}$ and $F_{\mu\nu}$. We thus obtain

$$\frac{d}{dm_Q^2}T_2=-\mathrm{Tr}\left[\frac{1}{((i\partial)^2-m_Q^2)^3}\left(\sigma\cdot H\right)\sigma\cdot\tilde{F}\right]+\mathrm{Tr}\left[\frac{1}{((iD)^2-m_Q^2)^5}H_{\mu\nu}H^{\mu\nu}\left(\sigma\cdot H\right)\sigma\cdot\tilde{F}\right].\tag{4.18}$$

where we ignore the derivatives acting on F. We can now replace iD by $i\partial$ in the last term to the order of our interest, and obtain

$$\frac{d}{dm_Q^2}T_2=-i\int d^4x\left[\frac{3eQ_Q}{4\pi^2m_Q^2}F_{\mu\nu}\tilde{F}^{\mu\nu}+\frac{1}{24\pi^2m_Q^6}\mathrm{tr}_c\left[H_{\mu\nu}H^{\mu\nu}H_{\rho\sigma}\tilde{F}^{\rho\sigma}\right]\right].\tag{4.19}$$

By integrating this we obtain

$$T_2=i\int d^4x\left[\frac{3eQ_Q}{4\pi^2}\ln\left(\frac{M_R^2}{m_Q^2}\right)F_{\mu\nu}\tilde{F}^{\mu\nu}+\frac{1}{48\pi^2m_Q^4}\mathrm{tr}_c\left[H_{\mu\nu}H^{\mu\nu}H_{\rho\sigma}\tilde{F}^{\rho\sigma}\right]\right],\tag{4.20}$$

where the additional mass scale M_R comes from the regularization which we did not write down explicitly. Next we compute T_3. By ignoring the derivatives acting on $\tilde{F}_{\mu\nu}$, we obtain

$$\begin{aligned}T_3=\frac{1}{4}\mathrm{Tr}\Bigg[&\frac{1}{((iD)^2-m_Q^2)^3}\left(\sigma\cdot H\right)^2\left(\sigma\cdot\tilde{F}\right)+\frac{1}{((iD)^2-m_Q^2)^4}\left[(iD)^2,\sigma\cdot H\right]\left(\sigma\cdot H\right)(\sigma\cdot\tilde{F})\\&-\frac{1}{((iD)^2-m_Q^2)^5}\left[(iD)^2,\sigma\cdot H\right]\left[(iD)^2,\sigma\cdot H\right]\sigma\cdot\tilde{F}+\cdots\Bigg],\end{aligned}\tag{4.21}$$

where the dots indicate terms that contain more than two commutators and thus correspond to higher dimensional operators that are out of our interest. The first term is

easily seen to generate only $\mathcal{O}(H^4\tilde{F})$ operators with the help of the identity (4.17). The second term is expanded as

$$\begin{aligned}
&\mathrm{Tr}\left[\frac{1}{((iD)^2-m_Q^2)^4}\left[(iD)^2,\sigma\cdot H\right](\sigma\cdot H)(\sigma\cdot\tilde{F})\right]\\
&=\mathrm{Tr}\left[\frac{1}{((iD)^2-m_Q^2)^4}iD^\alpha\left[iD_\alpha,\sigma\cdot H\right](\sigma\cdot H)\sigma\cdot\tilde{F}\right.\\
&\qquad+iD^\alpha\frac{1}{((iD)^2-m_Q^2)^4}\left[iD_\alpha,\sigma\cdot H\right](\sigma\cdot H)\sigma\cdot\tilde{F}\\
&\qquad\left.+\frac{1}{((iD)^2-m_Q^2)^4}\left[iD^\alpha,\sigma\cdot H\right]\left[iD_\alpha,\sigma\cdot H\right]\sigma\cdot\tilde{F}\right].
\end{aligned}\tag{4.22}$$

The first two terms induce only higher order terms [100], and thus we ignore them. The third term in Eq. (4.21) already contains three field strengths and two commutators, and hence we can ignore any further commutators between D and H. By taking the angular average, we obtain

$$\mathrm{Tr}\left[\frac{1}{((iD)^2-m_Q^2)^5}\left[(iD)^2,\sigma\cdot H\right]\left[(iD)^2,\sigma\cdot H\right]\sigma\cdot\tilde{F}\right]\tag{4.23}$$

$$=\mathrm{Tr}\left[\frac{(iD)^2}{((iD)^2-m_Q^2)^5}\left[iD^\alpha,\sigma\cdot H\right]\left[iD_\alpha,\sigma\cdot H\right]\sigma\cdot\tilde{F}\right].\tag{4.24}$$

By combining them, we obtain

$$\begin{aligned}
T_3&=-\frac{m_Q^2}{4}\mathrm{Tr}\left[\frac{1}{((iD)^2-m_Q^2)^5}\left[iD^\alpha,\sigma\cdot H\right]\left[iD_\alpha,\sigma\cdot H\right]\sigma\cdot\tilde{F}\right]\\
&=-\frac{g_s^2}{24\pi^2m_Q^4}\int d^4x\,\mathrm{tr}_c\left[(\mathcal{D}^\alpha G_{\mu\rho})(\mathcal{D}_\alpha G_\nu{}^\rho)\right]\tilde{F}^{\mu\nu}=0.
\end{aligned}\tag{4.25}$$

Finally we compute T_4. To the order of our interest, we can simply replace iD by $i\partial$ in the denominator. It is then easy to see that

$$T_4=-\frac{i}{48\pi^2m_Q^4}\int d^4x\,\mathrm{tr}_c\left[3H_{\mu\nu}H^{\mu\nu}H_{\rho\sigma}\tilde{F}^{\rho\sigma}-4H^\mu{}_\nu H^\nu{}_\rho H^\rho{}_\sigma\tilde{F}^\sigma{}_\mu\right].\tag{4.26}$$

Therefore we obtain

$$S_{\rm eff} = \frac{d_Q}{48\pi^2 m_Q^3}\int d^4x\,{\rm tr}_c\left[-H_{\mu\nu}H^{\mu\nu}H_{\rho\sigma}\tilde{F}^{\rho\sigma} + 2H^{\mu}{}_{\nu}H^{\nu}{}_{\rho}H^{\rho}{}_{\sigma}\tilde{F}^{\sigma}{}_{\mu}\right], \tag{4.27}$$

where we ignored the quadratic term that is irrelevant for our purpose, and ${\rm tr}_c$ is the trace only over the color. The action contains CP-odd photon-gluon operators as well as a CP-odd pure photon operator. For heavy quarks the pure photon operator is subdominant, the operator quadratic in the photon field is given by

$$\mathcal{L}_{G^2F\tilde{F}} = \frac{eQ_Q g_s^2 d_Q}{24\pi^2 m_Q^3}{\rm tr}_c\left[F_{\mu\nu}G^{\mu\nu}\tilde{F}_{\rho\sigma}G^{\rho\sigma} - \tilde{F}^{\mu}{}_{\nu}G^{\nu}{}_{\rho}F^{\rho}{}_{\sigma}G^{\sigma}{}_{\mu}\right], \tag{4.28}$$

while the one linear in the photon field is given by

$$\mathcal{L}_{G^3\tilde{F}} = \frac{g_s^3 d_Q}{48\pi^2 m_Q^3}{\rm tr}_c\left[-G_{\mu\nu}G^{\mu\nu}G_{\rho\sigma}\tilde{F}^{\rho\sigma} + 2G^{\mu}{}_{\nu}G^{\nu}{}_{\rho}G^{\rho}{}_{\sigma}\tilde{F}^{\sigma}{}_{\mu}\right]. \tag{4.29}$$

Carrying out color traces explicitly, one finds that (4.28) contains δ^{ab}, while (4.29) has d^{abc} structure. In that sense, (4.28) would exist for any choice of the gauge group for $G_{\mu\nu}$ including a U(1), while (4.29) requires $N \geq 3$ for SU(N), which includes of course the color group of the Standard Model.

For heavy leptons the CP-odd light-by-light operator becomes relevant. Focusing on the pure photon part of Eq.(4.27), we obtain

$$\mathcal{L}_{F^3\tilde{F}} = -\frac{d_L/e}{96\pi^2 m_L^3}e^4(\tilde{F}_{\mu\nu}F^{\mu\nu})(F_{\rho\sigma}F^{\rho\sigma}). \tag{4.30}$$

Based on the effective operators derived in this chapter, the nucleon and atomic EDMs induced by heavy fermion EDMs will be derived in Chapter 5 and 6. The experimental constraints on nucleon and atomic EDMs are then reinterpreted as constraints on heavy fermion EDMs.

Chapter 5

Indirect constraints on muon EDM

Latest interest to muons is fueled by the on-going discrepancy between theoretical predictions and experimental measurement of the muon anomalous magnetic moment [101–107]. It brings into focus a question of other observables that involve muons, and one such important quantity is the muon EDM, d_μ (see *e.g.* [108] on extended discussion on this point). At the moment, the auxiliary EDM measurement at the Brookhaven $g-2$ experiment sets the tightest bound on muon EDM [33],

$$|d_\mu| < 1.8 \times 10^{-19}\, e\text{cm}, \tag{5.1}$$

but there are proposals on significantly improving this bound with dedicated muon beam experiments [32, 109–111]. Given these upcoming efforts it is important to re-evaluate *indirect* bounds on muon EDM, especially given significant progress in precision of atomic/molecular EDM experiments in recent years.

In this chapter, we evaluate indirect limits on d_μ, finding superior bounds to (5.1) from Hg and ThO EDM experiments [21, 39]. Our results draw heavily on the fact that the closed muon loop with d_μ insertion is placed in a very strong electric field of a large nucleus (*e.g.* Hg or Th). The resulting interactions, derived in Chapter 4, is capable of generating Schiff moment [112], CP-odd electron-nucleus interaction [113], and magnetic quadrupole moment. Below, we elaborate on the details of our findings.

5.1 The E^3B interaction

The effective dimension eight electromagnetic operator generated by the muon EDM was derived in section 4.3, rewriting it in terms of the electric **E** and magnetic **B** fields gives

$$\begin{aligned}\mathcal{L} &= -e^4(\tilde{F}_{\alpha\beta}F^{\alpha\beta})(F_{\gamma\delta}F^{\gamma\delta}) \times \frac{d_\mu/e}{96\pi^2 m_\mu^3} \\ &= -\frac{d_\mu/e}{12\pi^2 m_\mu^3} e^4(\mathbf{E}\cdot\mathbf{B})(\mathbf{E}\cdot\mathbf{E} - \mathbf{B}\cdot\mathbf{B}).\end{aligned} \tag{5.2}$$

We note the differences with CP-even case: dimension four $(\tilde{F}_{\alpha\beta}F^{\alpha\beta})$ operator can be dropped, and there is only one dimension eight operator $(FF)(F\tilde{F})$, while CP-even case has two, $(FF)(FF)$ and $(F\tilde{F})(F\tilde{F})$. The effective CP-odd photon interactions were discussed recently in [114]. In principle, all terms in the expansion can be computed analytically. Neglecting $O(B^3)$ interaction that is subdominant due to no Z-enhancement leaves only E^3B effective operator that we write in a more generic form that can be applied to other sources of CP-violation as well:

$$H_{\text{eff}} = C_{E^3B} \times \int d^3x\, e^4(\mathbf{E}\cdot\mathbf{E})(\mathbf{E}\cdot\mathbf{B}), \tag{5.3}$$

with $C_{E^3B} = (12\pi^2 m_\mu^3)^{-1} d_\mu/e$ in our model.

It is important to note that the E^3B effective interaction does not always capture all relevant physics. For example, the muon-loop-mediated electron EDM derived in section 4.1 involves computation with loop momenta that can be comparable or even larger than m_μ. In that case, the entire CP-odd four-photon amplitude is needed. In what follows we evaluate the physical consequences of the E^3B interaction.

5.2 Muon EDM and nuclear CP-odd observables

Nuclear spin dependent EDMs (sometimes called diamagnetic EDMs) provide stringent tests of CP-violation via probing nuclear T, P-odd moments. At this step we address

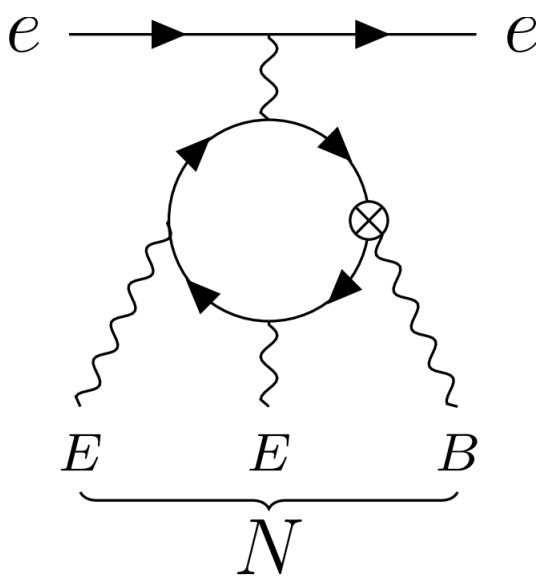

Figure 5.1: A representative diagram showing d_N and S_N are generated when E^2B is sourced by the nucleus.

the mechanisms that convert CP-even static nuclear moments to the CP-odd ones,

$$\mu_N, Q_N \xrightarrow{E^3B} d_N, S_N, M_N, \tag{5.4}$$

where subscript N stands for "nuclear", and μ, Q, d, S, M are magnetic dipole, electric quadrupole, electric dipole, Schiff and magnetic quadrupole moments. (Inside a neutral atom, d_N is not observable by itself, but in the linear combination that parametrizes the difference between EDM and charge distribution, the Schiff moment [112].) Consider a spin-$\frac{1}{2}$ nucleus, as in the most sensitive diamagnetic EDM experiment with ^{199}Hg [21]. Then M_N is absent by definition, but d_N and S_N can be induced as shown in Fig. 5.1. To calculate them we notice that the magnetic field of the $I = 1/2$ nucleus can be presented in the following form:

$$eB_i(\mathbf{r}) = b_1(r)n_{Ii} + b_2(r)(3n_in_j - \delta_{ij})n_{Ij}, \tag{5.5}$$

where we introduced the unit vector in the direction of the nuclear spin, $\mathbf{n}_I = \mathbf{I}/I$, $\mathbf{n} = \mathbf{r}/r$ and some scalar invariant functions $b_{1(2)}(r)$. Notice that in the limit of a very

small nuclear radius, $R_N \to 0$, the corresponding asymptotics of these functions are

$$b_1(r) \to \frac{2e\mu_N}{3}\delta(\mathbf{r}); \quad b_2(r) \to \frac{e\mu_N}{4\pi r^3}. \tag{5.6}$$

where μ_N is the nuclear magnetic dipole moment value. The nuclear electric field, to good accuracy, can be described by the radial ansatz,

$$e\mathbf{E} = \frac{\mathbf{n}}{r^2} \times Z\alpha f(r), \tag{5.7}$$

where Z is the atomic number, α is the fine structure constant and $f(r)$ is the fraction of nuclear charge within the radius r. For the uniform sphere charge distribution $f(r) = r^3/R_N^3$ for $r < R_N$ and $f(r) = 1$ for $r > R_N$. Substituting (5.7) and (5.5) into (5.3) and performing angular integration, we obtain intermediate expressions for d_N and S_N:

$$\frac{d_N}{eC_{E^3B}} = 4\pi(Z\alpha)^2 \int \frac{dr}{r^2} f^2 \left(\frac{5}{3}b_1 + \frac{4}{3}b_2\right), \tag{5.8}$$

$$\frac{S_N}{eC_{E^3B}} = \frac{2\pi(Z\alpha)^2}{15} \int dr f^2 \left[b_1\left(11 - \frac{25}{3}\frac{r_c^2}{r^2}\right) + b_2\left(16 - \frac{20}{3}\frac{r_c^2}{r^2}\right)\right]. \tag{5.9}$$

In these expressions, r_c^2 is the nuclear charge radius. We follow the standard definition of the Schiff moment that in non-relativistic limit and point-like nucleus leads to the effective nuclear-spin-dependent T, P-odd Hamiltonian for electrons

$$H_{T,P\text{-odd}} = -(S_N/e) \times 4\pi\alpha(\mathbf{n}_I \cdot \boldsymbol{\nabla}_e)\delta(\mathbf{r}_e). \tag{5.10}$$

Nuclear dependence in (5.8) and (5.9) is encapsulated in f and b_i. Electric field, *i.e.* f, is determined by the collective properties of the nucleus and has little to no dependence on the details of the nucleon's wave function inside a large nucleus. In contrast, the scalar functions b_i that describe magnetization are determined by mostly "outside" valence nucleons and carry more detail about nuclear structure. For any realistic choice of f and b_i, however, it is easy to see that radial integrals will be saturated by distances $r \sim R_N$.

Specializing our calculations to the ^{199}Hg nucleus, we adopt a simple shell model

description of it with a valence neutron in $n_r = 2, l = 1, j = 1/2$ state carrying all angular momentum dependence, and ignore configuration mixing. Its wave function can be conveniently written as

$$\psi(\mathbf{r}_n) = R_{2p}(r_n)\frac{(\boldsymbol{\sigma}_n \cdot \mathbf{n}_n)}{\sqrt{4\pi}}\chi, \tag{5.11}$$

where $\mathbf{r}_n = \mathbf{n}_n r_n$ and χ are neutron's coordinate and two component spinor, and R_{2p} is the radial wave function normalized as $\int R^2 r^2 dr = 1$. Nuclear spin in this case coincides with j, and $\mathbf{n}_I = \chi^\dagger \boldsymbol{\sigma}_n \chi$. The magnetic moment of the nucleus has a simple connection to the magnetic moment of the neutron, $e\mu_N = (-1/3)e\mu_n = (-1/3) \times (-1.91) \times 4\pi\alpha/(2m_p)$. The magnetization functions b_i defined earlier in (5.5) can be directly related to radial R_{2p} functions, and explicit calculations give

$$b_1(r) = \frac{-1.91\alpha}{2m_p} \times \frac{2}{3}\left(2\int_r^\infty \frac{dr_n}{r_n} R^2_{2p}(r_n) - R^2_{2p}(r)\right),$$
$$b_2(r) = \frac{-1.91\alpha}{2m_p} \times \frac{1}{3}\left(R^2_{2p}(r) - \frac{1}{r^3}\int_0^r dr_n r_n^2 R^2_{2p}(r_n)\right).$$

One can easily check that the corresponding boundary conditions (5.6) are satisfied. To learn about the parametric dependence of our answers we first explore the simplified case when not only the charge distribution but also $R(r)$ is taken to be constant inside the nuclear radius and zero outside, $R^2_{2p}(r) = 3R_N^{-3}\theta(R_N - r)$ [115]. In this approximation we get

$$\frac{d_N}{eC_{E^3B}} = \frac{1.91 \times 2\pi Z^2\alpha^3}{3m_p R_N^4}; \quad \frac{S_N}{eC_{E^3B}} = \frac{1.91 \times 39\pi Z^2\alpha^3}{245 m_p R_N^2}, \tag{5.12}$$

and consequently S_N scales as $Z^{4/3}$ since $R_N \propto Z^{1/3}$. In order to get a more realistic answer, we solve for R_{2p} numerically using the Woods-Saxon potential with parameters outlined in Ref. [116]. We check that our results reproduce $S_N(d_n)$ [115, 116] with reasonable $\propto 30\%$ accuracy. Performing two numerical integrals over r_n and r, and substituting explicit expression for C_{E^3B}, we obtain the following numerical result,

$$S_{^{199}\mathrm{Hg}}/e \simeq (d_\mu/e) \times 4.9 \times 10^{-7}\,\mathrm{fm}^2, \tag{5.13}$$

that lands itself very close (withing 20%) from the naive estimate (5.12). Given the

experimental constraint of $|S_{^{199}\mathrm{Hg}}| < 3.1 \times 10^{-13}\, e\,\mathrm{fm}^3$ [21], we arrive at the following final result

$$|d_\mu| < 6.4 \times 10^{-20}\, e\,\mathrm{cm}, \tag{5.14}$$

which is somewhat more stringent bound, by a factor of ~ 2.5 than (5.1). Result (5.13) carries a 25-30% uncertainty due to neglected contributions from the nuclear orbital mixing.

Future developments may bring about new experiments that would search for EDMs involving nuclei with $I \geq 1$ [117], opening the possibility of measuring magnetic quadrupole moments, and using nuclei with large deformations/large Q_N. We perform a simple estimate for the expected size of the magnetic quadrupole by taking the electric field created by Q_N outside the nucleus, and cutting divergent integrals at R_N. This way, we arrive at the following estimate

$$\frac{M_N}{eC_{E^3B}} \sim \frac{48\pi Z^2\alpha^3}{5}\frac{Q_N}{e}\int\frac{dr}{r^5} \simeq \frac{Q_N}{e}\frac{12\pi Z^2\alpha^3}{5R_N^4}. \tag{5.15}$$

Substituting expression (5.3), and normalizing electric quadrupole on large values observed in deformed nuclei, we get

$$\frac{M_N}{e} \sim 10^{-4}\,\mathrm{fm} \times \frac{Q_N}{e\,300\,\mathrm{fm}^2} \times (d_\mu/e). \tag{5.16}$$

Taking typical matrix elements and extrapolating future sensitivity to the current one of the ThO experiment, one could probe $M_N/e \propto 10^{-11}\,\mathrm{fm}^2$ and consequently achieving $d_\mu/e \propto 10^{-20}\, e\,\mathrm{cm}$.

5.3 Muon EDM and paramagnetic CP-odd observables

Finally we turn our attention to the electron-spin-dependent EDMs referred to as paramagnetic EDMs of atoms and molecules. As discussed in Chapter 2, it is convenient to introduce a linear combination of the electron EDM and the C_S operator referred to as "equivalent d_e" in Eq.(2.1). Current experimental limit stands as $|d_e^{\mathrm{equiv}}| < 1.1 \times 10^{-29}\, e\,\mathrm{cm}$ [39].

Muon EDM contributes both to d_e and C_S through loops. The bona fide three-loop

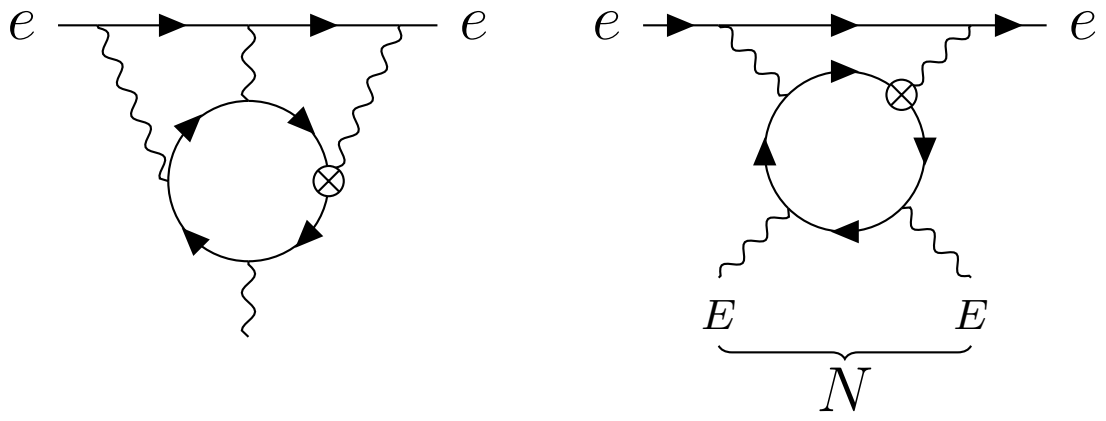

Figure 5.2: Three-loop contribution to d_e and two-loop contribution to equivalent C_S generated by d_μ.

$d_e(d_\mu)$ computation, Fig. 5.2, was performed in Section 4.1,

$$d_e = d_\mu \left(\frac{\alpha}{\pi}\right)^3 \frac{m_e}{m_\mu} \times 2.751 \simeq 1.6 \times 10^{-10} d_\mu. \tag{5.17}$$

If the direct bound (5.1) is saturated, d_e will be larger than the experimental limit by about a factor of two, as already noted in Ref. [108]. It turns out, however, that equivalent of C_S generated by E^3B interaction gives a larger contribution.

A representative diagram contributing to the T, P-odd electron-nucleus interaction via E^3B term is shown in Fig. 5.2. The two electric field lines can be sourced by a nucleon, or a nucleus, while the photon loop attached to electron line generates $m_e \bar{e} i\gamma_5 e$ interaction. There are two important considerations regarding this type of contribution: *i.* The photon loop is enhanced by $\log(\Lambda/m_e)$, and we calculate this loop to logarithmic accuracy, cutting it at $\Lambda = m_\mu$. (In practice, this cutoff will be supplied by the non-local nature of the muon loop in Fig. 5.1.) *ii.* In a large nucleus $\mathbf{E}^2$ is coherently enhanced and dominates over effects proportional to electromagnetic contribution of individual nucleons $\propto Z\langle p|\mathbf{E}^2|p\rangle$. Being concentrated inside and near the nucleus, $\mathbf{E}^2$ can be considered *equivalent* to the delta-functional contribution:

$$e^2(\mathbf{E}^2)_{\rm nucl} \to \delta(\mathbf{r}) \times \frac{4\pi(Z\alpha)^2}{R_N} \times \int_0^\infty \frac{f^2(R_N x)}{x^2} dx, \tag{5.18}$$

where $x = r/R_N$. For a constant density charge distribution, the integral in (5.18) is

6/5, and we adopt this number. Putting the results of the loop calculation together with (5.18), and using the explicit form for C_{E^3B} we arrive at the following prediction for the *equivalent* C_S value:

$$\frac{G_F}{\sqrt{2}} C_S^{\rm equiv} = \kappa \frac{4Z^2\alpha^4}{\pi A} \times \frac{m_e (d_\mu/e)}{m_\mu^3 R_N} \times \log\left(\frac{m_\mu}{m_e}\right). \tag{5.19}$$

As one can see, $C_S^{\rm equiv}$ scales as $Z^2 A^{-1} R_N^{-1} \propto Z^{2/3}$, which is the sign of coherent enhancement. A is the number of nucleons, and $A = 232$ for Th. In this expression, κ is a fudge factor to account for the change of the electronic matrix elements stemming from the fact that nuclear $\mathbf{E}^2$ extends beyond the nuclear boundary, while true nucleonic C_S effect is proportional to nuclear density and vanishes outside. Solving the Dirac equation near the nucleus for the outside $s_{1/2}$ and $p_{1/2}$ electron wave functions and finding a ratio of the matrix elements for these two distributions result in $\kappa \simeq 0.66$. We then arrive to the numerical result

$$C_S^{\rm equiv} = 3.1 \times 10^{-10} \left(\frac{d_\mu}{10^{-20}\, e\,{\rm cm}}\right). \tag{5.20}$$

Combining (5.20) with (5.17) into (2.1), we arrive at our main result

$$d_e^{\rm equiv} \simeq 5.8 \times 10^{-10}\, d_\mu \implies |d_\mu| < 1.7 \times 10^{-20}\, e\,{\rm cm}. \tag{5.21}$$

We observe that d_e and $C_S^{\rm equiv}$ interfere constructively, and C_S contribution is larger by a factor of $\simeq 4$. We believe (5.20)to be accurate within $\sim 15-20\%$ with uncertainties associated with modelling of $\mathbf{E}(r)$ and logarithmic approximation for the photon loop integral.

Recently, a measurement on the EDM of the HfF^+ is performed, giving an improved constraint on the paramagnetic EDM $|d_e^{\rm equiv}({\rm HfF}^+)| < 4.1 \times 10^{-29}\, e\,{\rm cm}$ [20]. With $d_e^{\rm equiv}({\rm HfF}^+) = d_e + C_S \times 0.9 \times 10^{-20}\, e\,{\rm cm}$, the constraint on the muon EDM is improved by another two-fold:

$$d_\mu({\rm HfF}^+) < 8.9 \times 10^{-21} e{\rm cm}. \tag{5.22}$$

5.4 Comments on the accuracy of calculations

Since the calculation of $S(d_\mu)$ and $C_S(d_\mu)$ involve many steps, it is appropriate to comment on the expected accuracy of the results. The uncertainties can be subdivided into three categories, coming from particle physics, nuclear and atomic physics.

Particle physics. In calculating the muon loop leading to $(\mathbf{BE})\mathbf{E}^2$ effective interaction, higher order terms in the electric field have been neglected. Such terms are additionally suppressed by powers of $(e\mathbf{E}^2)/m_\mu^4 \leq (Z\alpha m_\mu^{-1} R_N)^4 < 10^{-3}$, and therefore this approximation holds really well. The loop integral also neglects the change of electric field on the scale of the muon Compton wavelength. This correction can be at maximum $\sim (R_N m\mu)^{-2} \sim 7\%$. Notice that this can be consistently improved by numerically calculating the muon loop in the realistic $\mathbf{E}(r)$ background.

Photon loop calculation entering the calculation of C_S has been performed to logarithmic accuracy, *i.e.* $O(1)$ terms have been dropped relative to $\log(m_\mu^2/m_e^2) \sim O(10)$. This implies the accuracy of 10%, which again can be improved upon numerical calculation of the two-loop (muon and photon) diagram.

Nuclear physics. There are no nuclear uncertainties in the C_S calculation, other than the exact modelling of the electric field distribution inside the nucleus. The charge distributions used in our calculations are "anchored" by the measured values of the nuclear charge radii, but the exact shape can modeled by either constant-within-sphere, or Woods-Saxon form. This feeds into the calculation of the κ-factor, and we estimate that the possible variation does not exceed $\sim 10\%$.

The calculation of the Schiff moment involves modelling of the magnetic field inside the nucleus. In our work it is done in the simple shell model that predicts the magnetic moment to be $\mu_{^{199}\mathrm{Hg}} = -\mu_n/3 = 0.637$, while in practice the measured result for this quantity is 0.509. The rest of the magnetism comes from the mixing of different nuclear orbital configurations, and neglecting it generates $\sim 20 - 25\%$ errors. It has to be emphasized that this uncertainty is much smaller than a very large, order of magnitude uncertainty in calculations of the Schiff moment induced by the CP-odd nuclear forces, where there is no valence contribution, and subtle effects in the core polarization widely vary as function of adopted nuclear models.

Atomic physics. There is no change in atomic physics calculation (if the parameter

κ is treated as essentially a nuclear parameter). Therefore, same atomic calculations of molecular/atomic orbitals apply, and modern calculations are performed with estimated errors not exceeding 10%.

Combining different sources of errors, we conclude that the calculation of $C_S(d_\mu)$ and the resulting bounds on d_μ carry a theoretical error of $\sim 15-20\%$ which can be brought down to 10% level with more accurate modelling of the nuclear electric field distribution and full calculation of the two-loop diagram. Calculation of $S(d_\mu)$ carries a $\sim 30\%$ uncertainty, mostly due to our reliance on the simple shell model, but can be improved with a more sophisticated nuclear input.

5.5 Discussion

We have evaluated the electromagnetic transmission mechanisms of muon EDM to the observable EDMs that do not involve on-shell muons. We have found that muon-loop-induced E^3B effective interaction plays an important role and leads to novel indirect bounds, Eqs. (5.14) and (5.21) that are already stronger than the direct bound (5.1). Result (5.21) provides a new benchmark that future dedicated muon EDM experiments would have to overtake. We also notice that since both ^{199}Hg and ThO EDM results give an improvement, it is highly unlikely that a fine-tuned choice of d_e and hadronic CP-violation would lead to the relaxation of indirect bounds on d_μ.

In this chapter, we do not discuss the short-distance physics that may lead to the enhanced d_μ. We note that while in some models d_μ is predicted at the same level as d_e, it is also feasible that d_μ/d_e scales as $(m_\mu/m_e)^3$ and possibly even larger. (Given the on-going $g-2$ discrepancy in the muon sector, it is clear that d_μ deserves a separate treatment.) Still, it is instructive to equate d_μ to some simple scaling formula that involves an ultraviolet scale Λ_μ, and we choose $d_\mu = m_\mu/\Lambda_\mu^2$ scaling. Then our results translate to

$$\Lambda_\mu > 300\,\mathrm{GeV}, \tag{5.23}$$

which underscores that the (weak scale)$^{-1}$ distances start being probed. Depending on underlying model, there can be some scale dependence of the muon EDM form factor $d_\mu(Q^2)$ (see *e.g.* [90]). This, however, does not obscure comparison of direct ($Q^2 \simeq 0$) and indirect ($Q^2 \simeq m_\mu^2$) limits derived here as long as d_μ operator is generated at

distances $\Lambda^{-1} \ll m_\mu^{-1}$.

We also update the limit on the τ-lepton EDM d_τ derived in [90]. Our analysis is directly applicable to d_τ after replacing m_μ by the τ-lepton mass m_τ. In this case, the electron EDM plays the dominant role since $d_e \propto m_\tau^{-1}$ while $S_N, C_S \propto m_\tau^{-3}$ up to logarithm. For the ThO molecule, we obtain

$$d_e^{\text{equiv}} \simeq 1.0 \times 10^{-11}\, d_\tau \implies |d_\tau| < 1.1 \times 10^{-18}\, e\,\text{cm}. \tag{5.24}$$

This surpasses the constraint from the Belle experiment [118]. The constraint from ^{199}Hg is weaker by a factor of $\sim 2 \times 10^2$ than (5.24).

Finally, while the focus of this chapter was on d_μ, one could also derive limits on C_{E^3B} applicable to other models. We get constraints on C_{E^3B} at the level of $10^{-41}\,\text{eV}^{-4}$ and better, which would be challenging to match with photon-based experiments [114].

Chapter 6

Indirect constraints on heavy quark EDMs

Direct measurements of the heavy quark EDMs are difficult due to their short lifetimes. The current strongest direct bound is from $e^+e^- \to q\bar{q}$ at LEP and is only of the order of $10^{-17}\, e\,\mathrm{cm}$ [119]. Recently, an LHC based experiment is proposed that aims at directly measuring charm baryon dipole moments [34–38], potentially improving the direct bounds on the heavy quark EDMs. Given this situation, the goal of this chapter is to understand the current status of indirect limits on the heavy quark EDMs.

Indirect limits on the charm and bottom quark EDMs were previously considered in [120] and the CEDM case was also analyzed in [121]. There the authors derived limits based on the constraints on the heavy quark CEDMs. Indeed, the charm and bottom quark EDMs well above the heavy quark mass scales, say 1 TeV, generate the CEDM operators through the renormalization group (RG) running at a lower energy scale. These CEDMs in turn source the three-gluon Weinberg operator after integrating out the charm and bottom quark. The Weinberg operator then generates the neutron EDM, and this allows one to derive limits on the charm and bottom quark EDMs. We may phrase it a re-interpretation of bounds on the heavy quark CEDMs at the heavy quark mass threshold, with an assumption that there is no cancellation between the EDM and CEDM contributions (see also discussion at the end of Sec. 6.1). In contrast, in this chapter, we study CP-odd operators generated from the EDM operators at the

heavy quark mass threshold. Therefore our consideration directly applies to the heavy quark EDMs at the quark mass threshold and is independent of [120]. Even though the CP-odd operators induced by the heavy quark EDMs are formally higher dimensional, suppressions from the charm and bottom quark masses are not severe as there is only a little hierarchy between the quark masses and the QCD scale.

In order to make our limits robust, we derive indirect limits on charm and bottom quark EDMs based on multiple observables, paramagnetic and neutron EDMs. Indirect limits always have a potential of having a cancellation among different operators. For instance, paramagnetic EDM experiments are sensitive to only a particular linear combination of the electron EDM d_e and the CP-odd semi-leptonic operator C_S (see Sec. 6.1). Therefore a new physics contribution to d_e and C_S can be such that the linear contribution almost vanishes even though each term is sizable. Deriving constraints from two completely different observables, paramagnetic and neutron EDMs, makes the probability of having such a cancellation less likely. We also minimize the QCD uncertainty as much as possible. For this purpose the paramagnetic EDM plays an essential role as it is sensitive to the heavy quark EDM through the semi-leptonic operator C_S. The estimation of C_S is not polluted by hadronic uncertainties, and its uncertainty is theoretically well under control.

6.1 Paramagnetic EDM

In this section we study a constraint on the heavy quark EDM from paramagnetic atomic/molecule EDM experiments, in particular the ACME experiment [19]. Below the QCD scale, the CP-odd photon-gluon operator, in particular the two-photon two-gluon operator,

$$\mathcal{L}_{G^2F\tilde{F}} = \frac{eQ_Q g_s^2 d_Q}{48\pi^2 m_Q^3} G^a_{\mu\nu} G^a_{\alpha\beta} \left(F^{\mu\nu}\tilde{F}^{\alpha\beta} - F^{\nu\alpha}\tilde{F}^{\beta\mu} \right), \tag{6.1}$$

induces the C_S operator defined in Eq.(2.2).

Because our starting point here is explicitly isospin symmetric, it will result in the same C_S coupling for neutrons and protons. The nucleon matrix element of the gluon

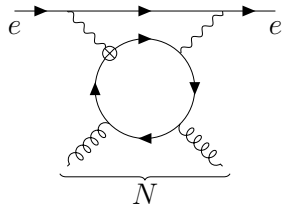

Figure 6.1: The diagram that generates the CP-odd semi-leptonic operator C_S. The photons are attached to the electron line and generate the structure $\bar{e}i\gamma_5 e$, while the gluons feed into the nucleon N.

part is given by

$$\langle N|\frac{g_s^2}{32\pi^2}G^a_{\mu\nu}G^a_{\alpha\beta}|N\rangle = -\frac{m_N}{108}\left(\eta_{\alpha\mu}\eta_{\beta\nu}-\eta_{\alpha\nu}\eta_{\beta\mu}\right)\bar{N}N+\cdots, \tag{6.2}$$

where N is the nucleon field (either p or n) with m_N its mass, and $\cdots$ denotes the traceless tensor part that is irrelevant for our purpose. Here we used that, in the chiral limit, the one-loop trace anomaly dominantly contributes to the nucleon mass,

$$\langle N|\frac{g_s^2}{32\pi^2}G^a_{\mu\nu}G^{a\mu\nu}|N\rangle = -\frac{m_N}{9}\bar{N}N, \tag{6.3}$$

where the coefficient in the right-hand-side is related to the beta function [122]. The photons are attached to the electron and induce the operator $\bar{e}i\gamma_5 e$ at one-loop [23] as shown in Fig. 6.1. This integral is logarithmically divergent, which is regulated by the heavy quark mass scale. Therefore, to the leading logarithmic accuracy, we obtain

$$C_S\frac{G_F}{\sqrt{2}} = -\frac{4Q_Q\alpha^2}{27}\frac{m_N m_e}{m_Q^3}\log\left(\frac{m_Q}{m_e}\right)\frac{d_Q}{e}, \tag{6.4}$$

where $\alpha = e^2/4\pi$ and m_e is the electron mass. By requiring $|d_e^{(\mathrm{equiv})}| < 1.1\times10^{-29}\,e\,\mathrm{cm}$, we obtain

$$|d_c| < 1.3\times10^{-20}\,e\,\mathrm{cm}, \tag{6.5}$$

for the charm quark and

$$|d_b| < 7.6 \times 10^{-19}\, e\,\mathrm{cm}, \tag{6.6}$$

for the bottom quark, respectively. The heavy quark EDM also induces the electron EDM at three-loop [90, 123], but its contribution to $d_e^{(\mathrm{equiv})}$ is negligible compared to C_S.

We now estimate the precision of our calculation. There is an uncertainty associated with Eq. (6.3), which is valid only in the chiral limit. However, the quark contribution to the nucleon mass is less than 10 % [124], and hence the uncertainty of Eq. (6.3) is also less than 10 %. Thanks to the lattice computations, these contributions are rather precisely known and the uncertainty in the non-perturbative matrix element can be further reduced by including the light quark contributions into our computation. Another uncertainty originates from our photon-loop computation, where we include only the leading logarithmic term. The uncertainty associated with this treatment may be estimated by changing the cut-off scale from m_Q to $2m_Q$, which results in $\lesssim 10\,\%$ change of the result for both the charm and bottom quarks. This can be further improved by performing the full two-loop computation, with the heavy quark and photon loops at the same time. Therefore, the precision of our C_S calculation is estimated to be 10 % and this can be further improved by properly including the quark contribution to the nucleon mass and performing the full two-loop computation of the photon-loop.

Our constraint is stronger than the one derived from $e^+e^- \to q\bar{q}$ at LEP by several orders of magnitude [119]. Although our constraint is weaker than [120] at its face value, there are two caveats. First, as we mentioned in the introduciton, the constraint in [120] is a re-interpretation of the bounds on the CEDMs $\tilde{d}_Q$ at the heavy quark mass scale, *i.e.*, $\tilde{d}_Q(m_Q)$. Both the quark EDM and CEDM at high energy scale Λ_{NP} contribute to the CEDM at lower energy due to the RG running, and hence $\tilde{d}_Q(m_Q)$ is given as a linear combination of $d_Q(\Lambda_{\mathrm{NP}})$ and $\tilde{d}_Q(\Lambda_{\mathrm{NP}})$. With only this information, one can put a constraint on only this particular linear combination of $d_Q(\Lambda_{\mathrm{NP}})$ and $\tilde{d}_Q(\Lambda_{\mathrm{NP}})$. Therefore the authors assume that there is no huge cancellation between $d_Q(\Lambda_{\mathrm{NP}})$ and $\tilde{d}_Q(\Lambda_{\mathrm{NP}})$, which allow them to derive a constraint solely on $d_Q(\Lambda_{\mathrm{NP}})$ and

thus on $d_Q(m_Q)$. Since our constraint directly applies to $d_Q(m_Q)$, it is an independent constraint, without any assumptions on the relative size of $d_Q(\Lambda_{\rm NP})$ and $\tilde{d}_Q(\Lambda_{\rm NP})$. Second, it is a complicated task to estimate the size of the neutron EDM induced by the Weinberg operator. Since [120] relies on the constraints on $\tilde{d}_Q(m_Q)$ from the Weinberg operator, it has a large hadronic uncertainty. In contrast, as we have just emphasized, our computation of C_S is precise and its uncertainty is well under control. Given the rapid progress of the paramagnetic EDM experiments, C_S will continue providing important and clean constraints on the heavy quark EDMs. In the next section, we will see that the neutron EDM provides a stronger constraint than C_S, comparable to [120], though with a larger hadronic uncertainty.

6.2 Neutron EDM

In Chapter 4 we have seen that the heavy quark EDM generates the CP-odd photon-gluon operator and the light quark EDM. Below the QCD scale, these CP-odd operators in turn generate the neutron EDM d_n, whose experimental upper bound is [22][1]

$$|d_n| < 1.8 \times 10^{-26}\, e\,\text{cm}. \tag{6.7}$$

In this section we translate this upper bound to the bound on the heavy quark EDM by estimating the size of the induced neutron EDM, with effects of the nonperturbative QCD taken into account (to the extent it is possible).

6.2.1 Light quark EDM contribution

We first study the neutron EDM induced by the light quark EDM $d_n^{(d_q)}$. Both the QCD sum rule and the quark model suggest that [18, 82, 125]

$$d_n^{(d_q)} = \frac{1}{3}\left(4d_d - d_u\right). \tag{6.8}$$

[1] The ^{199}Hg EDM experiment puts a similar constraint on the neutron EDM [21].

QCD sum rule calculations [82, 125] and more recently lattice calculations [126] give support to this simple formula within $\sim 30\%$ accuracy. We thus obtain

$$d_n^{(d_q)} = \frac{5(8\zeta(3)-7)}{72}\left(\frac{\alpha_s}{\pi}\right)^3 \frac{4m_d - m_u}{3m_Q} d_Q. \tag{6.9}$$

As we will see, there is another contribution to the neutron EDM from the CP-odd photon-gluon operator that leads to the QCD condensate power corrections in the light quark propagator. The rest of this section is devoted to estimate the size of this contribution.

6.2.2 CP-odd photon-gluon operator contribution

In Sec. 4.3 we saw that the heavy quark EDM generates the CP-odd photon-gluon operator

$$\mathcal{L}_{G^3\tilde{F}} = \frac{g_s^3 d_Q}{48\pi^2 m_Q^3}\mathrm{tr}_c\left[-G_{\mu\nu}G^{\mu\nu}G_{\rho\sigma}\tilde{F}^{\rho\sigma} + 2G^{\mu}{}_{\nu}G^{\nu}{}_{\rho}G^{\rho}{}_{\sigma}\tilde{F}^{\sigma}{}_{\mu}\right]. \tag{6.10}$$

Below the QCD scale the gluons confine and condense, and this operator feeds into the neutron EDM. We use the QCD sum rule technique [80] to estimate the size of the neutron EDM induced by this operator.

The starting point of the QCD sum rule is to define the two-point correlator

$$\Pi(p) \equiv i\int d^4x e^{ip\cdot x}\langle 0|\mathcal{T}\left\{\eta(x),\bar{\eta}(0)\right\}|0\rangle. \tag{6.11}$$

The interpolating function η is typically chosen as

$$\eta(x) = j_1(x) + \beta j_2(x), \tag{6.12}$$

and has an overlap with the neutron one-particle state. The functions j_1 and j_2 for the neutron are the same as the ones defined in Chapter 3:

$$j_1 = 2\epsilon_{ijk}\left(d_i^T\mathcal{C}\gamma_5 u_j\right)d_k, \quad j_2 = 2\epsilon_{ijk}\left(d_i^T\mathcal{C}u_j\right)\gamma_5 d_k, \tag{6.13}$$

As discussed in Chapter 3, the value of β cannot be chosen arbitrarily in the presence

of θ-dependent observables. However, it is not clear if there are similar caveats in other situations. Therefore, in this section, we treat β as a redundant parameter in our calculation. The QCD sum rule relies on the quark-hadron duality and evaluates this two-point correlator $\Pi(p)$ in the hadronic (phenomenological) side and the quark (OPE) side. On the phenomenological side, $\Pi(p)$ is expressed in terms of hadronic quantities such as the neutron mass and dipole moments. On the OPE side, $\Pi(p)$ is evaluated in terms of perturbative quarks and gluons with non-perturbative effects included in the form of the QCD condensates. One then obtains an estimation of the hadronic quantities by equating these two expressions, after the Borel transformation to reduce effects of excited states. In our case, we have external electromagnetic field $F_{\mu\nu}$ multiplying three Lorentz structures that in principle we can use to derive the sum rules: $\not{p}\sigma_{\mu\nu}\not{p}$, $\{\not{p}, \sigma_{\mu\nu}\}$ and $\sigma_{\mu\nu}$. In this chapter, we focus on the sum rule that follows from $\not{p}\sigma_{\mu\nu}\not{p}$ since it depends most strongly on the momentum and the vacuum susceptibilities are less relevant [127]. Moreover, it is computationally simple to derive the QCD sum rule based on this structure. In the following we evaluate $\Pi(p)$ in the OPE and phenomenological sides, respectively.

OPE side. We denote the light quark propagator as

$$\langle 0|\mathrm{T}\left\{q_i(x), \bar{q}_j(y)\right\}|0\rangle \equiv \delta_{ij} S(x,y), \tag{6.14}$$

where only the color-diagonal contribution is relevant for the QCD sum rule based on $\not{p}\sigma_{\mu\nu}\not{p}$ in our case. The CP-odd photon-gluon operator does not distinguish the up and down quarks, and thus we collectively denote u and d as q. With this expression, we obtain

$$\begin{aligned}\Pi_{\mathrm{OPE}}(p) = -24i \int d^4x e^{ip\cdot x} \big\{ &\mathrm{tr}\left[\gamma_5 S^c \gamma_5 S\right] S + S\gamma_5 S^c \gamma_5 S + \beta^2 \left(\gamma_5 S S^c S \gamma_5 + \mathrm{tr}\left[S^c S\right] \gamma_5 S \gamma_5\right) \\ &+\beta \left(S S^c \gamma_5 S \gamma_5 + \gamma_5 S \gamma_5 S^c S + \mathrm{tr}\left[S S^c \gamma_5\right] S \gamma_5 + \mathrm{tr}\left[S^c S \gamma_5\right] \gamma_5 S\right)\big\},\end{aligned} \tag{6.15}$$

where $S^c_{\alpha\beta} \equiv \left(\mathcal{C} S^T \mathcal{C}\right)_{\alpha\beta}$ and $S^T_{\alpha\beta} \equiv S_{\beta\alpha}$ with α and β being the spinor indices, and the trace is taken only over the spinor index. In our case the light quark propagator has

two contributions

$$S = S^{(0)} + S^{(CP)}, \tag{6.16}$$

where $S^{(0)}$ corresponds to the free quark propagator and is given by

$$S^{(0)}(x) = \frac{i\not{x}}{2\pi^2 x^4}, \tag{6.17}$$

while $S^{(CP)}$ is the CP-odd part which we compute from now.

The source inserted into the correlator has three gluon fields, and we follow the general idea of [128] where the Weinberg operator contribution to d_n was first evaluated, and where two gluons are treated perturbatively, while the third gluon field contributes to the quark-gluon condensate. With the QCD condensate background, we can write down the diagram

$$S_{ij}^{(CP)}(p) = $$ 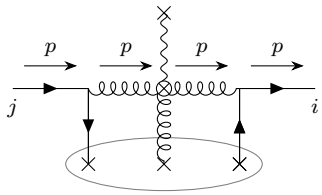

, (6.18)

where the crosses indicate the background fields, either the external photon or the QCD condensation of the quarks and gluons, and the cross dot is the insertion of the CP-odd photon-gluon operator (6.10). Since the QCD vacuum does not violate the Lorentz and color symmetries, we have

$$\left\langle q_i \bar{q}_j G^a_{\mu\nu} \right\rangle = -\frac{1}{192} T^a_{ij} \sigma_{\mu\nu} \left\langle \bar{q}\sigma \cdot Gq \right\rangle, \tag{6.19}$$

where $\sigma \cdot G = \sigma_{\mu\nu} G^{\mu\nu}$, and $\langle \cdots \rangle$ corresponds to the vacuum expectation value. We thus obtain

$$S_{ij}^{(CP)}(p) = \delta_{ij} S^{(CP)}(p) = i\delta_{ij} \frac{5\alpha_s^2 d_Q}{864 m_Q^3} \frac{g_s \langle \bar{q}\sigma \cdot Gq \rangle}{p^2} \frac{i}{\not{p}} \left[\sigma \cdot \tilde{F} - \frac{2p^\mu p^\nu}{p^2} \tilde{F}_{\mu\alpha} \sigma_\nu{}^\alpha \right] \frac{i}{\not{p}}. \tag{6.20}$$

Its Fourier transformation has an IR divergence, which in the dimensional regularization

leads

$$S^{(CP)}(x) = \frac{5\alpha_s^2 d_Q}{27648\pi^2 m_Q^3} g_s\langle\bar{q}\sigma\cdot Gq\rangle\Gamma(\epsilon_{\rm IR})\left(-\Lambda_{\rm IR}^2 x^2\right)^{-\epsilon_{\rm IR}}\tilde{F}\cdot\sigma, \tag{6.21}$$

where we take $d_{\rm IR} = 4+2\epsilon_{\rm IR}$ and keep only the logarithmic terms, with $\Lambda_{\rm IR}$ the IR cut-off scale. Due to the sensitivity to IR scale, calculations of further terms in the OPE are not possible. As a consequence, this evaluation should be viewed as an estimate, which cannot be systematically improved within QCD sum rule method. With the explicit forms of $S^{(0)}$ and $S^{(CP)}$, we obtain

$$\Pi_{\rm OPE}(p) = -\frac{5\alpha_s^2 d_Q}{2^{12}3^3\pi^4 m_Q^3}\langle\bar{q}\sigma\cdot g_s Gq\rangle\left[(1-\beta)^2\not{p}\tilde{F}\cdot\sigma\not{p} - 18\left(1-\beta^2\right)p^2\tilde{F}\cdot\sigma\right] I(p^2;\epsilon_{\rm IR},\epsilon_{\rm UV}), \tag{6.22}$$

where we perform the dimensional regularization to tame the UV divergence with $d_{\rm UV} = 4-2\epsilon_{\rm UV}$, and

$$I(p^2;\epsilon_{\rm IR},\epsilon_{\rm UV}) \equiv \Gamma(\epsilon_{\rm IR})\left(-\frac{\Lambda_{\rm IR}^2}{p^2}\right)^{-\epsilon_{\rm IR}}\Gamma(-\epsilon_{\rm UV}-\epsilon_{\rm IR})\left(-\frac{\mu^2}{p^2}\right)^{-\epsilon_{\rm UV}}, \tag{6.23}$$

with μ the renormalization scale. We then perform the Borel transformation, defined as [83]

$$\mathcal{B}\left[\Pi(p^2=-P^2)\right] = \frac{1}{\pi}\int_0^\infty \frac{dP^2}{M^2}e^{-P^2/M^2}\,{\rm Im}\left[\Pi(p)\right]_{p^2=-P^2}. \tag{6.24}$$

We thus obtain the $\not{p}\sigma_{\mu\nu}\not{p}$ part as

$$\mathcal{B}\left[\Pi_{\rm OPE}(p^2=-P^2)\right]_{\not{p}\tilde{F}\cdot\sigma\not{p}} = -\frac{5\alpha_s^2 d_Q}{2^{12}3^3\pi^4 m_Q^3}(1-\beta)^2\langle\bar{q}\sigma\cdot g_s Gq\rangle\log\left(\frac{M^2}{\Lambda_{\rm IR}^2}\right). \tag{6.25}$$

Taking the imaginary part of $I(p^2;\epsilon_{\rm IR},\epsilon_{\rm UV})$ is somewhat subtle, and we provide details in App. D. There we also clarify the physical meaning of the scale $\Lambda_{\rm IR}$; it should be identified with the mass of the constituent quarks. This expression is to be compared with the phenomenological expression.

Phenomenological side. On the phenomenological side, the two-point correlator with the neutron EDM insertion is expressed as

$$\Pi_{\rm pheno}(p) = -\lambda_n^2 \left[\frac{\not{p} + m_n}{p^2 - m_n^2} - \frac{d_n}{2(p^2 - m_n^2)^2} \not{p} \tilde{F} \cdot \sigma \not{p} + \cdots \right], \tag{6.26}$$

where m_n is the neutron mass and λ_n parametrizes the overlap between the interpolating function η and the neutron one-particle state. After the Borel transformation, we obtain

$$\mathcal{B}\left[\Pi_{\rm pheno}(p^2 = -P^2)\right]_{\not{p}\tilde{F}\cdot\sigma\not{p}} = \frac{\lambda_n^2 d_n}{2M^4} e^{-m_n^2/M^2} + \cdots, \tag{6.27}$$

where $\cdots$ expresses contributions from excited states which we ignore in the following.

Sum rule. The QCD sum rule of the neutron EDM is obtained by equating Eqs. (6.25) and (6.27). We thus obtain

$$\frac{\lambda_n^2 d_n^{(G^3\tilde{F})}}{2M^4} e^{-m_n^2/M^2} = -\frac{5\alpha_s^2 d_Q}{2^{12}3^3\pi^4 m_Q^3} (1-\beta)^2 \langle \bar{\psi}\sigma \cdot g_s G\psi \rangle \log\left(\frac{M^2}{\Lambda_{\rm IR}^2}\right), \tag{6.28}$$

where $d_n^{(\tilde{F}G^3)}$ is the neutron EDM induced by the CP-odd photon-gluon operator (to distinguish it from the one induced by the light quark EDM). We may use the Ioffe formula for the nucleon mass [85, 86][2]

$$\frac{\lambda_n^2 m_n}{M^4} e^{-m_n^2/M^2} = -\frac{7 - 2\beta - 5\beta^2}{16\pi^2} \langle \bar{q}q \rangle, \tag{6.29}$$

to eliminate λ_n. Then we obtain the QCD sum rule estimation of the neutron EDM

$$d_n^{(G^3\tilde{F})} = d_Q \times \frac{5\alpha_s^2}{2^7 3^3 \pi^2} \frac{m_n m_0^2}{m_Q^3} \frac{1-\beta}{7+5\beta} \log\left(\frac{M^2}{\Lambda_{\rm IR}^2}\right), \tag{6.30}$$

where we used $\langle q\sigma \cdot g_s G q \rangle = m_0^2 \langle \bar{q}q \rangle$ with $m_0^2 = 0.8\,\text{GeV}^2$ [129].

[2]The Ioffe formula in [86] is derived based on $\chi_{\rm SR}/2$ which is equivalent to our $-\eta/2$ with $\beta = -1$. Therefore the normalization of λ_n differs by a factor two.

6.2.3 Constraint on heavy quark EDM

The neutron EDM has two contributions, induced by the light quark EDM and the CP-odd photon-gluon operators, and is given by

$$d_n = d_n^{(d_q)} + d_n^{(G^3\tilde{F})}, \tag{6.31}$$

where

$$d_n^{(d_q)} = d_Q \times \frac{5(8\zeta(3)-7)}{72}\left(\frac{\alpha_s}{\pi}\right)^3 \frac{4m_d - m_u}{3m_Q}, \quad d_n^{(G^3\tilde{F})} = d_Q \times \frac{5\alpha_s^2}{2^7 3^3 \pi^2}\frac{m_n m_0^2}{m_Q^3}\log\left(\frac{M^2}{\Lambda_{\rm IR}^2}\right), \tag{6.32}$$

and we take $\beta = -1$ following [85, 130, 131]. The parameters should be evaluated at m_Q for the former contribution, and at the scale close to $\Lambda_{\rm QCD}$ for the latter contribution. We use $m_c = 1.27\,\text{GeV}$, $m_b = 4.18\,\text{GeV}$, $\alpha_s(m_c) = 0.38$ and $\alpha_s(m_b) = 0.223$ [132]. The light quark masses (in the $\overline{\rm MS}$ scheme) also depend on the energy scale, and we take $m_u(m_c) = 2.5\,\text{MeV}$ $m_d(m_c) = 5.4\,\text{MeV}$, $m_u(m_b) = 1.8\,\text{MeV}$ and $m_d(m_b) = 4.0\,\text{MeV}$ that we obtain by running the light quark masses at $2\,\text{GeV}$ following [132]. Finally we take $\alpha_s = 0.5$, $\Lambda_{\rm IR} = 300\,\text{MeV}$ and $M = 800\,\text{MeV}$ for the QCD sum rule estimation for definiteness. For these values, the contribution from the CP-odd photon-gluon operator is larger by a factor of 16 and 10 for the charm and bottom quarks, respectively. In the bottom quark case, the explicit quark mass suppression is compensated by the running of the strong coupling, and the CP-odd photon-gluon operator is still larger than the light quark EDM even with the relative suppression factor $1/m_b^2$. By requiring that $|d_n| < 1.8 \times 10^{-26}\,e\,\text{cm}$, we obtain

$$|d_c| < 6 \times 10^{-22}\,e\,\text{cm}, \tag{6.33}$$

for the charm quark, and

$$|d_b| < 2 \times 10^{-20}\,e\,\text{cm}, \tag{6.34}$$

for the bottom quark, respectively.

The constraint from d_n is stronger than that from C_S by more than an order of

magnitude. However, one should note that the estimation of d_n has a large hadronic uncertainty. Indeed, the final result is affected by a factor two if we use the sum rule of the nucleon kinetic term instead of the mass term for λ_n. There are also uncertainties related to the choice of M and β which can again result in a factor of a few difference in the final result. Therefore our constraint here should be understood as an order-of-magnitude estimation and the numerical factor should be taken with care. In contrast, our calculation of C_S is far more precise. Its uncertainty is estimated to be $\sim 10\,\%$ and can be further reduced if needed (see the end of Sec. 6.1). In this sense, the constraints from d_n and C_S are complementary to each other; d_n puts a stronger constraint on the heavy quark EDM, while the calculation of C_S is cleaner and its uncertainty is well under control.

Our constraint on d_c is stronger than [120] by a factor two, while the one on d_b is weaker by a factor two. However, as we noted in the introduction and the end of Sec. 6.1, our constraint directly applies to $d_c(m_c)$ and $d_b(m_b)$, and is independent of the one in [120].

6.3 Discussion

In this chapter, we have derived indirect limits on the charm and bottom quark EDMs. The charm and bottom quark EDMs generate the CP-odd photon-gluon operators and the light quark EDMs after integrating out the charm and bottom quarks. Photon-gluon operators contribute to the semi-leptonic CP-odd operator C_S (and ultimately to paramagnetic AMO EDMs) as well as to the neutron EDM at a non-perturbative level. Quark EDM dominantly contributes to the neutron and nuclear EDMs. Performing our evaluation and using the current limits, we obtain

$$|d_c| < 1.3 \times 10^{-20}\, e\,\mathrm{cm}, \quad |d_b| < 7.6 \times 10^{-19}\, e\,\mathrm{cm}, \tag{6.35}$$

from the paramagnetic EDM experiments, and

$$|d_c| < 6 \times 10^{-22}\, e\,\mathrm{cm}, \quad |d_b| < 2 \times 10^{-20}\, e\,\mathrm{cm}, \tag{6.36}$$

from the neutron EDM experiment, respectively. Although the constraint from the neutron EDM is stronger, it has a larger hadronic uncertainty. The uncertainty of the constraint from the paramagnetic EDM is estimated as 10 % and can be improved if needed, while the uncertainty from the neutron EDM can be a factor of a few. Our constraint is independent of the one given in [120] in the sense that our constraint directly applies to the EDM operators at the quark mass threshold. By assuming a simple scaling of $d_Q/e \propto (\alpha/\pi) m_Q/\Lambda_Q^2$, we may translate our constraint as a lower bound on CP-odd new physics scale: $\Lambda_c > 70\,\mathrm{GeV}$ and $\Lambda_b > 20\,\mathrm{GeV}$ from the paramagnetic EDM experiment, and $\Lambda_c > 300\,\mathrm{GeV}$ and $\Lambda_b > 100\,\mathrm{GeV}$ from the neutron EDM experiment.

Our result provides an important benchmark to overcome for the LHC based measurements of the charmed baryon EDMs [34–38]. The idea of using the bent crystal technique for studying electromagnetic properties of baryons containing a heavy quark is very appealing. However, given the strength of the bounds derived in our work, and the necessity to satisfy independent constraints from d_n and C_S (hence removing a chance of accidentally large $d_{c(b)}$ due to cancellations), one may want to re-evaluate the main goal of the charmed baryon experiment. While it will be difficult to match the indirect sensitivity to $d_{c(b)}$, the planned measurement may achieve sufficient accuracy to extract the values of the magnetic moments $\mu_{c(b)}$ and compare it with the QCD predictions.

Chapter 7

Summary and Outlook

In this thesis, an extensive discussion of the sources of CP violations and their connections to EDMs is provided from the perspective of particle theory. While a complete analysis of EDMs requires a broad spectrum of input ranging from the fundamental high energy scale all the way down to the nuclear and atomic scale, the leptonic and semi-leptonic nature of paramagnetic EDMs makes it possible for EDMs of such systems to be predicted based primarily on particle physics, and the experimental capability of measuring the neutron EDM opens a window for probing the physics at high energy scale without worrying about the nuclear and atomic effects. If any new CP-violating physics exists in nature, it is expected that it would contribute to the EDMs of the SM particles, which experiments can indirectly constrain. These aspects of EDMs are explored in this thesis.

In Chapter 2, the contribution to the C_S operator defined in Eq.(2.2) from the KM phase $\delta_{\rm KM}$ is revisited, the new contribution, generated by the Kaon change diagram in Fig. 2.1 at EW^3 order, is found to play the dominant role in the SM prediction for paramagnetic EDM. The uncertainty of the calculation is estimated in Eq.(2.15) and Eq.(2.16) and is under better control than previous estimates. The result, $C_S(\text{LO}+\text{NLO}) \simeq 6.9\times10^{-16}$, corresponds to an equivalent electron EDM for the ThO system given by $d_e^{\rm equiv} \simeq 1.0\times10^{-35}\, e\,\text{cm}$. While this is still below the current constraint by a few orders of magnitude, it is not unimaginable for the experimental sensitivity to reach a comparable size in the next few rounds of EDM experiments.

In Chapter 3, the caveat in calculating the θ-dependent quantity with interpolating

currents is discussed with the QCD sum rule. It is shown that an arbitrary choice of the interpolating current leads to an unphysical θ-dependence in the chiral limit. The origin of this unphysical phase is discussed in section 3.2. To avoid this issue, the choice of $\beta = \pm 1$ in the interpolating currents is required, and the procedure to remove the unphysical θ-dependence is discussed in section 3.4. The calculation for the θ-induced nucleon EDM is presented to show the validity of these procedures. The result, Eq.(3.40) and Eq.(3.54) shows reasonable agreement with the chiral perturbation theory calculation. While the QCD sum rule is used in the calculation, the issue arises from the choice of interpolating currents, and it is expected that lattice QCD calculations will have the same problem as well. Given the inconclusive status of lattice calculations on $d_n(\theta)$, the hope is that the same procedure could be checked on the lattice for consistency.

In Chapter 4, with the input of an effective heavy fermion EDM operator, the consequences below the corresponding fermion mass scale are discussed. When the momentum transfer is comparable to the heavy fermion mass, the heavy fermion EDMs induce light fermion EDMs, either through another three photons in the lepton case or another three gluons in the quark case. The results are given in Eq.(4.7), Eq.(4.8),and Eq.(4.9). When the momentum transfer is soft, integrating out the heavy fermion generates the CP-odd interaction among four gauge bosons, as given in Eq.(4.28), Eq.(4.29), and Eq.(4.30). These results are a starting point for discussing the indirect constraints on heavy fermion EDMs in Chapter 5 and 6.

In Chapter 5, the indirect constraints on the muon EDM are derived. With the magnetic field from the valence neutron and the electron field from the nucleus, the muon EDM generates a Schiff moment of the nucleus, contributing to the diamagnetic EDM. For the ^{199}Hg nucleus, the coefficient for this process is obtained in Eq.(5.13). With the electric field from the nucleus and the CP-odd $\boldsymbol{E}\cdot\boldsymbol{B}$ interaction on the electron side, the muon EDM generates an effective C_S operator as shown in Eq.(5.20), which together with the muon-EDM-induced electron EDM contributes to the paramagnetic EDM. Combining with the experimental constraints on paramagnetic and diamagnetic systems, the result $d_\mu(^{199}\text{Hg}) < 6\times10^{-20} e\text{cm}$ and $d_\mu(\text{HfF}^+) < 8.9\times10^{-21} e\text{cm}$, constitute approximately three- and twenty-fold improvements over the limits on d_μ extracted from the BNL muon beam experiment.

In Chapter 6, the indirect constraints on the charm and bottom EDM are derived. These heavy quarks induce the C_S operator through the diagram in Fig.6.1, and induce the neutron EDM both through the light quark EDM and through the $G^3\tilde{F}$ operator. The constraints on paramagnetic EDM and neutron EDM then provide indirect constraints on the charm and bottom quark EDM, given in Eq.(6.5) , Eq.(6.6), and Eq.(6.33) and Eq.(6.34), respectively.

The last few decades have seen rapid progress in the physics of EDMs, both theoretically and experimentally. With the efforts from particle physics and nuclear theory, it is finally possible to identify the SM contributions to the EDMs of all common experimental systems, and for the first time did EDM experiments reach the level of $10^{-30}e$cm, further paving the way towards the SM predictions and constraining the BSM physics. The next round of EDM experiments is expecting to further push the frontiers of experimental accuracy by another order of magnitude, as well as performing measurements for more systems with complementary sensitivity to various CP-violating parameters (See [133] for a review on proposed EDM experiments). Given that the orders-of-magnitude improvements in experiments continue to be possible, there is hope that, after the searches for EDMs for almost a century, a non-zero signal could eventually be detected in the next few decades. By that time, either the existence of extra sources of CP-violation is confirmed, which would provide hints for the energy scale and structure of new physics, or the SM continues to be the dominant source of EDMs, in which case the need for a precise determination of the SM contribution to EDMs at the percent level on the theory side would be stronger than ever before to identify possible BSM contributions.

To prepare for this exciting era of discovery, a significant amount of theoretical effort will be needed. Past experience has shown that, despite being a well-established theory, there may still be room for refining the predictions on EDMs from the SM side. Therefore, continuous attention to identifying all possible mechanisms for the SM to induce EDMs will be desirable. The next generation of neutrino experiments also brings the hope of probing CP-violation in the neutrino sector. If indeed confirmed by experiments, given that this would be the only known new source of CP-violation, it would be worthwhile to have a prediction on the EDMs induced by the neutrinos' CP violation, although the size of the EDMs induced is likely to be small. Further

going beyond the SM, further exploration of the CP-violations in new physics models is needed, and it would be vital to see how the baryogenesis requirements and EDM constraints could be satisfied simultaneously for any such models. Additionally, while most theoretical efforts on BSM CP violations are focused on the exploration of TeV-scale new physics, in principle, the exceptional precision of EDM experiments may also bring sensitivity to light new degrees of freedom, which may deserve further scrutiny. (See [134, 135] for some discussions.) Regardless of the source of CP-violation being considered, improving the precision of theoretical calculations is crucial for building a reliable connection between theory and experiment, and given the non-perturbative nature of QCD and the complexity of many-body interactions in nuclear physics, the progress along this direction is particularly challenging. The roles played by the quark CEDMs, the Weinberg operator, and the four-quark operator in nucleon EDMs and nucleon forces are still poorly understood. While it is possible and desirable to calculate their contributions on the lattice, the reliability of lattice calculations themselves has to be checked first, as discussed in this thesis. Further evaluation of how the nucleon EDMs and nucleon forces contribute to the nuclear and atomic EDMs requires nuclear many-body calculations, which are only possible for relatively light nuclei at this moment. A considerable improvement in both aspects, as well as a careful evaluation of uncertainties at each step in the tower of EFTs, is needed to build a complementary picture between theory and experiments.

References

[1] Y. Ema, T. Gao, and M. Pospelov, "Improved Indirect Limits on Muon Electric Dipole Moment," *Phys. Rev. Lett.* **128** (2022) no. 13, 131803, arXiv:2108.05398 [hep-ph].

[2] Y. Ema, T. Gao, and M. Pospelov, "Standard Model prediction for paramagnetic EDMs," arXiv:2202.10524 [hep-ph].

[3] Y. Ema, T. Gao, and M. Pospelov, "Improved indirect limits on charm and bottom quark EDMs," *JHEP* **07** (2022) 106, arXiv:2205.11532 [hep-ph].

[4] Y. Ema, T. Gao, and M. Pospelov, "Reevaluation of heavy-fermion-induced electron EDM at three loops," *Phys. Lett. B* **835** (2022) 137496, arXiv:2207.01679 [hep-ph].

[5] Y. Ema, T. Gao, M. Pospelov, and A. Ritz, "Chiral properties of the nucleon interpolating current and θ-dependent observables," *Phys. Rev. D* **110** (2024) no. 3, 034028, arXiv:2405.08856 [hep-ph].

[6] Y. Ema, T. Gao, and M. Pospelov, "Muon spin force," *Phys. Rev. D* **110** (2024) no. 7, 075024, arXiv:2308.01356 [hep-ph].

[7] Y. Ema, T. Gao, W. Ke, Z. Liu, K.-F. Lyu, and I. Mahbub, "Momentum shift and on-shell constructible massive amplitudes," *Phys. Rev. D* **110** (2024) no. 10, 105003, arXiv:2403.15538 [hep-ph].

[8] Y. Ema, T. Gao, W. Ke, Z. Liu, K.-F. Lyu, and I. Mahbub, "Momentum shift and on-shell recursion relation for electroweak theory," *Phys. Rev. D* **110** (2024) no. 10, 105002, arXiv:2407.14587 [hep-ph].

[9] T.-D. Lee and C.-N. Yang, "Question of parity conservation in weak interactions," *Physical Review* **104** (1956) no. 1, 254.

[10] C.-S. Wu, E. Ambler, R. W. Hayward, D. D. Hoppes, and R. P. Hudson, "Experimental test of parity conservation in beta decay," *Physical review* **105** (1957) no. 4, 1413.

[11] J. H. Christenson, J. W. Cronin, V. L. Fitch, and R. Turlay, "Evidence for the 2 π decay of the k 2 0 meson," *Physical Review Letters* **13** (1964) no. 4, 138.

[12] J. Schwinger, "The theory of quantized fields. i," *Physical Review* **82** (1951) no. 6, 914.

[13] G. Lüders, "On the equivalence of invariance under time reversal and under particle-antiparticle conjugation for relativistic field theories," *Dan. Mat. Fys. Medd.* **28** (1954) 1–17.

[14] W. Pauli, L. Rosenfeld, and V. Weisskopf, "Niels bohr and the development of physics," *British Journal for the Philosophy of Science* **7** (1957) no. 28, .

[15] A. D. Sakharov, "Violation of CP Invariance, C asymmetry, and baryon asymmetry of the universe," *Pisma Zh. Eksp. Teor. Fiz.* **5** (1967) 32–35.

[16] E. Purcell and N. Ramsey, "On the possibility of electric dipole moments for elementary particles and nuclei," *Physical Review* **78** (1950) no. 6, 807.

[17] I. B. Khriplovich and S. K. Lamoreaux, *CP violation without strangeness: electric dipole moments of particles, atoms, and molecules*. Springer Science & Business Media, 2012.

[18] M. Pospelov and A. Ritz, "Electric dipole moments as probes of new physics," *Annals Phys.* **318** (2005) 119–169, arXiv:hep-ph/0504231.

[19] **ACME** Collaboration, V. Andreev *et al.*, "Improved limit on the electric dipole moment of the electron," *Nature* **562** (2018) no. 7727, 355–360.

[20] T. S. Roussy *et al.*, "An improved bound on the electron's electric dipole moment," *Science* **381** (2023) no. 6653, adg4084, arXiv:2212.11841 [physics.atom-ph].

[21] B. Graner, Y. Chen, E. G. Lindahl, and B. R. Heckel, "Reduced Limit on the Permanent Electric Dipole Moment of Hg199," *Phys. Rev. Lett.* **116** (2016) no. 16, 161601, arXiv:1601.04339 [physics.atom-ph]. [Erratum: Phys.Rev.Lett. 119, 119901 (2017)].

[22] C. Abel *et al.*, "Measurement of the Permanent Electric Dipole Moment of the Neutron," *Phys. Rev. Lett.* **124** (2020) no. 8, 081803, arXiv:2001.11966 [hep-ex].

[23] V. V. Flambaum, M. Pospelov, A. Ritz, and Y. V. Stadnik, "Sensitivity of EDM experiments in paramagnetic atoms and molecules to hadronic CP violation," *Phys. Rev. D* **102** (2020) no. 3, 035001, arXiv:1912.13129 [hep-ph].

[24] H. Mulder, R. Timmermans, and J. de Vries, "Probing the QCD $\bar{\theta}$ term with paramagnetic molecules," arXiv:2502.06406 [hep-ph].

[25] W. Dekens, J. De Vries, J. Bsaisou, W. Bernreuther, C. Hanhart, U.-G. Meißner, A. Nogga, and A. Wirzba, "Unraveling models of cp violation through electric dipole moments of light nuclei," *Journal of high energy physics* **2014** (2014) no. 7, 1–57.

[26] V. F. Dmitriev and R. A. Sen'kov, "P violating and T violating Schiff moment of the mercury nucleus," *Phys. Atom. Nucl.* **66** (2003) 1940–1945, arXiv:nucl-th/0304048.

[27] R. J. Crewther, P. Di Vecchia, G. Veneziano, and E. Witten, "Chiral Estimate of the Electric Dipole Moment of the Neutron in Quantum Chromodynamics," *Phys. Lett. B* **88** (1979) 123. [Erratum: Phys.Lett.B 91, 487 (1980)].

[28] R. Crewther, P. Di Vecchia, G. Veneziano, and E. Witten, "Erratum: Chiral estimate of the electric dipole moment of the neutron in quantum chromodynamics [phys. lett. 88b (1979) 123]," *Physics Letters B* **91** (1980) no. 3-4, 487–487.

[29] M. Pospelov and A. Ritz, "Theta induced electric dipole moment of the neutron via QCD sum rules," *Phys. Rev. Lett.* **83** (1999) 2526–2529, arXiv:hep-ph/9904483.

[30] A. Shindler, T. Luu, and J. de Vries, "Nucleon electric dipole moment with the gradient flow: The θ-term contribution," *Phys. Rev. D* **92** (2015) no. 9, 094518, arXiv:1507.02343 [hep-lat].

[31] C.-Y. Seng, "Reexamination of The Standard Model Nucleon Electric Dipole Moment," *Phys. Rev. C* **91** (2015) no. 2, 025502, arXiv:1411.1476 [hep-ph].

[32] A. Adelmann *et al.*, "Search for a muon EDM using the frozen-spin technique," arXiv:2102.08838 [hep-ex].

[33] **Muon (g-2)** Collaboration, G. W. Bennett *et al.*, "An Improved Limit on the Muon Electric Dipole Moment," *Phys. Rev. D* **80** (2009) 052008, arXiv:0811.1207 [hep-ex].

[34] V. G. Baryshevsky, "The possibility to measure the magnetic moments of short-lived particles (charm and beauty baryons) at LHC and FCC energies using the phenomenon of spin rotation in crystals," *Phys. Lett. B* **757** (2016) 426–429.

[35] F. J. Botella, L. M. Garcia Martin, D. Marangotto, F. M. Vidal, A. Merli, N. Neri, A. Oyanguren, and J. R. Vidal, "On the search for the electric dipole moment of strange and charm baryons at LHC," *Eur. Phys. J. C* **77** (2017) no. 3, 181, arXiv:1612.06769 [hep-ex].

[36] A. S. Fomin *et al.*, "Feasibility of measuring the magnetic dipole moments of the charm baryons at the LHC using bent crystals," *JHEP* **08** (2017) 120, arXiv:1705.03382 [hep-ph].

[37] E. Bagli *et al.*, "Electromagnetic dipole moments of charged baryons with bent crystals at the LHC," *Eur. Phys. J. C* **77** (2017) no. 12, 828, arXiv:1708.08483 [hep-ex]. [Erratum: Eur.Phys.J.C 80, 680 (2020)].

[38] S. Aiola *et al.*, "Progress towards the first measurement of charm baryon dipole moments," *Phys. Rev. D* **103** (2021) no. 7, 072003, arXiv:2010.11902 [hep-ex].

[39] **ACME** Collaboration, V. Andreev *et al.*, "Improved limit on the electric dipole moment of the electron," *Nature* **562** (2018) no. 7727, 355–360.

[40] A. C. Vutha, M. Horbatsch, and E. A. Hessels, "Oriented polar molecules in a solid inert-gas matrix: a proposed method for measuring the electric dipole moment of the electron," *Atoms* **6** (2018) no. 1, 3, arXiv:1710.08785 [physics.atom-ph].

[41] A. C. Vutha, M. Horbatsch, and E. A. Hessels, "Orientation-dependent hyperfine structure of polar molecules in a rare-gas matrix: A scheme for measuring the electron electric dipole moment," *Phys. Rev. A* **98** (2018) no. 3, 032513, arXiv:1806.06774 [physics.atom-ph].

[42] T. Fleig and D. DeMille, "Theoretical aspects of radium-containing molecules amenable to assembly from laser-cooled atoms for new physics searches," *New J. Phys.* **23** (2021) no. 11, 113039, arXiv:2108.02809 [physics.atom-ph].

[43] E. P. Shabalin, "Electric Dipole Moment of Quark in a Gauge Theory with Left-Handed Currents," *Sov. J. Nucl. Phys.* **28** (1978) 75.

[44] I. B. Khriplovich, "Quark Electric Dipole Moment and Induced θ Term in the Kobayashi-Maskawa Model," *Phys. Lett. B* **173** (1986) 193–196.

[45] M. E. Pospelov and I. B. Khriplovich, "Electric dipole moment of the W boson and the electron in the Kobayashi-Maskawa model," *Sov. J. Nucl. Phys.* **53** (1991) 638–640.

[46] A. Czarnecki and B. Krause, "Neutron electric dipole moment in the standard model: Valence quark contributions," *Phys. Rev. Lett.* **78** (1997) 4339–4342, arXiv:hep-ph/9704355.

[47] I. B. Khriplovich and A. R. Zhitnitsky, "What Is the Value of the Neutron Electric Dipole Moment in the Kobayashi-Maskawa Model?," *Phys. Lett. B* **109** (1982) 490–492.

[48] M. B. Gavela, A. Le Yaouanc, L. Oliver, O. Pene, J. C. Raynal, and T. N. Pham, "CP Violation Induced by Penguin Diagrams and the Neutron Electric Dipole Moment," *Phys. Lett. B* **109** (1982) 215–220.

[49] V. V. Flambaum, I. B. Khriplovich, and O. P. Sushkov, "On the Possibility to Study P Odd and T Odd Nuclear Forces in Atomic and Molecular Experiments," *Sov. Phys. JETP* **60** (1984) 873.

[50] J. F. Donoghue, B. R. Holstein, and M. J. Musolf, "Electric Dipole Moments of Nuclei," *Phys. Lett. B* **196** (1987) 196–202.

[51] B. H. J. McKellar, S. R. Choudhury, X.-G. He, and S. Pakvasa, "The Neutron Electric Dipole Moment in the Standard K^-m Model," *Phys. Lett. B* **197** (1987) 556–560.

[52] Y. Yamaguchi and N. Yamanaka, "Large long-distance contributions to the electric dipole moments of charged leptons in the standard model," *Phys. Rev. Lett.* **125** (2020) 241802, arXiv:2003.08195 [hep-ph].

[53] M. Pospelov and A. Ritz, "CKM benchmarks for electron electric dipole moment experiments," *Phys. Rev. D* **89** (2014) no. 5, 056006, arXiv:1311.5537 [hep-ph].

[54] V. A. Dzuba, V. V. Flambaum, and C. Harabati, "Relations between matrix elements of different weak interactions and interpretation of the PNC and EDM measurements in atoms and molecules," *Phys. Rev. A* **84** (2011) no. 5, 052108, arXiv:1109.6082 [physics.atom-ph].

[55] T. Inami and C. S. Lim, "Effects of Superheavy Quarks and Leptons in Low-Energy Weak Processes k(L) —> mu anti-mu, K+ —> pi+ Neutrino anti-neutrino and K0 <—> anti-K0," *Prog. Theor. Phys.* **65** (1981) 297. [Erratum: Prog.Theor.Phys. 65, 1772 (1981)].

[56] M. Gorbahn and U. Haisch, "Charm Quark Contribution to K(L) —> mu+ mu- at Next-to-Next-to-Leading," *Phys. Rev. Lett.* **97** (2006) 122002, arXiv:hep-ph/0605203.

[57] A. J. Buras, J. Girrbach, D. Guadagnoli, and G. Isidori, "On the Standard Model prediction for BR(Bs,d to mu+ mu-)," *Eur. Phys. J. C* **72** (2012) 2172, arXiv:1208.0934 [hep-ph].

[58] G. Isidori and R. Unterdorfer, "On the short distance constraints from K(L,S) —> mu+ mu-," *JHEP* **01** (2004) 009, arXiv:hep-ph/0311084.

[59] G. D'Ambrosio and T. Kitahara, "Direct CP Violation in $K \to \mu^+\mu^-$," *Phys. Rev. Lett.* **119** (2017) no. 20, 201802, arXiv:1707.06999 [hep-ph].

[60] J. Bijnens, H. Sonoda, and M. B. Wise, "On the Validity of Chiral Perturbation Theory for Weak Hyperon Decays," *Nucl. Phys. B* **261** (1985) 185–198.

[61] M. A. Shifman, A. I. Vainshtein, and V. I. Zakharov, "Light Quarks and the Origin of the Delta I = 1/2 Rule in the Nonleptonic Decays of Strange Particles," *Nucl. Phys. B* **120** (1977) 316–324.

[62] J. Tandean and G. Valencia, "CP violation in hyperon nonleptonic decays within the standard model," *Phys. Rev. D* **67** (2003) 056001, arXiv:hep-ph/0211165.

[63] E. E. Jenkins, "Hyperon nonleptonic decays in chiral perturbation theory," *Nucl. Phys. B* **375** (1992) 561–581.

[64] D. McKeen, M. Pospelov, and A. Ritz, "Electric dipole moment signatures of PeV-scale superpartners," *Phys. Rev. D* **87** (2013) no. 11, 113002, arXiv:1303.1172 [hep-ph].

[65] W. Dekens, J. de Vries, M. Jung, and K. K. Vos, "The phenomenology of electric dipole moments in models of scalar leptoquarks," *JHEP* **01** (2019) 069, arXiv:1809.09114 [hep-ph].

[66] M. A. Shifman, A. I. Vainshtein, and V. I. Zakharov, "Can Confinement Ensure Natural CP Invariance of Strong Interactions?," *Nucl. Phys. B* **166** (1980) 493–506.

[67] S. Aoki and A. Gocksch, "The Neutron Electric Dipole Moment in Lattice QCD," *Phys. Rev. Lett.* **63** (1989) 1125. [Erratum: Phys.Rev.Lett. 65, 1172 (1990)].

[68] D. Guadagnoli, V. Lubicz, G. Martinelli, and S. Simula, "Neutron electric dipole moment on the lattice: A Theoretical reappraisal," *JHEP* **04** (2003) 019, arXiv:hep-lat/0210044.

[69] M. Abramczyk, S. Aoki, T. Blum, T. Izubuchi, H. Ohki, and S. Syritsyn, "Lattice calculation of electric dipole moments and form factors of the nucleon," *Phys. Rev. D* **96** (2017) no. 1, 014501, arXiv:1701.07792 [hep-lat].

[70] J. Dragos, T. Luu, A. Shindler, J. de Vries, and A. Yousif, "Confirming the Existence of the strong CP Problem in Lattice QCD with the Gradient Flow," arXiv:1902.03254 [hep-lat].

[71] C. Alexandrou, A. Athenodorou, K. Hadjiyiannakou, and A. Todaro, "Neutron electric dipole moment using lattice QCD simulations at the physical point," *Phys. Rev. D* **103** (2021) no. 5, 054501, arXiv:2011.01084 [hep-lat].

[72] T. Bhattacharya, V. Cirigliano, R. Gupta, E. Mereghetti, and B. Yoon, "Contribution of the QCD Θ-term to the nucleon electric dipole moment," *Phys. Rev. D* **103** (2021) no. 11, 114507, arXiv:2101.07230 [hep-lat].

[73] T. Bhattacharya, V. Cirigliano, R. Gupta, E. Mereghetti, and B. Yoon, "Calculation of neutron electric dipole moment due to the QCD topological term, Weinberg three-gluon operator and the quark chromoelectric moment," *PoS* **LATTICE2021** (2022) 567, arXiv:2203.03746 [hep-lat].

[74] χ**QCD** Collaboration, J. Liang, A. Alexandru, T. Draper, K.-F. Liu, B. Wang, G. Wang, and Y.-B. Yang, "Nucleon electric dipole moment from the θ term with lattice chiral fermions," *Phys. Rev. D* **108** (2023) no. 9, 094512, arXiv:2301.04331 [hep-lat].

[75] F. He, M. Abramczyk, T. Blum, T. Izubuchi, H. Ohki, and S. Syritsyn, "The calculations of Nucleon Electric Dipole Moment using background field on Lattice QCD," in *40th International Symposium on Lattice Field Theory*. 11, 2023. arXiv:2311.06106 [hep-lat].

[76] G. Schierholz, "Absence of strong CP violation," arXiv:2403.13508 [hep-ph].

[77] A. Pich and E. de Rafael, "Strong CP violation in an effective chiral Lagrangian approach," *Nucl. Phys. B* **367** (1991) 313–333.

[78] A. S. Zhevlakov, M. Gorchtein, A. N. Hiller Blin, T. Gutsche, and V. E. Lyubovitskij, "Bounds on rare decays of η and η' mesons from the neutron EDM," *Phys. Rev. D* **99** (2019) no. 3, 031703, arXiv:1812.00171 [hep-ph].

[79] A. S. Zhevlakov and V. E. Lyubovitskij, "Deuteron EDM induced by CP violating couplings of pseudoscalar mesons," *Phys. Rev. D* **101** (2020) no. 11, 115041, arXiv:2003.12217 [hep-ph].

[80] M. A. Shifman, A. I. Vainshtein, and V. I. Zakharov, "QCD and Resonance Physics. Theoretical Foundations," *Nucl. Phys. B* **147** (1979) 385–447.

[81] M. Pospelov and A. Ritz, "Theta vacua, QCD sum rules, and the neutron electric dipole moment," *Nucl. Phys. B* **573** (2000) 177–200, arXiv:hep-ph/9908508.

[82] J. Hisano, J. Y. Lee, N. Nagata, and Y. Shimizu, "Reevaluation of Neutron Electric Dipole Moment with QCD Sum Rules," *Phys. Rev. D* **85** (2012) 114044, arXiv:1204.2653 [hep-ph].

[83] B. L. Ioffe and A. V. Smilga, "Nucleon Magnetic Moments and Magnetic Properties of Vacuum in QCD," *Nucl. Phys. B* **232** (1984) 109–142.

[84] D. Djukanovic, G. von Hippel, H. B. Meyer, K. Ottnad, M. Salg, and H. Wittig, "Electromagnetic form factors of the nucleon from $N_f = 2 + 1$ lattice QCD," arXiv:2309.06590 [hep-lat].

[85] B. L. Ioffe, "Calculation of Baryon Masses in Quantum Chromodynamics," *Nucl. Phys. B* **188** (1981) 317–341. [Erratum: Nucl.Phys.B 191, 591–592 (1981)].

[86] D. B. Leinweber, "QCD sum rules for skeptics," *Annals Phys.* **254** (1997) 328–396, arXiv:nucl-th/9510051.

[87] V. M. Belyaev and Y. I. Kogan, "CALCULATION OF QUARK CONDENSATE MAGNETIC SUSCEPTIBILITY BY QCD SUM RULE METHOD," *Yad. Fiz.* **40** (1984) 1035–1038.

[88] A. Vainshtein, "Perturbative and nonperturbative renormalization of anomalous quark triangles," *Phys. Lett. B* **569** (2003) 187–193, arXiv:hep-ph/0212231.

[89] G. S. Bali, F. Bruckmann, M. Constantinou, M. Costa, G. Endrodi, S. D. Katz, H. Panagopoulos, and A. Schafer, "Magnetic susceptibility of QCD at zero and at finite temperature from the lattice," *Phys. Rev. D* **86** (2012) 094512, arXiv:1209.6015 [hep-lat].

[90] A. G. Grozin, I. B. Khriplovich, and A. S. Rudenko, "Electric dipole moments, from e to tau," *Phys. Atom. Nucl.* **72** (2009) 1203–1205, arXiv:0811.1641 [hep-ph].

[91] S. Laporta and E. Remiddi, "The Analytical value of the electron light-light graphs contribution to the muon (g-2) in QED," *Phys. Lett. B* **301** (1993) 440–446.

[92] D. J. Broadhurst, "Three loop on-shell charge renormalization without integration: Lambda-MS (QED) to four loops," *Z. Phys. C* **54** (1992) 599–606.

[93] L. V. Avdeev, "Recurrence relations for three loop prototypes of bubble diagrams with a mass," *Comput. Phys. Commun.* **98** (1996) 15–19, arXiv:hep-ph/9512442.

[94] M. Steinhauser, "MATAD: A Program package for the computation of MAssive TADpoles," *Comput. Phys. Commun.* **134** (2001) 335–364, arXiv:hep-ph/0009029.

[95] K. G. Chetyrkin and F. V. Tkachov, "Integration by Parts: The Algorithm to Calculate beta Functions in 4 Loops," *Nucl. Phys. B* **192** (1981) 159–204.

[96] F. V. Tkachov, "A Theorem on Analytical Calculability of Four Loop Renormalization Group Functions," *Phys. Lett. B* **100** (1981) 65–68.

[97] S. P. Martin and D. G. Robertson, "Evaluation of the general 3-loop vacuum Feynman integral," *Phys. Rev. D* **95** (2017) no. 1, 016008, arXiv:1610.07720 [hep-ph].

[98] A. V. Smirnov and F. S. Chuharev, "FIRE6: Feynman Integral REduction with Modular Arithmetic," *Comput. Phys. Commun.* **247** (2020) 106877, arXiv:1901.07808 [hep-ph].

[99] J. H. Kuhn, A. I. Onishchenko, A. A. Pivovarov, and O. L. Veretin, "Heavy mass expansion, light by light scattering and the anomalous magnetic moment of the muon," *Phys. Rev. D* **68** (2003) 033018, arXiv:hep-ph/0301151.

[100] V. A. Novikov, M. A. Shifman, A. I. Vainshtein, and V. I. Zakharov, "Calculations in External Fields in Quantum Chromodynamics. Technical Review," *Fortsch. Phys.* **32** (1984) 585.

[101] M. Davier, A. Hoecker, B. Malaescu, and Z. Zhang, "Reevaluation of the hadronic vacuum polarisation contributions to the Standard Model predictions of the muon $g-2$ and $\alpha(m_Z^2)$ using newest hadronic cross-section data," *Eur. Phys. J. C* **77** (2017) no. 12, 827, arXiv:1706.09436 [hep-ph].

[102] G. Colangelo, M. Hoferichter, and P. Stoffer, "Two-pion contribution to hadronic vacuum polarization," *JHEP* **02** (2019) 006, arXiv:1810.00007 [hep-ph].

[103] M. Hoferichter, B.-L. Hoid, and B. Kubis, "Three-pion contribution to hadronic vacuum polarization," *JHEP* **08** (2019) 137, arXiv:1907.01556 [hep-ph].

[104] M. Davier, A. Hoecker, B. Malaescu, and Z. Zhang, "A new evaluation of the hadronic vacuum polarisation contributions to the muon anomalous magnetic moment and to $\boldsymbol{\alpha(m_Z^2)}$," *Eur. Phys. J. C* **80** (2020) no. 3, 241, arXiv:1908.00921 [hep-ph]. [Erratum: Eur.Phys.J.C 80, 410 (2020)].

[105] A. Keshavarzi, D. Nomura, and T. Teubner, "$g-2$ of charged leptons, $\alpha(M_Z^2)$, and the hyperfine splitting of muonium," *Phys. Rev. D* **101** (2020) no. 1, 014029, arXiv:1911.00367 [hep-ph].

[106] T. Aoyama *et al.*, "The anomalous magnetic moment of the muon in the Standard Model," *Phys. Rept.* **887** (2020) 1–166, arXiv:2006.04822 [hep-ph].

[107] **Muon g-2** Collaboration, B. Abi *et al.*, "Measurement of the Positive Muon Anomalous Magnetic Moment to 0.46 ppm," *Phys. Rev. Lett.* **126** (2021) no. 14, 141801, arXiv:2104.03281 [hep-ex].

[108] A. Crivellin, M. Hoferichter, and P. Schmidt-Wellenburg, "Combined explanations of $(g-2)_{\mu,e}$ and implications for a large muon EDM," *Phys. Rev. D* **98** (2018) no. 11, 113002, arXiv:1807.11484 [hep-ph].

[109] Y. K. Semertzidis *et al.*, "Sensitive search for a permanent muon electric dipole moment," in *KEK International Workshop on High Intensity Muon Sources (HIMUS 99)*. 12, 1999. arXiv:hep-ph/0012087.

[110] H. Iinuma, H. Nakayama, K. Oide, K.-i. Sasaki, N. Saito, T. Mibe, and M. Abe, "Three-dimensional spiral injection scheme for the g-2/EDM experiment at J-PARC," *Nucl. Instrum. Meth. A* **832** (2016) 51–62.

[111] M. Abe *et al.*, "A New Approach for Measuring the Muon Anomalous Magnetic Moment and Electric Dipole Moment," *PTEP* **2019** (2019) no. 5, 053C02, arXiv:1901.03047 [physics.ins-det].

[112] L. I. Schiff, "Measurability of Nuclear Electric Dipole Moments," *Phys. Rev.* **132** (1963) 2194–2200.

[113] I. B. Khriplovich and S. K. Lamoreaux, *CP violation without strangeness: Electric dipole moments of particles, atoms, and molecules*. 1997.

[114] M. Gorghetto, G. Perez, I. Savoray, and Y. Soreq, "Probing CP Violation in Photon Self-Interactions with Cavities," arXiv:2103.06298 [hep-ph].

[115] J. S. M. Ginges and V. V. Flambaum, "Violations of fundamental symmetries in atoms and tests of unification theories of elementary particles," *Phys. Rept.* **397** (2004) 63–154, arXiv:physics/0309054 [physics].

[116] V. F. Dmitriev and R. A. Sen'kov, "Schiff moment of the mercury nucleus and the proton dipole moment," *Phys. Rev. Lett.* **91** (2003) 212303, arXiv:nucl-th/0306050.

[117] V. V. Flambaum, D. DeMille, and M. G. Kozlov, "Time-reversal symmetry violation in molecules induced by nuclear magnetic quadrupole moments," *Phys. Rev. Lett.* **113** (2014) 103003, arXiv:1406.6479 [physics.atom-ph].

[118] **Belle** Collaboration, K. Inami *et al.*, "Search for the electric dipole moment of the tau lepton," *Phys. Lett. B* **551** (2003) 16–26, arXiv:hep-ex/0210066.

[119] A. E. Blinov and A. S. Rudenko, "Upper Limits on Electric and Weak Dipole Moments of tau-Lepton and Heavy Quarks from e+ e- Annihilation," *Nucl. Phys. B Proc. Suppl.* **189** (2009) 257–259, arXiv:0811.2380 [hep-ph].

[120] H. Gisbert and J. Ruiz Vidal, "Improved bounds on heavy quark electric dipole moments," *Phys. Rev. D* **101** (2020) no. 11, 115010, arXiv:1905.02513 [hep-ph].

[121] U. Haisch and G. Koole, "Beautiful and charming chromodipole moments," *JHEP* **09** (2021) 133, arXiv:2106.01289 [hep-ph].

[122] M. A. Shifman, A. I. Vainshtein, and V. I. Zakharov, "Remarks on Higgs Boson Interactions with Nucleons," *Phys. Lett. B* **78** (1978) 443–446.

[123] A. G. Grozin, I. B. Khriplovich, and A. S. Rudenko, "Upper limits on electric dipole moments of tau-lepton, heavy quarks, and W-boson," *Nucl. Phys. B* **821** (2009) 285–290, arXiv:0902.3059 [hep-ph].

[124] J. Ellis, N. Nagata, and K. A. Olive, "Uncertainties in WIMP Dark Matter Scattering Revisited," *Eur. Phys. J. C* **78** (2018) no. 7, 569, arXiv:1805.09795 [hep-ph].

[125] M. Pospelov and A. Ritz, "Neutron EDM from electric and chromoelectric dipole moments of quarks," *Phys. Rev. D* **63** (2001) 073015, arXiv:hep-ph/0010037.

[126] T. Bhattacharya, V. Cirigliano, S. Cohen, R. Gupta, H.-W. Lin, and B. Yoon, "Axial, Scalar and Tensor Charges of the Nucleon from 2+1+1-flavor Lattice QCD," *Phys. Rev. D* **94** (2016) no. 5, 054508, arXiv:1606.07049 [hep-lat].

[127] H.-x. He and X.-D. Ji, "QCD sum rule calculation for the tensor charge of the nucleon," *Phys. Rev. D* **54** (1996) 6897–6902, arXiv:hep-ph/9607408.

[128] D. A. Demir, M. Pospelov, and A. Ritz, "Hadronic EDMs, the Weinberg operator, and light gluinos," *Phys. Rev. D* **67** (2003) 015007, arXiv:hep-ph/0208257.

[129] V. M. Belyaev and B. L. Ioffe, "Determination of Baryon and Baryonic Resonance Masses from QCD Sum Rules. 1. Nonstrange Baryons," *Sov. Phys. JETP* **56** (1982) 493–501.

[130] B. L. Ioffe, "ON THE CHOICE OF QUARK CURRENTS IN THE QCD SUM RULES FOR BARYON MASSES," *Z. Phys. C* **18** (1983) 67.

[131] U. Haisch and A. Hala, "Sum rules for CP-violating operators of Weinberg type," *JHEP* **11** (2019) 154, arXiv:1909.08955 [hep-ph].

[132] **Particle Data Group** Collaboration, P. A. Zyla *et al.*, "Review of Particle Physics," *PTEP* **2020** (2020) no. 8, 083C01.

[133] R. Alarcon *et al.*, "Electric dipole moments and the search for new physics," in *Snowmass 2021*. 3, 2022. arXiv:2203.08103 [hep-ph].

[134] M. Le Dall, M. Pospelov, and A. Ritz, "Sensitivity to light weakly-coupled new physics at the precision frontier," *Phys. Rev. D* **92** (2015) no. 1, 016010, arXiv:1505.01865 [hep-ph].

[135] K. Fuyuto, X.-G. He, G. Li, and M. Ramsey-Musolf, "CP-violating Dark Photon Interaction," *Phys. Rev. D* **101** (2020) no. 7, 075016, arXiv:1902.10340 [hep-ph].

[136] L. D. Landau and E. M. Lifshits, *Quantum Mechanics: Non-Relativistic Theory*, vol. v.3 of *Course of Theoretical Physics*. Butterworth-Heinemann, Oxford, 1991.

[137] V. B. Berestetskii, E. M. Lifshitz, and L. P. Pitaevskii, *QUANTUM ELECTRODYNAMICS*, vol. 4 of *Course of Theoretical Physics*. Pergamon Press, Oxford, 1982.

Appendix A

Conventions

The thesis uses natural units, where

$$\hbar = c = 1. \tag{A.1}$$

In addition, the following conventions are used throughout this thesis

$$\begin{aligned}
&e = |e|, \quad e^2 = 4\pi\alpha, \quad \eta_{\mu\nu} = \mathrm{diag}(1,-1,-1,-1), \quad \sigma_{\mu\nu} = \frac{i}{2}[\gamma_\mu, \gamma_\nu], \\
&\epsilon^{0123} = +1, \quad \gamma^5 = -\frac{i}{4!}\epsilon^{\mu\nu\alpha\beta}\gamma_\mu\gamma_\nu\gamma_\alpha\gamma_\beta, \quad P_L = \frac{1-\gamma^5}{2}, \quad P_R = \frac{1+\gamma^5}{2} \\
&F_{\mu\nu} = \partial_\mu A_\nu - \partial_\nu A_\mu, \quad \tilde{F}^{\mu\nu} = \frac{1}{2}\epsilon^{\mu\nu\alpha\beta}F_{\alpha\beta}, \\
&G^a_{\mu\nu} = \partial_\mu G^a_\nu - \partial_\nu G^a_\mu + g_s f^{abc} G^b_\mu G^c_\nu, \quad G_{\mu\nu} = G^a_{\mu\nu} T^a.
\end{aligned} \tag{A.2}$$

These conventions imply

$$\sigma^{\mu\nu}\gamma^5 = \frac{i}{2}\epsilon^{\mu\nu\alpha\beta}\sigma_{\alpha\beta}, \quad \sigma\tilde{F} = -i\sigma F\gamma^5. \tag{A.3}$$

The charge conjugation matrix is defined by

$$\mathcal{C} = i\gamma^0\gamma^2. \tag{A.4}$$

The Fourier transform in 4D is defined by

$$\mathcal{F}\left[f(x)\right] = \int d^4x e^{ipx} f(x), \quad \mathcal{F}\left[f(p)\right] = \int \frac{d^4p}{(2\pi)^4} e^{-ipx} f(p). \tag{A.5}$$

When switching from the 4D spacetime coordinates to the 3D spatial coordinates, the upper and lower indices in 3D are not distinguished, and x^μ, p^μ, A^μ are "naturally raised" and ∂_μ is "naturally lowered", i.e.

$$x^\mu = (x^0, x^i), \quad p^\mu = (p^0, p^i), \quad A^\mu = (A^0, A^i), \quad \partial_\mu = (\partial_0, \partial_i). \tag{A.6}$$

The Levi-Civita tensor in 3D satisfies

$$\epsilon_{123} = \epsilon^{123} = 1 \tag{A.7}$$

The Fourier transform in 3D is defined by

$$\mathcal{F}\left[f(\boldsymbol{x})\right] = \int d^3x e^{-i\boldsymbol{p}\cdot\boldsymbol{x}} f(\boldsymbol{x}), \quad \mathcal{F}\left[f(\boldsymbol{q})\right] = \int \frac{d^3p}{(2\pi)^3} e^{i\boldsymbol{p}\cdot\boldsymbol{x}} f(\boldsymbol{p}). \tag{A.8}$$

The QCD SR calculation involves the use of dimensionally-regularized Fourier transforms, which are defined by

$$\mathcal{F}\left[f(x)\right] = \left(\frac{\mu_{UV}^2 e^{\gamma_E}}{4\pi}\right)^{-\epsilon_{UV}} \int d^{4-2\epsilon_{UV}} x \, e^{ipx} f(x), \tag{A.9}$$

$$\mathcal{F}\left[f(p)\right] = \left(\frac{\mu_{IR}^2}{4\pi e^{\gamma_E}}\right)^{-\epsilon_{IR}} \int \frac{d^{4+2\epsilon_{IR}} p}{(2\pi)^{4+2\epsilon_{IR}}} \, e^{-ipx} f(p), \tag{A.10}$$

The Borel transform is defined as

$$\mathcal{B}[f(Q^2)] = \lim_{\substack{Q^2, n\to\infty \\ Q^2/n = M^2}} \frac{(Q^2)^n}{(n-1)!} (-\frac{\mathrm{d}}{\mathrm{d}Q^2})^n f(Q^2). \tag{A.11}$$

Appendix B

Technical details for nucleon correlator calculations

Here we provide some additional technical details about the calculation of the nucleon correlators in external fields that form the basis of the QCD sum rule calculations used in Chapter 3. Further details are available in Refs. [18, 29, 81, 82].

B.1 Sum rules for $\beta = +1$

We begin with the sum rule for $\beta = +1$ nucleon interpolating currents. In this case, it is sufficient to retain just the leading terms in the the quark propagator as given by (3.28) and its corresponding charge conjugate given by

$$S_q^c = \frac{i\not{x}}{2\pi^2 x^4} + \frac{ie_q}{8\pi^2}\frac{x^\mu}{x^2}\tilde{F}_{\mu\nu}\gamma^\nu\gamma_5 + \frac{i\tilde{\chi}_q}{24}m_*\bar{\theta}F_{\mu\nu}x^\mu\gamma^\nu\gamma_5. \tag{B.1}$$

The nucleon current correlator relevant for the leading order calculation of the MDM and EDM can then be simplified to the form,

$$\Pi_n^+ = 48i\int d^4x\, e^{ip\cdot x}\left[\mathrm{tr}\left[S_d^c S_u\right] S_d + 2S_d S_u^c S_d\right]. \tag{B.2}$$

By using

$$\int d^4x\, e^{ip\cdot x}\frac{x^\mu}{x^6} = -\frac{\pi^2 p^\mu}{4}\log\left(-\frac{p^2}{\mu^2}\right) + \cdots, \tag{B.3}$$

$$\int d^4x\, e^{ip\cdot x}\frac{x^\mu}{x^8} = \frac{\pi^2 p^2 p^\mu}{48}\log\left(-\frac{p^2}{\mu^2}\right) + \cdots, \tag{B.4}$$

and the relations,

$$\{\not{p}, F\cdot\sigma\gamma_5\} = 4ip^\mu F_{\mu\nu}\gamma^\nu\gamma_5, \quad \{\not{p}, F\cdot\sigma\} = -4p^\mu\tilde{F}_{\mu\nu}\gamma^\nu\gamma_5, \tag{B.5}$$

we arrive at the expression (3.29), where we retain only the terms relevant after the Borel transformation.

B.2 Sum rules for $\beta = -1$

We next consider the sum rule for $\beta = -1$ nucleon interpolating currents. In this case, to subtract the unphysical chiral phase, we compute both the two-point function and three-point function with the external electromagnetic field.

We begin with the two-point function. The terms in the quark propagator (3.41) relevant in this case are given by

$$\begin{aligned} S_q = {} & \frac{i\not{x}}{2\pi^2x^4} - \frac{m_q}{4\pi^2x^2}\left(1 - i\gamma_5\theta_m\frac{m_*}{m_q}\right) \\ & - \frac{1}{12}\left(1 + i\gamma_5\theta_G\frac{m_*}{m_q}\right)\langle\bar{q}q\rangle, \end{aligned} \tag{B.6}$$

with the charge conjugate,

$$\begin{aligned} S_q^c = {} & \frac{i\not{x}}{2\pi^2x^4} + \frac{m_q}{4\pi^2x^2}\left(1 - i\gamma_5\theta_m\frac{m_*}{m_q}\right) \\ & + \frac{1}{12}\left(1 + i\gamma_5\theta_G\frac{m_*}{m_q}\right)\langle\bar{q}q\rangle. \end{aligned} \tag{B.7}$$

By focusing on the leading order terms, we can reduce the nucleon correlator in this

case to the form

$$\Pi_n^-\big|_{\mathbb{1},\gamma_5} = -24i \int d^4x e^{ip\cdot x} \times \left[S_d \left(S_u + \gamma_5 S_u^c \gamma_5\right) S_d - S_d \{S_u^c, \gamma_5\} S_d \gamma_5\right]_{\mathbb{1},\gamma_5} . \tag{B.8}$$

It follows that we need to retain the chirality flipping part of S_u^c, and we then obtain the expression (3.42) by using

$$\int d^4x\, e^{ip\cdot x} \frac{1}{x^6} = -\frac{i\pi^2 p^2}{8} \log\left(-\frac{p^2}{\mu^2}\right) + \cdots , \tag{B.9}$$

$$\int d^4x\, e^{ip\cdot x} \frac{1}{x^8} = \frac{i\pi^2 p^4}{192} \log\left(-\frac{p^2}{\mu^2}\right) + \cdots , \tag{B.10}$$

where we exhibit just the terms relevant for the Borel transform.

We now calculate the three-point function, or rather the two-point function expanded to leading order in the background electromagnetic field, by focusing on the leading terms of order $\tilde{\chi}_q/x^6$ or m_q/x^6 (as terms of order $\langle\bar{q}q\rangle/x^4$ do not enter to the double-pole contribution). At this order, the quark propagator is given by (3.41), along with its charge conjugate,

$$\begin{aligned} S_q^c = {} & \frac{i\not{x}}{2\pi^2 x^4} \\ & + \frac{m_q}{4\pi^2 x^2}\left(1 - i\gamma_5\theta_m \frac{m_*}{m_q}\right) + \frac{\langle\bar{q}q\rangle}{12}\left(1 + i\gamma_5\theta_G \frac{m_*}{m_q}\right) \\ & + \frac{ie_q}{8\pi^2}\frac{x^\mu}{x^2}\tilde{F}_{\mu\nu}\gamma^\nu\gamma_5 - \frac{\tilde{\chi}_q}{24} F\cdot\sigma\left(1 + i\gamma_5\theta_G \frac{m_*}{m_q}\right) \\ & + \frac{e_q m_q}{32\pi^2}\log\left(-\mu_{\rm IR}^2 x^2\right) F\cdot\sigma\left(1 - i\gamma_5\theta_m \frac{m_*}{m_q}\right) . \end{aligned} \tag{B.11}$$

Nontrivial contributions require picking up one of the last three terms. The latter two terms have the same Dirac structure and are combined with two $\not{x}$ propagators, while the first term is combined with one $\not{x}$ and one m_q or $\langle\bar{q}q\rangle$ term. One can show that, for both contributions, the traces cancel and thus we can simplify the nucleon correlator to

the form,

$$\Pi_n^-\big|_{\mu,\tilde{d}} = -24i \int d^4x e^{ip\cdot x} \times \left[S_d \left(S_u + \gamma_5 S_u^c \gamma_5\right) S_d - S_d \{S_u^c, \gamma_5\} S_d \gamma_5\right]_{\mu,\tilde{d}}. \tag{B.12}$$

It follows, as in the case of the two-point function, that we need to retain the chirality flipping part of S_u^c, and we then obtain expressions (3.46) and (3.47) after some computation, where the relevant Fourier transforms are given by

$$\int d^4x\, e^{ip\cdot x} \frac{x^\alpha x^\mu}{x^6} = \frac{i\pi^2 \eta^{\alpha\mu}}{4} \log\left(-\frac{p^2}{\mu^2}\right) + \cdots, \tag{B.13}$$

$$\int d^4x\, e^{ip\cdot x} \frac{x^\alpha x^\mu}{x^8} = -\frac{i\pi^2 (p^2 \eta^{\alpha\mu} + 2p^\alpha p^\mu)}{48} \log\left(-\frac{p^2}{\mu^2}\right) + \cdots. \tag{B.14}$$

Appendix C

Technical details for muon EDM calculations

Here we provide some technical details about the evaluation of the Schiff moment and the semi-leptonic CP-odd operator used in Chapter 5.

C.1 Schiff moment

Here we start from the CP-odd photon operator (5.3) and derive the Schiff moment (5.9). We focus on the part linear in the electric field induced by the electron as shown in Fig. 5.1. The E^3B operator is then evaluated as

$$H_{\text{eff}} = -C_{E^3B} \times \int d^3x \left(\boldsymbol{\nabla} \frac{\alpha}{|\mathbf{x} - \mathbf{r}_e|} \right) \cdot \left(2e\mathbf{E} \left(e\mathbf{E} \cdot e\mathbf{B} \right) + e\mathbf{B} \left(e\mathbf{E} \cdot e\mathbf{E} \right) \right), \tag{C.1}$$

where $\mathbf{E}$ and $\mathbf{B}$ in this expression are understood to be the nuclear electromagnetic field, and $\mathbf{r}_e$ is the position vector of the electron. With Eqs. (5.5) and (5.7), we obtain

$$H_{\text{eff}} = \int d^3x \left(\boldsymbol{\nabla}_e \frac{\alpha}{|\mathbf{x} - \mathbf{r}_e|} \right) \cdot \mathbf{P}_d, \tag{C.2}$$

where the nuclear EDM distribution is given by

$$\mathbf{P}_d = C_{E^3B} \frac{Z^2 \alpha^2 f^2}{r^4} \left[\frac{5b_1 + 4b_2}{3} \mathbf{n}_I + \frac{2b_1 + 7b_2}{3} \left(3(\mathbf{n} \cdot \mathbf{n}_I)\mathbf{n} - \mathbf{n}_I \right) \right]. \tag{C.3}$$

We thus obtain the nuclear EDM as

$$\frac{\mathbf{d}_N}{e} = \int d^3x\, \mathbf{P}_d = \mathbf{n}_I \times C_{E^3B} \int d^3x \frac{Z^2\alpha^2 f^2}{r^4} \left(\frac{5b_1 + 4b_2}{3}\right), \tag{C.4}$$

reproducing Eq. (5.8). Due to the screening effect, the atomic EDM is induced not solely by the nuclear EDM distribution but by the interaction of the form

$$H_{\text{eff}} = \int d^3x \left(\boldsymbol{\nabla}_e \frac{\alpha}{|\mathbf{x} - \mathbf{r}_e|}\right) \cdot \left(\mathbf{P}_d - \rho_q \frac{\mathbf{d}_N}{e}\right), \tag{C.5}$$

where ρ_q is the nuclear charge distribution normalized as $\int d^3x \rho_q = 1$. Since the atomic scale is much larger than the nuclear scale, we may expand the electric field induced by the electron as

$$\boldsymbol{\nabla}_e \frac{1}{|\mathbf{x} - \mathbf{r}_e|} = \boldsymbol{\nabla}_e \left[\frac{1}{r_e} - \mathbf{x} \cdot \boldsymbol{\nabla}_e \frac{1}{r_e} + \frac{1}{2} (\mathbf{x} \cdot \boldsymbol{\nabla}_e)^2 \frac{1}{r_e} + \cdots\right]. \tag{C.6}$$

The first two terms do not contribute and we obtain to the leading order

$$H_{\text{eff}} = \frac{\alpha}{2} \left(\nabla_i \nabla_j \nabla_k \frac{1}{r_e}\right) \int d^3x \left[(P_d)_i - \rho_q \frac{d_{Ni}}{e}\right] x_j x_k, \tag{C.7}$$

where we omit the subscript e from ∇ for notational ease but the derivatives still act on r_e as the bracket indicates. After the angular integration, we obtain

$$H_{\text{eff}} = -\frac{S_N}{e} \times 4\pi\alpha\, (\mathbf{n}_I \cdot \boldsymbol{\nabla}_e)\, \delta(\mathbf{r}_e), \tag{C.8}$$

where the Schiff moment is given by Eq. (5.9).

Up until this point, the treatment was completely general, and used only the symmetry considerations applied to $\mathbf{E}$ and $\mathbf{B}$. To move further and evaluate the Schiff moment, we adopt the model where $\mathbf{E}$ is created collectively by all protons inside the nucleus, while $\mathbf{B}$ is generated by a valence nucleon in a shell model of the nucleus. Evaluations of the magnetic moment of the ^{199}Hg show that the latter approximation holds to $\sim 20\%$ accuracy. In our evaluation, we simply take $f(r) = r^3/R_N^3$ for $r < R_N$ and $f(r) = 1$ for $r > R_N$ for the nuclear electric field. We have checked that the result is affected only within 10% if we instead use the Woods-Saxon type charge distribution. The nuclear

magnetic field induced by the magnetic moment of the valence neutron is given by [136] (notice the different normalization of e)

$$e\mathbf{B}(\mathbf{x}) = \frac{e\mu_n}{4\pi}\int d^3x_n \left[\boldsymbol{\nabla}_n \times \left(\psi_n^\dagger(\mathbf{x}_n)\boldsymbol{\sigma}_n\psi_n(\mathbf{x}_n)\right)\right] \times \boldsymbol{\nabla}_n \frac{1}{|\mathbf{x}_n - \mathbf{x}|}, \tag{C.9}$$

where $\mathbf{x}_n$ is the position vector of the valence neutron and $\boldsymbol{\sigma}_n$ is the Pauli matrix. The wave function of the valence neutron ψ_n is normalized as

$$\int d^3x_n \, |\psi_n|^2 = 1. \tag{C.10}$$

After integration by parts we obtain

$$e\mathbf{B}(\mathbf{x}) = \frac{2e\mu_n}{3}\psi_n^\dagger(\mathbf{x})\boldsymbol{\sigma}_n\psi_n(\mathbf{x}) + \frac{e\mu_n}{4\pi}\left[\boldsymbol{\nabla}\left(\boldsymbol{\nabla}\cdot\right) - \frac{\boldsymbol{\nabla}^2}{3}\right]\int d^3x_n \frac{\psi_n^\dagger(\mathbf{x}_n)\boldsymbol{\sigma}_n\psi_n(\mathbf{x}_n)}{|\mathbf{x}_n - \mathbf{x}|}. \tag{C.11}$$

With Eq. (5.11), the spin density for $p_{1/2}$ neutron orbital is given by

$$\psi_n^\dagger(\mathbf{x}_n)\boldsymbol{\sigma}_n\psi_n(\mathbf{x}_n) = \frac{R_{2p}^2(r_n)}{4\pi}\left[2\left(\mathbf{n}_n\cdot\mathbf{n}_I\right)\mathbf{n}_n - \mathbf{n}_I\right]. \tag{C.12}$$

The angular integral can be performed with the multipole expansion of the Coulomb potential

$$\frac{1}{|\mathbf{x}_n - \mathbf{x}|} = \frac{\Theta(r_n - r)}{r_n}\sum_{l=0}^{\infty}\left(\frac{r}{r_n}\right)^l P_l(\cos\theta) + \frac{\Theta(r - r_n)}{r}\sum_{l=0}^{\infty}\left(\frac{r_n}{r}\right)^l P_l(\cos\theta), \tag{C.13}$$

where $\cos\theta = \mathbf{x}_n\cdot\mathbf{x}/rr_n$, and we obtain

$$e\mathbf{B}(\mathbf{x}) = b_1(r)\mathbf{n}_I + b_2(r)\left(3(\mathbf{n}\cdot\mathbf{n}_I)\mathbf{n} - \mathbf{n}_I\right), \tag{C.14}$$

where

$$\begin{aligned} b_1(r) &= \frac{\mu_n}{6\pi}\left(2\int_r^\infty \frac{dr_n}{r_n}R_{2p}^2(r_n) - R_{2p}^2(r)\right), \\ b_2(r) &= \frac{\mu_n}{12\pi}\left(R_{2p}^2(r) - \frac{1}{r^3}\int_0^r dr_n r_n^2 R_{2p}^2(r_n)\right), \end{aligned} \tag{C.15}$$

thus reproducing the equations in Chapter 5. As a cross check, one can show that these

expressions satisfy Maxwell's equation $\nabla \cdot \mathbf{B} = 0$.

In order to obtain R_{2p}, we numerically solved the Schrödinger equation for the valence neutron moving in the Woods-Saxon potential. The parameters of the potential [116] are tuned to reproduce single-particle energies and collective properties of heavy nuclei. We have checked that our numerical results are consistent with other single-particle calculations, of *e.g.* Schiff moment induced by the neutron EDM [115]. Final numerical results for $S_{^{199}\mathrm{Hg}}$ are given in Eq. (5.13).

C.2 Semi-leptonic CP-odd operator

Here we provide details on our evaluation of the semi-leptonic CP-odd operator C_S. We again start from the CP-violating photon operator

$$\mathcal{L} = \frac{e^4 C_{E^3B}}{8} (\tilde{F}_{\alpha\beta} F^{\alpha\beta})(F_{\gamma\delta} F^{\gamma\delta}). \tag{C.16}$$

We contract two photons with the electron line as shown in Fig. 5.2. At the level of effective operators, this diagram is logarithmically divergent. However, since we have integrate out the muon, the logarithmic divergence is tamed by the muon mass scale, and hence we obtain

$$\mathcal{L} = C_{E^3B} \times 10\alpha^2 m_e \log\left(\frac{m_\mu}{m_e}\right) |e\mathbf{E}|^2 \, \bar{e} i\gamma_5 e, \tag{C.17}$$

to the leading log accuracy, where $\mathbf{E}$ is the nuclear electric field and we ignore $\mathbf{B}^2$ that is subdominant. We use the same character e for both gauge coupling and the electron spinor, but there should be no confusion.

It is well-known that the strength of atomic EDMs in heavy atoms is determined mostly by the mixing of $s_{1/2}$ and $p_{1/2}$ atomic orbitals. It is easy to see that both the $\mathbf{E}^2$-proportional interaction (C.17) and the usual form of C_S-interaction (2.2) induce a mixing between the atomic $s_{1/2}$ and $p_{1/2}$ states. Near/inside the nucleus where $\bar{N}N$ and $\mathbf{E}^2$ operators peak, the electron wave functions satisfy the Dirac equations and are

given by

$$\psi_{jlm} = e^{-iEt}\begin{pmatrix} f_{jl}(r)\Omega_{jlm} \\ (-)^{j-l-1/2} g_{jl}(r)\Omega_{jl'm} \end{pmatrix}, \quad l' = 2j - l, \tag{C.18}$$

where Ω_{jlm} is the spherical harmonics spinor (see *e.g.* [137]). Thus the atomic matrix element induced by (2.2) is

$$\int d^3x_N\, \rho_N(\mathbf{x}_N)\psi_p^\dagger(\mathbf{x}_N)\gamma^0\gamma_5\psi_s(\mathbf{x}_N) = A\int dr_N\, r_N^2 \bar{\rho}_N\left(f_p g_s + f_s g_p\right), \tag{C.19}$$

where ρ_N is the nucleon density distribution inside the nucleus, $A = 232$ is the atomic number of Th and we made the index $j = 1/2$ implicit for notational ease.

Atomic/molecular theory connects the small-r asymptotic form of the wave functions (C.18) with the full numerically determined atomic orbitals. CP-violation, on the other hand, comes exclusively from the atomic short-distance matrix element (C.19). Therefore, in order to determine the atomic matrix element induced by (C.17) we need to replace (C.19) with

$$\int d^3x_N\, |e\mathbf{E}(\mathbf{x}_N)|^2\, \psi_p^\dagger(\mathbf{x}_N)\gamma^0\gamma_5\psi_s(\mathbf{x}_N) = \frac{24\pi Z^2\alpha^2}{5R_N}\int dr_N\, r_N^2 \bar{\rho}_{E^2}\left(f_p g_s + f_s g_p\right). \tag{C.20}$$

Here the normalized distributions are taken as

$$\bar{\rho}_N(r_N) \propto \frac{1}{1+e^{(r_N-R_N)/a}}, \quad \bar{\rho}_{E^2}(r_N) \propto \frac{r_N^2}{R_N^6}\Theta(R_N - r_N) + \frac{1}{r_N^4}\Theta(r_N - R_N),$$
$$\int dr_N r_N^2 \bar{\rho}_N = \int dr_N r_N^2 \bar{\rho}_{E^2} = 1. \tag{C.21}$$

Therefore the effective C_S-coupling induced by (C.17) is estimated as

$$\frac{G_F}{\sqrt{2}} C_S^{\text{equiv}} = C_{E^3B} \times \kappa \frac{48\pi Z^2\alpha^4 m_e}{R_N A}\log\left(\frac{m_\mu}{m_e}\right), \quad \kappa = \frac{\int dr_N\, r_N^2 \bar{\rho}_{E^2}\left(f_p g_s + f_s g_p\right)}{\int dr_N\, r_N^2 \bar{\rho}_N\left(f_p g_s + f_s g_p\right)}. \tag{C.22}$$

In order to evaluate the correction factor κ, that ultimately accounts for the difference of spatial distribution between $\bar{N}N$ and $\mathbf{E}^2$ operators in the atomic matrix element,

we solve the Dirac equation for the radial functions f and g numerically. We take $R_N = r_0 A^{1/3}$ with $r_0 = 1.27\,\mathrm{fm}$ and $a = 0.742\,\mathrm{fm}$ following [116], and obtain

$$\kappa \simeq 0.66. \tag{C.23}$$

This is used for our estimation of the upper limit on d_μ in Chapter 5.

Appendix D

Borel transformation and IR divergence

In this appendix we discuss the Borel transformation of Eq. (6.22) that contains both the UV and IR divergences. As the Borel transformation is related to the imaginary part, it is equivalent to taking the imaginary part of

$$I(p^2;\epsilon_{\rm IR},\epsilon_{\rm UV}) \equiv \Gamma(\epsilon_{\rm IR})\left(-\frac{\Lambda_{\rm IR}^2}{p^2}\right)^{-\epsilon_{\rm IR}}\Gamma(-\epsilon_{\rm UV}-\epsilon_{\rm IR})\left(-\frac{\Lambda_{\rm UV}^2}{p^2}\right)^{-\epsilon_{\rm UV}}. \tag{D.1}$$

The limit of this function at $\epsilon_{\rm UV}\to 0$, $\epsilon_{\rm IR}\to 0$ is not well defined. For example, if the limit is taken along the line $\epsilon_{\rm UV} = a\,\epsilon_{\rm IR}$ with fixed a, one would get an a-dependent result:

$$\begin{aligned}&\lim_{\epsilon_{\rm IR}\to 0} I(p^2;\epsilon_{\rm IR},a\,\epsilon_{\rm IR})\\ &= -\frac{1}{2\,(1+a)}\left[\log^2\left(-\frac{\Lambda_{\rm IR}^2}{p^2}\right)+2a\log\left(-\frac{\Lambda_{\rm IR}^2}{p^2}\right)\log\left(-\frac{\Lambda_{\rm UV}^2}{p^2}\right)+a^2\log^2\left(-\frac{\Lambda_{\rm UV}^2}{p^2}\right)\right],\end{aligned} \tag{D.2}$$

where we only kept the double logarithmic terms. The purpose of this subsection is to understand the correct prescription of evaluating the imaginary part of this function.

In order to understand the correct prescription, it is helpful to consider a simpler example: a scalar three-body decay. Indeed, the two point correlator $\Pi(p)$ contains three quark propagators, and thus the imaginary part of this function is related a three-body

decay phase space integral. Therefore we consider the following Lagrangian

$$\mathcal{L} = \frac{1}{2}(\partial\phi)^2 - \frac{m_\phi^2}{2}\phi^2 + \frac{1}{2}(\partial\chi)^2 - \frac{m_\chi^2}{2}\chi^2 - \frac{\lambda}{6}\phi\chi^3, \tag{D.3}$$

and study the three-body decay $\phi \to 3\chi$. The two-loop diagram is evaluated as

$i\mathcal{M}_2 =$ 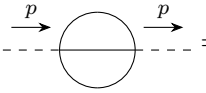 $= \frac{i\lambda^2}{6}\int\frac{d^4l_1}{(2\pi)^4}\int\frac{d^4l_2}{(2\pi)^4}D_F(l_1)D_F(l_2)D_F(l_1+l_2-p),$ (D.4)

where $D_F(p)$ is the Feynman propagator,

$$iD_F(p) = \frac{i}{p^2 - m_\chi^2 + i0}, \tag{D.5}$$

and the solid line is χ while the dashed line is ϕ. The cutting rule tells us that

$$\mathrm{Im}\mathcal{M}_2 = \frac{1}{2}\frac{\lambda^2}{6}\int d\Pi_{\mathrm{LIPS}}, \tag{D.6}$$

where $d\Pi_{\mathrm{LIPS}}$ is the three-body Lorentz invariant phase space integral. This is expanded with respect to m_χ^2/m_ϕ^2 as

$$\int d\Pi_{\mathrm{LIPS}} = \frac{1}{32\pi^3}\left[\frac{m_\phi^2}{8} + \frac{3m_\chi^2}{4}\left(\log\left(\frac{4m_\chi^2}{m_\phi^2}\right) - 1\right) + \cdots\right], \tag{D.7}$$

where we used $p^2 = m_\phi^2$. We now evaluate the left hand side of Eq. (D.6) in an analogous way as the main text. We may expand the propagator as

$$iD_F(p) = \frac{i}{p^2 - m_\chi^2} = i\left(\frac{1}{p^2} + \frac{1}{p^2}m_\chi^2\frac{1}{p^2} + \cdots\right), \tag{D.8}$$

where we omit $i\epsilon$ for notational simplicity. In the coordinate space this is given by

$$iD_F(x) = -\frac{1}{4\pi^2x^2} - \frac{m_\chi^2}{16\pi^2}\Gamma(\epsilon_{\mathrm{IR}})\left(-\Lambda_{\mathrm{IR}}^2x^2\right)^{-\epsilon_{\mathrm{IR}}} + \cdots. \tag{D.9}$$

The first order term in m_χ^2 is IR divergent and this is analogous to our propagator with

the CP-odd operator insertion in Sec. 6.2.2. The two-loop amplitude is given by

$$i\mathcal{M}_2(p) = \frac{(i\lambda)^2}{6}\mu_{\rm UV}^{d_{\rm UV}-4}\int d^{d_{\rm UV}}x\, e^{ip\cdot x} iD_F(x) iD_F(x) iD_F(x). \tag{D.10}$$

To the first order in m_χ^2 we obtain

$$\mathcal{M}_2|_{\mathcal{O}(m_\chi^2)} = -\frac{\lambda^2 m_\chi^2}{512\pi^4} I(p^2;\epsilon_{\rm IR},\epsilon_{\rm UV}). \tag{D.11}$$

Note that we get exactly the same function $I(p^2;\epsilon_{\rm IR},\epsilon_{\rm UV})$ here. Eq. (D.6) tells us that

$$\mathrm{Im}\mathcal{M}_2|_{\mathcal{O}(m_\chi^2)} = \left[\frac{1}{2}\frac{\lambda^2}{6}\int d\Pi_{\rm LIPS}\right]_{\mathcal{O}(m_\chi^2)} = \frac{\lambda^2 m_\chi^2}{512\pi^3}\log\left(\frac{m_\chi^2}{m_\phi^2}\right), \tag{D.12}$$

where we focus on the leading logarithmic term on the right hand side. Thus the correct prescription of evaluating the imaginary part of I is

$$\mathrm{Im}\left[I(p^2;\epsilon_{\rm IR},\epsilon_{\rm UV})\right] = -\pi\log\left(\frac{\Lambda_{\rm IR}^2}{p^2}\right), \tag{D.13}$$

where we identify $\Lambda_{\rm IR}^2 = m_\chi^2$ in the present case. This agrees with the Borel transformation formula in [131]. For the example in Eq.(D.2), this prescription is equivalent to neglecting the real part of the UV logarithm.

Our discussion clarifies the physical meaning of $\Lambda_{\rm IR}$ that appears in Eq. (6.25). This IR divergence originates from the phase space integral and is regulated by the mass of the daughter particles. In the neutron EDM case, the daughter particles are the constituent quarks. Therefore $\Lambda_{\rm IR}$ is identified with the mass of the constituent up and down quarks that we take $\Lambda_{\rm IR} = 300\,\mathrm{MeV}$ in Chapter 6.

Appendix E

Acronyms

This appendix contains a table of acronyms and their meaning.

Table E.1: Acronyms

Acronym	Meaning
AMO	atomic, molecular, and optical physics
BSM	beyond Standard Model
CEDM	color electric dipole moment
CKM	Cabibbo–Kobayashi–Maskawa
EDM	electric dipole moment
EFT	effective field theory
EM	electromagnetic
EW	electroweak
IR	infrared
KM	Kobayashi-Maskawa
LO	leading order
NLO	next-to-leading order
MDM	magnetic dipole moment
OPE	operator product expansion
QCD	quantum chromodynamics

Continued on next page

Table E.1 – Continued from previous page

Acronym	Meaning
QCD SR	QCD sum rule
SM	Standard Model
SMEFT	Standard Model effective field theory
UV	ultraviolet